Design and Production of a Wooden Thames A Rater Class Sailing Yacht

SOUPPEZ

Jean-Baptiste Roger Guillaume

jeanbaptiste.souppez@gmail.com
jsou443@aucklanduni.ac.nz

Master of Engineering Studies in Yacht Engineering
Department of Mechanical Engineering
The University of Auckland
June 2015

Abstract

The niche market for modern classics, combining traditional wooden boats with the latest design and manufacturing technology, has been expanding in the past decade, particularly in the United-Kingdom. Yachts such as the Thames A Raters remain among the most competitive racing classes, featuring extreme high aspect ratio carbon rigs and wooden hulls over a century old. This example of a modern classic motivated the conception of the next generation of A Raters.

The design was developed under the strict class rule and in close relation with the class association and sailors to ensure that the original spirit of the yachts would be conserved. Furthermore, the design brief incorporated the client's requirements, as well as the shipyard's restrictions and environmental constraints. Finally, the RCD/ISO standard regulation has been adopted.

Hydrodynamic optimisation has been a major interest to improve the performance, despite the imposed hull shape. Indeed, only an exact replica of an existing A Rater is allowed. However, a loop-hole in the class regulation allowed for some modifications to the hull shape. Based on the Delft systematic yacht hull series, parametric optimisation has been utilised to reduce the hull resistance. Furthermore, multiple centreplate and rudder planforms have been compared using computational fluid dynamics to adopt the most efficient ones.

Coupled with the decrease in hydrodynamic resistance, the more powerful sails led to a higher level of performance, quantified thanks to a six degrees of freedom velocity prediction program. In order to reflect the planning capabilities of the boat, the fundamental principles of Savitzky's planning theory have been adapted and incorporated to maximise the accuracy.

In terms of design, the main priorities were to create an aesthetically pleasing yacht, taking advantage of the natural beauty of vanished woods, as well as a more practical layout, better suited to modern racing. As a result, the cockpit was a particular area of interest: a simpler and more ergonomic layout has been developed, with a higher level of comfort for the crew.

To achieve a light boat that can be built faster and at a lesser cost than the traditional carvel technique, cold moulding has been preferred. The structural design was developed in accordance with the relevant regulatory bodies and considering the manufacturing constraints. Eventually, a realistic cost estimate and detailed planning were elaborated.

A complete set of drawings have been provided to detail the multiple aspects of the design, as well as specify the materials and production methods involved.

The final design fully answers the pre-established specifications, with significant improvement in performance while retaining the traditional spirit of the class. The complete design and production allows for the building to be started, and the careful consideration of the various regulations ensures that the boat will be classified, with the inherent reliability in terms of safety.

The qualities of the yacht are demonstrated in this report, and further supported by the excellent feedback obtained from the client, extremely satisfied by the design proposed.

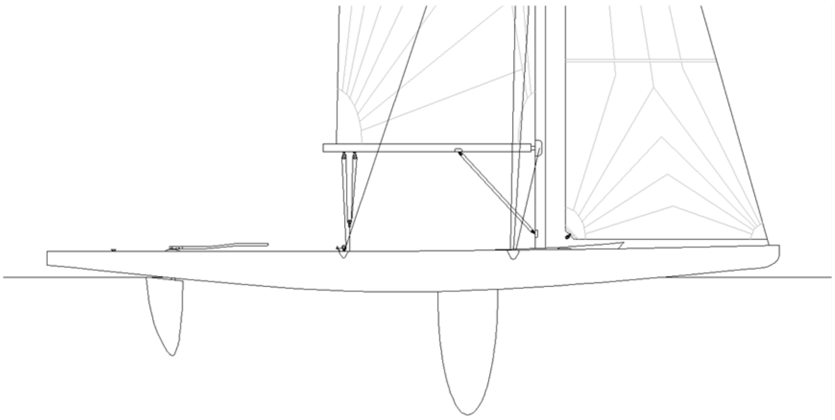

Table of Contents

List of Figures

List of Tables

List of Symbols

$1+k$	Form factor
AR	Aspect ratio
AR_e	Effective aspect ratio
Aw	Waterplane area
BAD	Boom above deck
BM	Metacentric radius
BOA	Beam overall
Bwl	Waterline beam
Cb	Block coefficient
C_D	Drag coefficient
C_{Di}	Induced drag coefficient
Cf	Friction coefficient
C_L	Lift coefficient
Cm	Midship coefficient
Cp	Prismatic coefficient
Cv	Speed coefficient
D	Drag
Dr	Drive force
E	Main foot length
E	Young's modulus
f	Flat
F	Freeboard
Fh	Side force
g	Acceleration due to gravity
GM	Metacentric height
Gz	Righting lever
HA	Heeling arm
I	Jib height
I_{xx}	Second moment of area
J	Jib foot length
KN	Base-line righting lever
L	Lift
LOA	Length overall
Lwl	Length on waterline
P	Main luff height
r	Reef
Rf	Fritcion resistance
Ri	Induced drag
RM	Righting moment
Rn	Reynolds nulmber
Rr	Residuary resistance
Rt	Total resistance
Rv	Viscous resistance
Rw	Wave resistance
SA	Sail area
Sc	Wetted surface area
SM	Section modulus
Tc	Canoe body draft
T	Overall draft
Va	Apparent wind speed
$Veff$	Effective wind speed
Vs	Boat speed
Vt	True wind speed

List of Greek Symbols

α	Angle of attack
β	Yaw angle
βa	Apparent wind angle
βeff	Effective wind angle
βt	True wind angle
Δ	Displacement
∇c	Canoe body displacement
θ	Pitch angle
λ	Leeway angle
μ	Viscosity
ρ	Density
σ_d	Design stress
σ_y	Yield stress
τ_d	Design sheer stress
φ	Roll angle

List of Acronyms

CE	Centre of effort
CFD	Computational fluid dynamics
CLR	Centre of lateral resistance
CPA	Critical path analysis
DSYHS	Delft systematic yacht hull series
IBTC	International boatbuilding training college
KSF	Keel side force
LCB	Longitudinal centre of buoyancy
LCF	Longitudinal centre of flotation
LCG	Longitudinal centre of gravity
SSF	Sail side force
TCG	Transverse centre of gravity
VCG	Vertical centre of gravity
VLM	Vortex lattice method
VMG	Velocity made good
VPP	Velocity prediction program

Conversion Factors

Although this report will be based on the International System of Units (SI) (or 'nautical' units in special cases), the Thames A Raters have been designed using the imperial system, and imperial units remain predominant in wooden boatbuilding; conversion factors are therefore provided hereafter.

Metric Unit	Imperial Unit	Conversion factor: Metric to Imperial	Conversion factor: Imperial to Metric
Millimetres (mm)	Inches (in)	0.039	25.4
Meters (m)	Inches (in)	39.37	2.54
Meters (m)	Feet (ft)	3.281	0.305
Square meters (m^2)	Square feet (ft^2)	10.764	0.0929
Cubic meters (m^3)	Cubic feet (ft^3)	35.315	0.0283
Kilograms (kg)	Pounds (lbs)	2.2046	0.4536
Meters per second (m/s)	Knots (kts)	1.9425	0.5148

Chapter 1: Introduction

In over a century of racing, the Thames A Rater class evolved with the technological advances that enabled it to last through history and remain one of the most exciting inland racing classes in the world. The aim of this project is to conceive the next generation of A Raters, combining a classic yacht with the latest design and technology, and to introduce the boat into a new location: the Norfolk Broads, on the East coast of England. The history and evolution of the class will first be presented; a detailed design brief considering all stakeholders to be involved will then be developed, leading to an overall outline of the project.

1.1 Thames A Rater

1.1.1 Historical Background

Created in 1870, the Thames Sailing Club (TSC) is the second oldest inland sailing club in Britain. The success of the first years of racing quickly highlighted two major issues: boats of highly different performances were competing together and no racing rules were applied. Despite those two constraints, the Thames Sailing Club became so important that in 1887, Queen Victoria herself awarded the Thames Champions Cup. This particular event revealed the potential of inland sailing events, and called for a prompt remedy to previously mentioned issues. The following year (1888) saw the creation of the Sailing Boat Association (SBA) that established racing rules, and later introduced a handicap system, based on the popular Dixon Kemp's rating formula [13]:

$$Rating = \frac{Lwl \times SA}{6000} \qquad \textit{Eq. 1}$$

In which:

Lwl	Waterline length.	ft
SA	Sail area.	ft^2

This gave birth to the term '*Rater*', defining yachts designed under this particular rule; a One-Rater rating 1, a Half-Rater rating 0.5, etc… Later, a class gathering boats rating from 0.8 to 1 was created: the A Rater class.

1.1.2 Thames A Rater Class

Towards the end of the 19^{th} century, the design of inland racing yachts is generally defined as a '*skimming dish*', a philosophy that reached a plateau with the A Rater's fleet. Out of the 13 original A Raters still racing today, twelve were built between 1898 and 1911 and the last one post WWI in 1922.

The majority of the A Raters were designed by Alfred Burgoine and Linton Hope, each having a radically different approach to the rating rule that only accounts for the waterline length and the sail area.

Burgoine's yachts are characterized by a large sail area, the counterpart being a shorter waterline length. While the latter restricts the speed for a given Froude number, the larger sail area will offer a more powerful boat that therefore has to be made wider to increase form stability and the ability to carry sail.

On the other hand, Hope favoured a longer waterline and narrower beam, and consequently a smaller sail area. The opposition of those two design philosophies is illustrated in Table 1, comparing two original A Raters, namely *Ulva* (1898) and *Scamp* (1902), respectively drawn by Burgoine and Hope.

Yacht	Lwl (m)	Bwl (m)	SA (m^2)	Rating
Ulva	4.80	2.15	35.00	0.99
Scamp	5.15	1.66	33.00	1.00

Table 1: *Burgoine and Hope designs comparison.*

The radically opposed specifications led to different performances, the Hope yachts being better suited to upwind sailing while the Burgoine ones sailed faster downwind.

As always with rating rules, if something is not strictly written as prohibited, it can be considered as part of the design, and the A Rater class is no exception.

1.1.3 Cheating the Rule

Looking at the various attempts to '*cheat*' the A Rater class rules provides some insights into the critical design areas to be improved; in this case the waterline length, the stability and the mast weight.

Firstly, the work of William Froude published a few decades before the A Raters [25, 26] identified the waterline length as the main speed restricting factor, hence the interest in a longer waterline length. For the typical resistance hump occurring at a Froude number of 0.33, *Ulva* would achieve 4.40 knots, while *Scamp* would reach 4.56 knots. As a result, some boats were fitted with rods and wires at each end. By winding up the wires, the yacht could artificially be sagged to offer a shorter waterline length when measured. The wires would then be loosened when racing, thus extending the actual waterline length.

Secondly, stability is a major factor for such a light displacement craft carrying a large sail area. Some of the main innovations with regard to stability have been experimented on Vagabond, designed in 1907 by Hope. The ancestor of the trapeze (now standard on most dinghies) was named the '*bell rope*': a crew (the '*bell boy*') holding onto a rope attached at the top of the mast could stand to windward, as depicted in Figure 1, thus increasing the righting moment.

Figure 1: *The 'bell boy' and the 'bell rope' [74].*

Once made illegal, Vagabond was fitted with sliding seats (see Figure 2), with the same effect of increasing the righting moment, and the same fate of being banned.

Figure 2: *Sliding seats on Vagabond [74].*

Finally, removable top masts have been introduced to minimise the heeling moment in high winds. While this practice was prohibited, the masts would undergo several improvements in the future.

1.1.4 Mast Evolution

While the hulls and appendages have been untouched since the beginning of the 20th century, the rig and sails have significantly evolved. Originally designed as a low aspect ratio gaff rig, as presented in Figure 3, the masts technology changed from bamboo to the current carbon fibre, via solid and hollow wooden spars and aluminium.

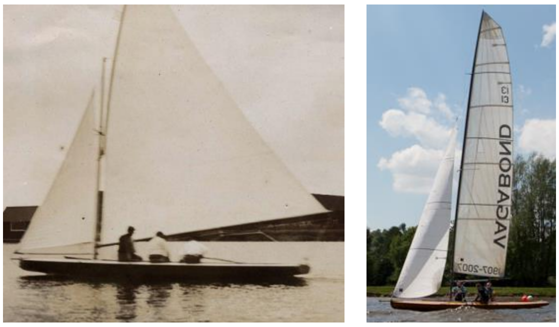

Figure 3: *Rig in 1907 (left) [74] and 2014 (right) [112].*

With the improving mast technology, higher spans could be achieved, and the A Raters are now famous for their impressive 43 feet (13.1m) tall rigs, which allows better performance due to the high aspect ratio as well as a better control downwind.

Indeed, one of the downsides of the early gaff rigs was the eccentric location of the centre of effort of the sails downwind, requiring tremendous efforts from the helmsman to keep the boat on course in the narrow waterways.

Remains of this behaviour can still be seen today with some of the original tillers, clearly made for the helmsman to brace himself onto it, as shown in Figure 4.

Figure 4: *The bracing tiller of Ulva [93].*

Along with the masts, cotton sails have been replaced with more advanced materials. Those innovations contributed to the success of the A Rater class, and so did the Glass Reinforced Plastics (GRP) technology that sparked a regain of interest in the class in the late 1970s.

1.1.5 Modern Days

The A Rater class is one of the rare racing classes that survived after World War II, but with the last wooden A Rater dating from 1922, the number of boats was becoming smaller and smaller over time. In 1978, a female mould tool of *Ulva* was made, and new GRP hulls were built, thus ensuring the future of the class. Around this time also came into place a change in the rules: no new design would be allowed, any new A Rater would have to be an exact replica of an original one; this will be further discussed in Section 1.2.6. In addition, to stop the '*arms race*' resulting from the new composite manufacturing, a minimum class weight was imposed.

In 2002, J. Stewart [110] proposed a modern version of an A Rater; while the design is not an exact replica and therefore cannot be considered a strict A Rater, it constitutes relevant previous work that will be studied for the purpose of this project.

Finally, the early 2010s saw the appearance of the first full carbon boats, fitted with a new deck inspired from the 5o5 class; the latest A Rater built is illustrated in Figure 5.

Figure 5: *The latest A Rater built [112].*

The challenge set for this project is to design and produce the next generation of wooden A Raters.

1.2 Design Brief

The design brief is possibly the most crucial part of the project, and is often not appreciated as such. Indeed, a design can only meet and satisfy the requirements of the various stakeholders involved if they are all carefully considered, leading to a well thought and complete brief. The proposed one takes into account the client's requirements, the restrictions inherent to the shipyard and the production, the environment for which the yacht is intended, feedback from the sailors, as well as the class rule and regulatory body to be involved.

1.2.1 Aims

The Thames A Rater class owes part of its name to its location on the river Thames. The aim of this project is to provide the next generation of A Raters, and introduce the class to a new location: the Norfolk Broads, located on the far East coast of England, 180km North-East of London. The Norfolk Broads offer large inland waterways, i.e. similar racing conditions as the river Thames. Furthermore, this particular location benefits from a very strong local knowledge and workforce in traditional wooden boatbuilding, to the extent that many A Raters are maintained and refitted in this particular region.

1.2.2 Client's Expectations

The design brief starts with the client's requirements and expectations that are of primary importance and must be satisfied.

First of all, a wooden A Rater to operate on the Norfolk Broads is to be conceived, with particular emphasis on:

- Performance, to be able to compete with the existing fleet and win races.
- Elegance, the design must be aesthetically pleasing and conserve the tradition of the original A Raters. Moreover, the wood must be highlighted with visible varnished wood.
- Low cost, to make the boat affordable to buy, race and maintain over time.

Further and more specific demands were also made:

- Reefing must be provided on the mainsail (currently no reef on the mainsails), so the A Rater can be handled in higher wind speeds.
- The mast is to be easy to drop and raise again in order to go under bridges (as it is part of races) and make most of the Norfolk Broads accessible for sailing; this consideration will involve a draft constraint, further discussed in Section 1.2.4
- Water flowing over the deck and into the cockpit should be minimised, and a self-bailer should be installed.

The basis of the design brief is set by the client, then implemented by additional stakeholders to be involved with the project, such as the shipyard.

1.2.3 Shipyard's Restrictions

The new vessel is to be built on the Southern end of the area of operation, at the International Boatbuilding Training College (IBTC).

For the past 35 years, the IBTC has been at the heart of the preservation of the traditional maritime skills, with one of the most renown wooden boatbuilding courses in the world. Since the yacht is to be constructed by students, the manufacturing implications are atypical.

Firstly, the labour being provided by students, it is not charged for: only the materials have to be paid. When building a wooden boat, labour is the primary expense that reflects on the selling price; free labour thus ensures that an inexpensive A Rater can be achieved.

The quality of the work is of a high standard, and perhaps higher than a commercial standard. Indeed, commercial work (that accounts for labour) will not be able to spend an extended amount of time on a task, or repeat it until perfection is reached, which is the case at the IBTC since the primary purpose is the formation of students. It must however be noted that the quality of the work can vary from one worker to another, and inconsistency is a potential issue.

Nevertheless, the free labour and high standard of craftsmanship come at a price: time. The time to complete a given task is likely to be higher than for a typical shipyard; this aspect must therefore be carefully considered, with efficient manufacturing techniques and the allocation of extra time in the production planning.

In addition to the work-force specificities, the shipyard restrictions are as follows:

- All wooden machining can be done in-house, and a composite workshop is available.
- Being part of a training course, the yacht must offer relevant experience for the students.
- The main wood species available at the IBTC are: oak, larch, mahogany and Douglas fir. Where possible, the use of those species will be privileged.
- While the yard can accommodate larger crafts, the lofting floor is restricted to 28ft in length, which happens to be the size of A Rater: the boat can therefore be lofted at the shipyard.

Last but not least, traditional boatbuilding is particularly attached to its traditions, of varying importance. For instance, the boat is to be set up back to the water (as doing otherwise would be seen as bad luck); this particular tradition is enforced at the IBTC, which will impact on the location of the yacht in the shipyard. While other traditions such as never launching the boat on a Friday or placing a silver coin under the mast are not of primary concern, they will still be met to comply with the spirit of tradition inherent to the A Rater.

The location of the IBTC on the edge of the Norfolk Broads makes it particularly convenient, as it is the intended area of operation.

1.2.4 Environmental Constraints

Since the yacht is designed to operate in a particular location, environmental restrictions apply in terms of height and draft constraints, in order to make the majority of the waterways accessible [20].

As previously stated, the mast must be lowered so the yacht can go under bridges, the lowest one being the Potter Heigham bridge, with a clearance of 6 feet and 6 inches (1.98m) [20], illustrated in Figure 6.

Figure 6: *Potter Heigham bridge [112].*

In terms of draft, the average depth is 1.8m. The Broads Authority [20] specifies that the large majority of the Broads is accessible to vessels having a 5 feet (1.52m) or less draft; this will therefore be set as the maximum draft allowed.

1.2.5 Sailors' Feedback

The A Rater class having over a hundred years of history, feedback has been sought among experienced sailors from the Thames Sailing Club to identify areas of possible improvement as well as suggestions relevant to the project.

- The foremost requirement was to design a boat that would carry on the class legacy and be able to race alongside the rest of the fleet, and not an ultra-light full carbon yacht.
- The carbon mast could be improved: the current ones are too flexible, and attempts at a stiffer rig resulted in a mast so heavy the crew could not raise it again after going under a bridge, and had to retire from the race.
- Crew often have to stand on the foredeck: a heavily curved one is very uncomfortable to stand on, especially if polished or varnished. This calls for a more suited and safer foredeck.
- Mainsails are not fitted with reefing points, which restricts the ability to handle the boats in higher wind speeds. This is coupled with the stability issue in strong winds, where the crew cannot counteract the heeling moment.

The improvements suggested by the sailors will be added to the design brief that now needs to incorporate the relevant regulation.

1.2.6 Thames A Rater Class Rule

The main design implications of the Thames A Rater class rule [111] are summarised in this section.

- For a new hull to be considered an A Rater, it must be an exact replica of an original A Rater, with a tolerance of one and a half inch (Rule D2).
- 800 lbs (363kg) of buoyancy are to be provided (Rule D3).
- The rubbing strake shall not exceed 2.5 inches in plan width (Rule D4).
- The minimum lightship weight is 750 lbs (340kg), excluding sheets, sails, mast, stays, halyards, boom, whisker pole or jib boom (Rule D5).
- Two mooring points (one at the bow, one at the stern) are required on the centreline and at a maximum of 36 inches from the extremities, with a minimum diameter of 1.5 inches (Rule D6).
- Each mooring line must be at least 30 feet in length (Rule D7).
- A single mast is allowed, with an overall length less than 44 feet and 6 inches, at a maximum height from the sheerline of 43 feet (Rule E2 (a)).
- The gooseneck shall be fitted at least 3 feet above the sheerline (Rule E2 (d)).
- The bow sprit shall extend less than 24 inches from the bow (Rule E2 (g)).
- Only two sails are allowed and spinnakers are prohibited (Rule E4 (a)).
- The sail area shall not exceed 350 ft^2 (32.51 m^2) (Rule E4 (b)).
- The number of crew onboard is to be three (Rule F2).
- Are prohibited: bumpkins, outriggers, sliding seats, trapeze wires, bilge boards, double rudders and similar contrivances (Rule F3 (b)); as well as: hydraulic, electrical or electronic equipment other than watches and bilge pumps (Rule F3 (c)).

The two major aspects of the class rule are the need for the hull to be an exact replica of an existing A Rater, and the minimum lightship weight and inherent exclusions.

On the one hand, for the hull to be an exact replica, the linesplan of an existing boat must be obtained, which will represent a research challenge as the original drawings are over a century old. This also highly restricts the design of the hull, although part of the one and a half inch building tolerance could be used to slightly modify it while still meeting the tolerance required to be considered an exact replica. Furthermore, the very limited design changes allowed suggest that a greater proportion of time should be spent on the appendages, not concerned by the replica criterion, and where most of the hydrodynamics can be improved.

On the other hand, the imposed minimum lightship sets a target displacement, where any weight saved can be added as ballast in the centreplate to improve stability and performance. It is also important to note the exclusion of sheets, sails, mast, stays, halyards and boom. Since those are not concerned by the lightship, they are to be made as light as possible to achieve a lighter craft.

The Thames A Rater class rule is to be met for the boat to be recognised as an A Rater. Furthermore, the yacht is to meet the requirements of a relevant regulatory body.

1.2.7 Regulations

As a leisure craft intended for the European market, the new A Rater must comply with the regulation of a classification society.

In this instance, the Recreational Craft Directive (RCD) [95] and the ISO standard [54] will be considered. The main reason for choosing the ISO standard is the ability for the builder to self-certify any category C or D yacht less than 12m long. As the A Rater falls under this category, the ISO standard will result in a simpler classification procedure.

The intended area of operation being inland waters, the vessel appears as a Category D, as defined in Table 2.

Design Category		Wave height (m)	Wind Speed (Bft)
A	Ocean	7+	8+ (40+ kts)
B	Offshore	4	8 (40 kts)
C	Inshore	2	6 (27 kts)
D	Inland	0.5	4 (16 kts)

Table 2: ISO design categories [95].

However, the boat will be designed as a Category C. This is primarily motivated by the extreme racing nature of the A Rater and the higher wind speed it can operate in. A Category C boat involves only minor upgrades compared to a Category D, and will induce additional reliability. Furthermore, as a Category C, the A Rater can operate as an inshore craft. The Norfolk Broads being located by the sea, this offers alternative sailing opportunities.

The implications of the regulation on the various aspects of the design and production will be highlighted throughout the report.

1.2.8 Conclusions

The design brief was laid out as accurately as possible by involving all the stakeholders concerned by the project in order to meet all possible requirements. The client provided the core of the specifications, then refined based on restrictions of the shipyard and intended area of operation, also taking into account sailors' feedback. Finally, the Thames A Rater class rule and the RCD/ISO standard have been considered.

The conception of a modern A Rater meeting the design brief can now be undertaken.

1.3 An Outline of the Project

1.3.1 Aims

The new design is intended to be the next generation of A Raters, and to be introduced to the Norfolk Broads. The aim is to provide a complete design, supported by a thorough conception process to achieve a competitive and aesthetically attractive yacht.

The ambition to realise a complete design therefore involves going through the four main stages of conception.

1.3.2 Design Process

1.3.2.1 Design Spiral

The conception of a yacht is generally characterized by the design spiral. Indeed, the process is iterative, and the initial assumptions are then replaced by educated guesses, followed by a more in-depth analysis, to eventually satisfy pre-established requirements. Each '*turn*' around the spiral then leads to a more refined version, until a satisfactory one is reached, at which stage a more detailed design is developed. Those various levels of depth and accuracy can be separated into four main phases.

1.3.2.2 Design Brief

As mentioned in Section 1.2, the design brief defines the intended use and operation of the yacht, as well as the demands from the different stakeholders.

1.3.2.3 Conceptual Design

This is primarily based on rule of thumbs and experience, and is largely speculative. The principal dimensions and overall layout are determined, as well as primary sketches.

1.3.2.4 Preliminary Design

At this stage, the design is definitive: the hull and inherent arrangements are fixed, and the yacht is checked against strict criteria, such as structural analysis and stability.

1.3.2.5 Detailed Design

The final phase of the project is strongly linked to production. All required drawings are produced, defining all the manufacturing details, leading to a bill of materials and inherent cost estimate.

1.3.2.6 Conclusions

The four main phases of the design undertaken are documented together with the overall schedule in the project planning to be found in Appendix A.

1.3.3 Areas of Investigation

As part of the project, the hull and appendages (centreplate and rudder) will be designed, as well as the sails, rig and the cockpit layout.

Structural analysis, weight and centres estimates and resulting stability assessment will be performed, and checked against the relevant regulatory body.

In order to optimise and evaluate the performance of the yacht, a velocity prediction program will be developed, thus concluding the preliminary design phase.

Finally, the detailed design will be undertaken, with production considerations, to accurately evaluate the schedule and associated costs. All drawings will be provided to illustrate the detailed design, which constitutes the finality of the project.

Chapter 2: Hull Design

Research has been conducted in order to meet the class rule requirement of the hull being an exact replica of an existing A Rater. From the original linesplan, the yacht has been redrawn and modelled in 3D. The one and a half inch tolerance allowed by the rule has also been exploited, with 20mm being dedicated to the modification of the hull. Based on the Delft Systematic Yacht Hull Series, parametric optimisation has been used to refine the hydrodynamics and decrease the resistance. The final modified A Rater has been adopted as the new boat.

2.1 Research

The main condition and priority for the new yacht to be considered an A Rater is to find the plans for an existing one. Initial investigations revealed that original linesplans for at least three boats are still in existence, held by either the Thames Sailing Club or owners. Unfortunately, none was made available for the purpose of this research. It is indeed understandable that the owner of a century old racing yacht may not want to share its design. The same reason justifies why lines could not be physically taken from an existing boat.

The research was therefore orientated towards openly available sources. The British Pathé Archives offers racing videos dating as early as 1923 [12]; while this is of historical importance and enables to identify the original rigs, there is no relevant design information that can be extracted. The databases of various maritime museums across the United-Kingdom were explored, but no mention of an A Rater was found. While articles relating the history of the Thames A Rater have been published [72, 73, 74], none provides any relevant information or reference. The closest design to an A Rater was found in the relatively widely available ninth edition of *Dixon Kemp's manual of yacht and boat sailing* [59] which contains the plans for the One-Rater *Sorceress*, designed by Linton Hope and illustrated in Figure 7.

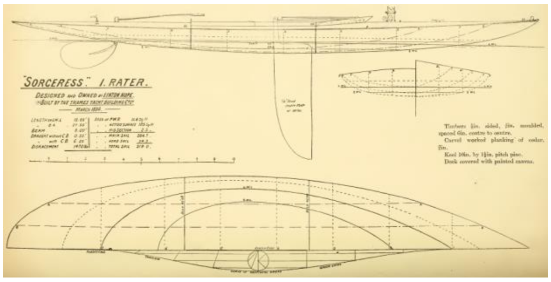

Figure 7: *L. Hope One-Rater Sorceress [59].*

As a One-Rater, *Sorceress* would have been considered an A Rater under the old class rule, defined as boats rating from 0.8 to 1. However, *Sorceress* does no match the current definition of an A Rater since it is not an existing one.

Further investigation revealed that an eleventh edition of *Dixon Kemp's manual of yacht and boat sailing* was published in 1913, after being reviewed and modified by Linton Hope, one of the main A Rater designers.

Given Hope's tendency to implement his publications with case studies of its own designs [49], the latest edition of the book was consulted. One of the very few remaining copies is held at the British Library in London, and did indeed contain the linesplan of an existing A Rater, still racing nowadays: *Scamp*.

Ideally, various designs would have been compared and the best one would have been selected; regrettably, despite further research, no other one appeared to be publicly available.

2.2 Modelling Scamp

2.2.1 Introduction

Designed in 1902, *Scamp* has always been a successful boat, and being one of the original Thames A Rater, it qualifies as an exact replica of an existing A Rater as defined by the class rule and will therefore be adopted as the hull for the purpose of this project.

2.2.2 Taking the Lines

When dealing with one of the last drawings of an historic boat, the priority is to ensure the integrity of the document and avoid any form of damage to it. With this is mind, the state of the art facilities available at the British Library have been utilised to obtain a digital copy of the linesplan, the result is shown in Figure 8.

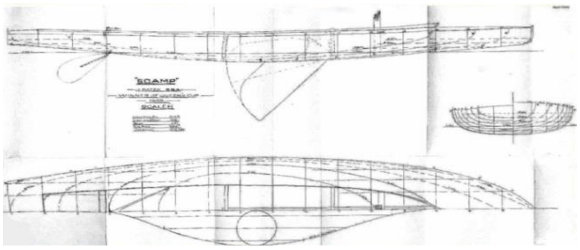

Figure 8: *Original linesplan of Scamp (1902) [60].*

Unfortunately, the folds on the paper, coupled with deformation due to aging and the will not to risk any damage to the document led to a slightly deformed drawing. While it constitutes a good graphical representation, it does not allow for an accurate enough modelling of the boat. As a result, the lines were manually taken off by physical measurements of all the offsets to the closest 1/64th of an inch, i.e. an accuracy of ±1/128th of an inch.

2.2.3 2D Drawing

2.2.3.1 2D Lofting

The table of offsets realised was then scaled up to full size, converted from imperial to metric, and numerically lofted using Computer Aided Design (CAD). The drawing of the boat was mostly focussed on the body plan. Indeed, since the body plan was drawn over a small area, it has been less affected by distortion and aging of the paper compared to the half-breadth and profile view extending the full length of the plan. This process enabled a redraw of the 2D linesplan, ensuring an exact replica is achieved, as shown in Figure 9 and further detailed in Drawing 01.

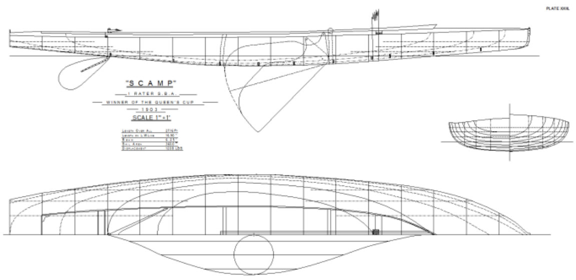

Figure 9: *Replica of the Scamp linesplan.*

Note that this linesplan is an exact replica of the original one, reproducing every detail, even where discrepancies have been noticed, as it is the case with the centreboard.

2.2.3.2 Design Discrepancy

The linesplan of *Scamp* offers two illustrations of the centreboard: one lowered under the hull (centreboard 1), and one retracted inside (centreboard 2). Careful analysis of the drawing revealed that those two centreboards are clearly not identical, as illustrated in Figure 10.

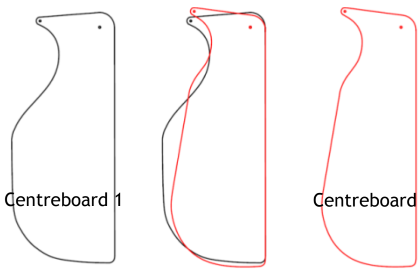

Figure 10: *Centreboards discrepancy.*

This difference is too extreme to simply result from a deformation of the plan, and is assumed to be a drawing error. Whilst it is impossible to know for sure which one is the intended planform and which one is the mistake, two arguments would suggest that centreboard 1 is the original design.

First, centreboard 1 is drawn as a solid thick line in the lowered position, where the centreboard is to operate. Conversely, centreboard 2 is a thin dotted line that would typically be drawn as a rotation of the lower one, and therefore prone to a drawing mistake.

In addition, the choice of the appendages area was often taken as a percentage of the sail area; an approach still employed by many designers today.

Centreboard 1 represents 2.30% of the sail area, which gives a total 3.00% when added to the rudder area, both round numbers suggesting they are the intended proportions. Conversely, centreboard 2 has an area equal to 2.12% of the sail area, as summarised in Table 3.

Appendage	Area (m²)	% of Sail Area
Centreboard 1	0.76	2.30%
Centreboard 2	0.70	2.12%
Rudder	0.23	0.70%

Table 3: *Appendage areas.*

There is therefore evidence to suggest Centreboard 1 is the intended planform. However, at this stage, only the hull will be considered since the appendages will undergo an advanced design process to be found in Chapter 3.

2.2.4 3D Modelling

Scamp has been modelled in 3 dimensions thanks to the Rhinoceros 3D [97] software; the process is very similar to the one of traditional boatbuilding. First, the stations are positioned along the length of the craft; a surface is then lofted along those stations with a specified accuracy of 0.01 mm. The process is depicted in Figure 11.

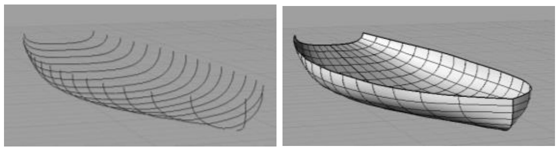

Figure 11: *3D modelling of Scamp.*

The hull surface is then exported as an initial graphics exchange specification (IGES) file, and imported into Maxsurf [9] for the hydrostatic analysis.

2.3 Hydrostatics

The Maxsurf model has been used to compare the hydrostatics with those determined from the replica of the 2D linesplan. The results in Table 4 reveal a very accurate modelling, with an average 0.46% difference.

Parameter	Linesplan	3D Model	Diff.	Diff. (%)
LOA (m)	8.28	8.28	0.000	0.00%
Lwl (m)	5.15	5.17	0.019	0.37%
BOA (m)	1.9	1.9	0.000	0.00%
Bwl (m)	1.66	1.64	-0.020	-1.20%
Tc (m)	0.16	0.16	-0.002	-1.25%
F (m)	0.31	0.31	0.000	0.00%
Disp. (m^3)	0.548	0.545	-0.003	0.00%
Awp (m²)	6.58	6.60	0.020	0.30%
LCB (m)	2.84	2.80	-0.043	-1.53%
LCF (m)	2.81	2.78	-0.033	-1.16%
Cb	0.40	0.40	-0.003	-0.71%
Cp	0.59	0.59	-0.006	-1.04%
Cm	0.68	0.68	0.002	0.34%

Table 4: *Hydrostatics comparison.*

An exact replica of *Scamp* has therefore been achieved, thus complying with the class rule, which does allow a one and a half inches (31.8mm) building tolerance. The high standard of craftsmanship that can be expected from the IBTC where the boat will be built means that part of that tolerance can be utilised to modify and improve the hull design while still meeting the rule.

2.4 Design Tolerance

2.4.1 Introduction

In order to establish how much of the tolerance can be used to modify the design, the accuracy lost in modelling the hull from the original linesplan must be evaluated, and building tolerances must be estimated.

2.4.2 Modelling Accuracy

By taking the lines off, the accuracy was maximised compared to simply drawing over the top of the linesplan that has been distorted over time. As a result, the replica of the linesplan can be considered as accurate as the measurement tolerance, i.e. 1/128th of an inch (0.20mm), which translates into 1/128th of a foot (2.38mm) full size. To this must be added the Rhinoceros 3D modelling accuracy of 0.01mm, giving a total uncertainty of 2.39 mm.

2.4.3 Building Tolerance

While a high standard of manufacturing can be expected, it is important to allow for building inaccuracies, such as the lofting of the station moulds, the natural expansions and contractions of the wood, and the possibility of a slightly wrong measurement or human error. An overall margin of 3/8th inch (9.53mm) has therefore been allocated to the construction, leaving 19.88mm to modify the hull shape. This value has been rounded up to 20mm, thus decreasing the building tolerance to 9.41mm.

2.4.4 Design Tolerance

The 20mm margin offers an opportunity to improve the hull design. It is to be noted that, while the overall one and a half inch tolerance will be respected, it is in practice quite hard to enforce this aspect of the class rule. Indeed, while some physical dimensions such as the length and breadth of the boat can physically be measured, a change in curve in the middle of a section cannot however be clearly identified.

This is supported by the International Towing Tank Conference (ITTC) standard for towing tank models manufacturing [52], where a tolerance is allowed for the length, breadth and depth of the model, while other deviations of the hull shape from the intended geometry are neglected due to the impracticalities of comparing the two.

2.5 Resistance (DSYHS)

The 20mm allocated to design modification will aim at improving the hull shape by reducing its resistance thanks to parametric optimisation based on the Delft Systematic Yacht Hull Series (DSYHS) [63].

The DSYHS offers regression equations (fully detailed in Section 10.2.3) that enable to assess the resistance of yacht from its principal dimensions. The two main drag components of an upright bare hull are namely the frictional and the residuary resistance.

At low Froude numbers (slow speeds), the frictional resistance is the major component, and is dependent on the wetted surface area of the hull (and inherent roughness). At higher Froude numbers, the residuary resistance becomes the primary drag component. In this instance, efforts have been focussed on decreasing the resistance at high Froude number since it would have the most significant impact. The upright hull residuary resistance Rrh is given by [63]:

$$\frac{Rrh}{\nabla c \times \rho \times g} = a_0 + \left(a_1 \times \frac{LCB_{fpp}}{Lwl} + a_2 \times Cp + a_3 \times \frac{\nabla c^{2/3}}{Aw} + a_4 \times \frac{Bwl}{Lwl} + a_5 \times \frac{LCB_{fpp}}{LCF_{fpp}} + a_6 \times \frac{Bwl}{Tc} + a_7 \times Cm \right) \times \frac{\nabla c^{1/3}}{Lwl} \quad \textit{Eq. 2}$$

In which:

Rrh	Residuary resistance.	N
∇c	Canoe body displacement.	m^3
ρ	Water density.	$kg.m^{-3}$
g	Acceleration due to gravity.	$m.s^{-2}$
LCB_{fpp}	LCB location from the FPP.	m
Lwl	Waterline length.	m
Cp	Prismatic coefficient.	-
Aw	Waterplane area.	m^2
Bwl	Waterline beam.	m
LCF_{fpp}	LCF location from the FPP.	m
Tc	Canoe body draft.	m
Cm	Midship area coefficient.	-
a_0 to a_7	Regression coefficients.	-

Thanks to the DSYHS, the most influent parameters on the resistance can be identified. It is to be noted that the regression coefficients (a_0 to a_7 in Eq. 2) have a varying influence between displacement mode and semi-displacement mode; the sailing regime transition has been identified at a Froude number of 0.45 [96].

The hull of the original *Scamp* has therefore been modified based on parametric optimisation to reduce the resistance at higher Froude number. The objective was reached with an average 3% reduction in overall resistance in a fully loaded condition replicating the sailing displacement past a Froude number of 0.45, as illustrated in Figure 12.

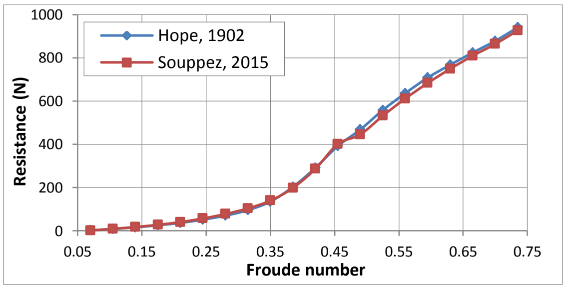

Figure 12: *Resistance comparison.*

The reduction is clearly visible with the sudden discontinuity in the resistance curve occurring at a Froude number of 0.45.

2.6 Modified Scamp

The main modifications realised using the 20mm margin include an extended overall length and breadth, to respectively increase the Froude number and form stability. The angle of the bottom of the boat with the waterline being so acute, a 20mm increase in overall length resulted in an impressive 160mm increase in waterline length. The draft has been shortened to provide a shallower and flatter craft; effectively increasing the values of the midship and prismatic coefficient, desirable for the purpose of the parametric optimisation. Furthermore, the LCB was shifted forward as much as possible within the design tolerance. The modifications induced a 6% increase in wetted surface area, which implies a slight increase in frictional drag, largely over-compensated by the resistance reduction at higher Froude number. The comparison between the original Hope design and the modified one is summarized in Table 5.

Measurement	Hope	Souppez	Diff. (%)
Length over all (m)	8.28	8.30	0.24%
Length on waterline (m)	5.46	5.62	2.93%
Beam over all (m)	1.90	1.92	1.05%
Beam on waterline (m)	1.67	1.70	1.80%
Canoe body draft (m)	0.185	0.166	-10.27%
Displacement (m^3)	0.652	0.652	0.00%
Midship coefficient	0.734	0.762	3.81%
Prismatic coefficient	0.528	0.546	3.41%
Wetted surface area (m^2)	7.112	7.552	6.19%
Waterplane area (m^2)	6.887	7.330	6.43%

Table 5: *Original and new Scamp design comparison.*

Furthermore, the tendency for yachts to experience an increase in waterline length and decrease in wetted area when heeling has been accentuated in order to offer a decreased frictional resistance and lower Froude number when sailing at angle of heel. Those behaviours are highlighted in Figure 13.

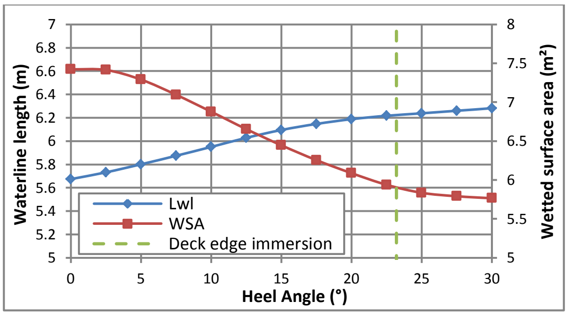

Figure 13: *Lwl and WSA evolution with heel.*

The final hull design is to be found in Drawing 02.

2.7 Conclusions

The original linesplan of an existing Thames A Rater has been considered for the new design, thus complying with the class rule. *Scamp* was accurately redrawn in 2D and then converted to 3D to verify the hydrostatics of the yacht.

By accounting for the modelling uncertainties and estimating the building margins required, a 20mm tolerance has been employed to improve the hull shape.

Thanks to parametric optimisation, the resistance at high Froude numbers was reduced by 3%, and enhancements in terms of hydrostatics and stability have been achieved, giving the final hull design for the new A Rater.

No further work has been conducted on refining the hull with other methods, such as computational fluid dynamics (CFD). Indeed, a large amount of time would be required to only provide very minor improvements. Instead, the work has been focussed on the appendages design: since the centreplate and rudder do not have to be replicas, they offer a great opportunity to elaborate the hydrodynamics and will concentrate the majority of the implementation efforts.

Chapter 3: Appendages Design

While the hull shape is restricted by the Thames A Rater class rule to being a replica, the appendages are not. As a result, significant improvements can be made. This justifies the larger amount of time dedicated to the appendages design and the use of more advanced resources, namely computational fluid dynamics (CFD). The CFD analysis will first of all be described and detailed, before being applied to the centreplate and rudder respectively, aiming to improve the lift/drag ratio of both foils by comparing a range of planforms.

3.1 Computational Fluid Dynamics

3.1.1 Modelling and Simplifications

At this stage, CFD has been employed to provide an initial comparison of a range of planforms for both the centreplate and rudder. The modelling has been heavily simplified: the presence of the hull and free surface and inherent impact on the appendages has been neglected. The appendage tested is therefore modelled alone in a domain of water. This is motivated by the restricted computational power available: 7 central processing units (CPU) at 1.73 GHz and 6.00 Go of random access memory (RAM). All simulations have been performed with Ansys CFX [4], a Reynolds-Averaged Navier-Stokes Equations (RANSE) solver, due to the availability of the software.

Since the structural and manufacturing constraints are not known at this stage, the appendages have been treated as thin flat plates. Indeed, the actual section will have to consider the structural requirements (in terms of section modulus, thus dictating the thickness/chord ratio), and the manufacturing capabilities (whether a NACA section can be accurately made or not).

3.1.2 Governing Equations

The steady state analysis performed is to satisfy both the continuity (conservation of mass) and the momentum (conservation of linear momentum) equations, respectively given by:

$$\nabla.(\rho\langle u_k\rangle) = 0 \qquad \textit{Eq. 3}$$

And:

$$\nabla.(\rho\langle u_k\rangle\langle u_k\rangle) = -\nabla\langle p\rangle + \nabla.\overline{\tau_k} + \rho\vec{g} \qquad \textit{Eq. 4}$$

Where:

$$\overline{\tau_k} = \mu_{eff}\left(\nabla\langle u_k\rangle + (\nabla\langle u_k\rangle)^T - \frac{2}{3}\mu_{eff}\nabla.\langle u_k\rangle I\right) \qquad \textit{Eq. 5}$$

The k-ε turbulence model [76] has been chosen as it is an industry standard and has been extensively studied [106]. For the purpose of this analysis, a typical turbulence intensity I_T of 5% has been considered. The model is governed by two equations, the turbulence kinetic energy and energy dissipation rate:

$$\nabla.((\langle u_k\rangle\rho k) = \nabla.\left[\left(\mu + \frac{\mu_t}{\sigma_k}\right)\nabla.k\right] + G_k \qquad \textit{Eq. 6}$$

And:

$$\frac{\partial(\rho\varepsilon\langle u_k\rangle)}{\partial x_k} = \frac{\partial}{\partial x_k}\left(\left(\mu + \frac{\mu_t}{\sigma_k}\right)\frac{\partial\varepsilon}{x_k}\right) + C_{\varepsilon 1}\frac{\varepsilon}{k}G_k - C_{\varepsilon 2}\frac{\varepsilon^2}{k} \qquad \textit{Eq. 7}$$

Where:

$$G_k = \tau_{ik}\frac{\partial\langle u_i\rangle}{\partial x_k} \qquad \sigma_k = 1.00$$

$$\sigma_\varepsilon = 1.3$$

$$\nu_T = C_\mu\frac{k^2}{\varepsilon} \qquad C_{\varepsilon 1} = 1.44$$

$$C_\mu = 0.09 \qquad C_{\varepsilon 2} = 1.92$$

3.1.3 Domain Size

The domain size, normally expressed in terms of boat length L has been kept as small as possible to minimise computation time. The dimensions are: 2L long (0.5L upstream, 1.5L downstream), 0.5L wide, and 0.5L deep. Investigations into wider domains proved not to impact on the results, suggesting that the selected domain is wide enough to avoid blockage issues.

3.1.4 Meshing

3.1.4.1 Mesh

Meshing was performed using an unstructured mesh, easier and faster to create and better suited to flow around appendages than a structured mesh [107]. In addition, inflation layers have been built around the surface of the appendage to better capture the boundary layer and inherent viscous components. A typical cross section through the domain is illustrated in Figure 14.

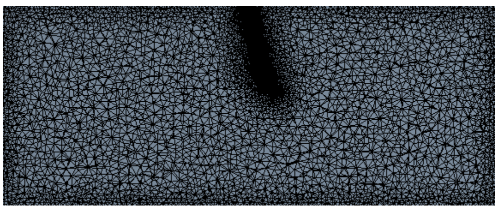

Figure 14: Cross section through the meshed domain.

3.1.4.2 Convergence

To maximise accuracy while minimizing computational resources, a mesh convergence study and error estimation have been conducted; results are shown in Figure 15.

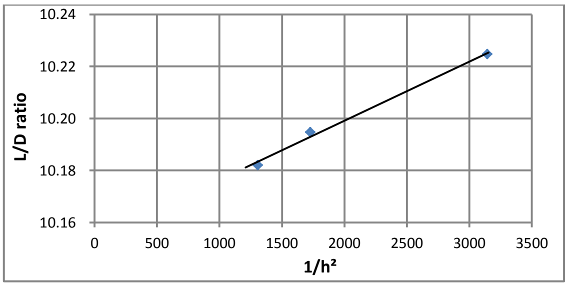

Figure 15: *Convergence study.*

The results reveal the second order nature of the solver (straight line achieved for 1/h²), and suggest that the region of monolithic convergence has been reached. The mesh is therefore fine enough.

3.1.4.3 Error Estimation

The discretization error and grid convergence index (GCI) have been evaluated following the Richardson extrapolation procedure and the Roach and Celik error estimation, both discussed in [21].

The grid size h is calculated for 3 meshes (fine h_1, medium h_2 and coarse h_3, where $h_1 < h_2 < h_3$), using:

$$h = \left[\frac{1}{N}\sum_{i=1}^{N}(\Delta V_i)\right]^{\frac{1}{3}} \qquad \textbf{\textit{Eq. 8}}$$

In which:

h	Grid size.	m
N	Number of elements.	-
ΔV_i	Volume of the i^{th} cell.	m³

The grid refinement factor r, to be higher than 1.3, is:

$$r_{21} = \frac{h_2}{h_1} \qquad \textbf{\textit{Eq. 9}}$$

In which:

r_{21}	Grid refinement factor.	-
h_2	Medium grid size.	m
h_1	Fine grid size.	m

And the apparent order p is:

$$p = \frac{1}{\ln(r_{21})}\left|ln\left|\frac{\varepsilon_{32}}{\varepsilon_{21}}\right| + ln\left|\frac{r_{21}^p - s}{r_{32}^p - s}\right|\right| \qquad \textbf{\textit{Eq. 10}}$$

In which:

p	Apparent order.	-
r_{21}	Fine grid refinement factor.	-
ε_{32}	$= f_3 - f_1$	N
ε_{21}	$= f_2 - f_1$	N
f_k	Solution on the k^{th} grid.	N
r_{32}	Medium grid refinement factor.	-
s	$= 1 \cdot sign\left(\frac{\varepsilon_{32}}{\varepsilon_{21}}\right)$	-

The extrapolated solution f_{ext}^{21}, based on the solutions f_k for the different grid sizes, is given by:

$$f_{ext}^{21} = \frac{r_{21}^p f_1 - f_2}{r_{21}^p - 1} \qquad \textbf{\textit{Eq. 11}}$$

In which:

f_{ext}^{21}	Extrapolated solution.	N
r_{21}	Fine grid refinement factor.	-
p	Apparent order.	-
f_k	Solution on the k^{th} grid.	N

The approximate relative error e_a^{21} can be found:

$$e_a^{21} = \left|\frac{f_1 - f_2}{f_1}\right| \qquad \textbf{\textit{Eq. 12}}$$

In which:

e_a^{21}	Approximate relative error.	%
f_k	Solution on the k^{th} grid.	N

As well as the extrapolated relative error e_{ext}^{21}:

$$e_{ext}^{21} = \left|\frac{f_{ext}^{21} - f_1}{f_{ext}^{21}}\right| \qquad \textbf{\textit{Eq. 13}}$$

In which:

e_{ext}^{21}	Extrapolated relative error.	%
f_{ext}^{21}	Extrapolated solution.	N
f_1	Solution on the fine grid.	N

Finally, considering a factor of safety Fs of 1.25 (justified by the three grids modelled [21]); the grid convergence index GCI is assessed:

$$GCI^{21} = \frac{Fs \times |e_a^{21}|}{r_{21}^p - 1} \qquad \textbf{\textit{Eq. 14}}$$

In which:

GCI^{21}	Grid convergence index.	%
Fs	Factor of safety.	-
e_a^{21}	Approximate relative error.	%
r_{21}	Fine grid refinement factor.	-
p	Apparent order.	-

The results are summarized in Table 6.

Discretization Error Results						
r_{21}	r_{32}	p	F^{12}_{ext}	e^{21}_a	e^{21}_{ext}	GCI^{21}
1.35	1.35	2.58	10.25	0.29%	0.25%	0.32%

Table 6: *Discretization error.*

The negligible errors demonstrate the level of accuracy achieved with the finer mesh; no further refinement appears to be necessary. Indeed, a finer mesh would only negligibly increase the accuracy, but induce a tremendous increment in solving time.

3.1.5 Boundary Conditions

The boundary conditions specified in the domain are described in Table 7.

Boundary	Applied Condition
Upstream end	Inlet, specified U velocity.
Downstream end	Outlet, specified U velocity
Surrounding walls	No slip, smooth walls, U velocity
Centreplate	No slip, smooth wall, stationary.

Table 7: *Boundary conditions.*

3.1.6 Solving Time

In order to perform the calculations as efficiently as possible, an investigation into the optimum run mode has been conducted; the results based on 5 iterations are introduced in Figure 16.

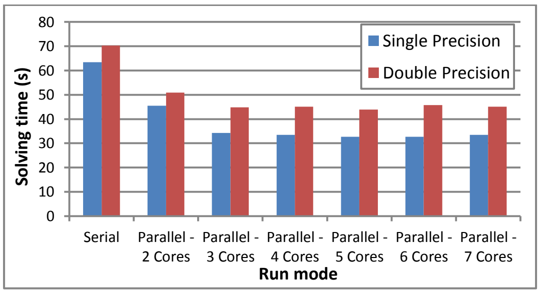

Figure 16: Solving time comparison.

Past 3 cores, there is no more significant decrease in solving time. As a result, the 3 cores configuration with double precision will be used throughout the analysis. Indeed, single precision did not prove to be sufficient to achieve convergence, with characteristic round-up errors occurring. Double precision enabled to reach the desired convergence of RMS residuals decreasing down to 10^{-6}.

Investigation into speedup and efficiency revealed that linear speedup was not achieved, presumably due to communication overhead and sequential components to the program. The speedup behaviour was determined to be approximately 50% according to Amdahl's law [1].

3.1.7 Results

The lift and drag coefficient and inherent lift/drag ratio proved to be very similar to theoretical [117] and experimental [70] data for a tapered appendage of similar aspect ratio, thus validating the analysis conducted. However, no strict benchmark could be found (wind tunnel tested appendage for instance), further validation of the CFD analysis could therefore be performed. Finally, post-processing revealed very satisfactory streamlines, highlighting the characteristic '*horse shoe*' vortex at the tip.

3.1.8 Conclusions

In order to provide initial comparison between a range of planforms using a RANSE solver, the problem had to be simplified due to the limited computational resources available. The method presented and validated in the section will be applied to the centreboard and rudder design, respectively tackled in Section 3.2 and Section 3.3.

3.2 Centreboard

3.2.1 Area

The planform area can lead to a large loss of performance if too little or too much is provided, respectively resulting in high leeway angle and added frictional resistance. The area is generally expressed as a percentage of the sail area.

One option could be to keep the original design area (2.30%). Alternatively, an empirical estimate can be calculated [119]:

$$\frac{KA}{SA} = 0.039 \times \frac{Tk}{LOA} + C \qquad \textbf{Eq. 15}$$

In which:

KA/SA	Keel/sail area ratio.	%
Tk	Keel draft.	m
LOA	Length overall.	m
C	0.018 for racing yachts.	-

This method would advise a 2.51% ratio.

Finally, a more advanced method developed by the author [105] and based on the area required when coming out of a tack in light winds has been applied. A keel area of 2.27% of the sail area has been ascertained, i.e. very close to the original 2.30%. The later value has therefore been conserved.

Having established the keel area (2.30% or 0.76m²), and remembering the draft restriction mentioned in Section 1.2.4, a range of possible designs will be investigated. Indeed, the class rule does not specify that the appendages have to be replicas of the original, thus allowing hydrodynamic improvements.

3.2.2 Profile

3.2.2.1 Designs

A range of 10 possible planforms will be investigated based on the setup suggested in Section 3.1. The centreboards, illustrated in Figure 17, are briefly described in Table 8.

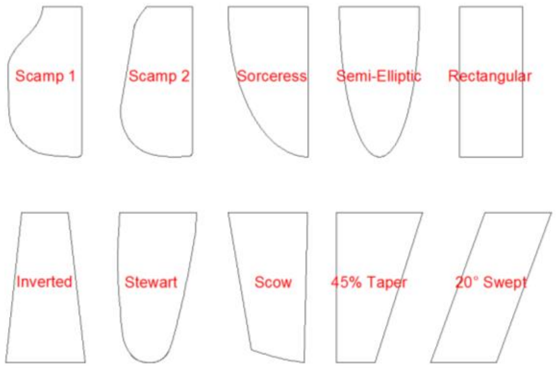

Figure 17: Centreboard designs investigated.

Design	Characteristics
Scamp 1	Original Scamp centreboard [60].
Scamp 2	Misdrawn centreboard (see 2.1.2.2) [60].
Sorceress	L. Hope design for Sorceress [59].
Semi-Elliptic	Elliptical loading (cf. Spitfire wings).
Rectangular	Easiest to manufacture.
Inverted	Increased ballast lever (cf. Australia II).
Stewart	Stewart modern A Rater design [110].
Scow	Found on modern scows (cf. E-Scow).
45% Taper	Hydrodynamic optimum taper ratio [75]
20° Swept	Popular dinghy design [75].

Table 8: Centreboard designs.

The analysis has been performed at 15° of heel and 5° of leeway, for speeds of 1, 2, 3, 4 and 5 m/s, representative of typical sailing conditions.

3.2.2.2 Results

The delta in lift/drag ratio L/D compared to the original centreboard (Scamp 1), are depicted in Figure 18.

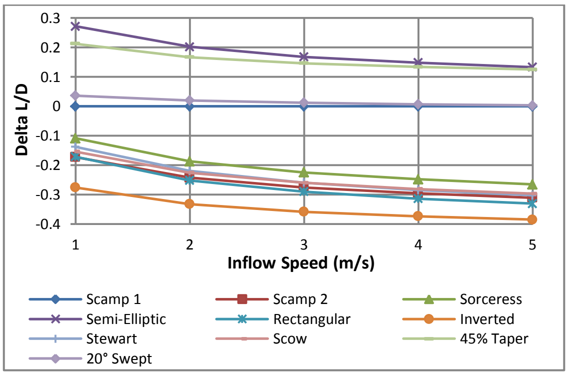

Figure 18: *Centreplates delta in Lift/Drag ratio.*

First of all, it is to be noted that the overall design ranking is as expected: the semi-elliptic and 45% taper ratio, both promoting elliptical spanwise loading, proved to be the most efficient, especially at low speeds. The better hydrodynamic performance of the semi-elliptic centreboard constitutes a 1.8% improvement in terms of lift/drag ratio compared to the original.

3.2.2.3 Streamlines

In addition to the improved lift/drag ratio, the semi-elliptic centreboard offers a large reduction in tip vortex which contrasts with the original, as shown in Figure 19.

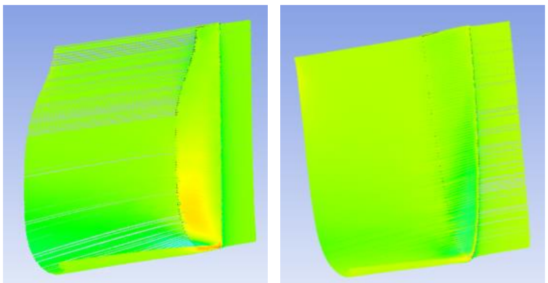

Figure 19: *Original (left) and new (right) centreplate.*

3.2.2.4 Conclusions

Based on the hydrodynamic analysis, the semi-elliptic centreboard appears to be the most efficient, and will therefore be the proposed design. In addition, due to its geometrical properties, the centreplate offers one of the smallest lever for its centre of lateral resistance (CLR), thus decreasing the heeling arm, contributing to an improved stability.

3.2.3 Section

The foil section of yachts are generally NACA 00 series, due to their better hydrodynamic performance, with a higher lift/drag ratio and a delayed stall angle compared to NACA 63, 64, and 65 series. A closer analysis revealed further advantages of the NACA 00 series.

Indeed, as detailed in Table 9, the NACA 00 series has the highest sectional area coefficient. Consequently, the ballast/WSA ratio will be the highest, meaning a lower wetted area and frictional resistance for a given volume.

Moreover, the section modulus/WSA ratio is also the highest, meaning that for a given structural requirement, a NACA 00 will have a lower wetted area and friction resistance.

Section	Area Coeff.	Ballast/WSA	SM_T/WSA
NACA 0012	0.676	100%	100%
NACA 63 012	0.659	97.65%	95.19%
NACA 64 012	0.628	92.90%	86.30%
NACA 65 012	0.644	95.29%	90.79%

Table 9: *NACA series comparison.*

At this stage, the thickness/chord ratio is still undecided as it is primarily driven by the structural constraints that will be tackled in Section 7.3.

3.2.4 Conclusions

CFD was employed to select the optimum hydrodynamic design in terms of lift/drag ratio, also contributing to reduce the heeling arm. While a NACA 00 section has been chosen, the thickness/chord ratio is still to be defined based on the structural analysis.

3.3 Rudder

3.3.1 Area

As per the centreboard, the rudder area is generally expressed as a ratio of the sail area. For small yachts, 1.5% is usually advised [75]. This value however appears to be excessive for the A Rater, having less than half the area suggested. Studying the appendages of *Sorceress* and *Scamp*, designed a decade apart by Linton Hope showed that both the rudder and centreboard areas have been decreased for the latest A Rater, revealing that only a minimum area is required. As a result, the original rudder area of $0.23m^2$, or 0.70% of the sail area, will be kept. The rudder planform will however be redesigned.

3.3.2 Profile

3.3.2.1 Designs

Using the same CFD approach as for the centreplate, various rudder planforms will be investigated; aiming at increasing the rudder aspect ratio to improve the hydrodynamic performances. The 10 designs are introduced in Table 10 and depicted in Figure 20.

Design	Characteristics
Scamp	Original Scamp rudder [60]
Sorceress	L. Hope design for Sorceress [59].
Stewart	Stewart modern A Rater design [110].
Scow	Found on modern scows (cf. E-Scow).
Rectangular	Easiest to manufacture
1/4 Ellipse	Popular hydrodynamic design [75].
Semi-Elliptic	Elliptical spanwise loading.
Straight 1/4 Chord	Popular hydrodynamic design [75].
Jeffa	Typical modern cruiser/racer design.
IMOCA	Typical modern fast racing design.

Table 10: *Rudder designs.*

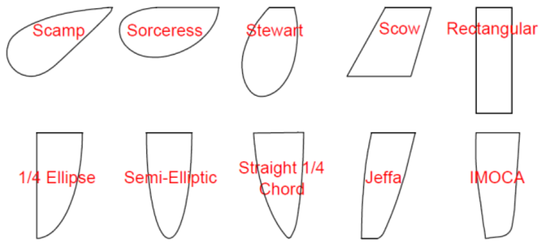

Figure 20: *Rudder designs investigated.*

3.3.2.2 Results

The analysis has been performed at 15° of heel and 5° of leeway, for speeds of 1, 2, 3, 4 and 5 m/s. The differences in lift/drag ratio compared to the original rudder (Scamp) are shown in Figure 21.

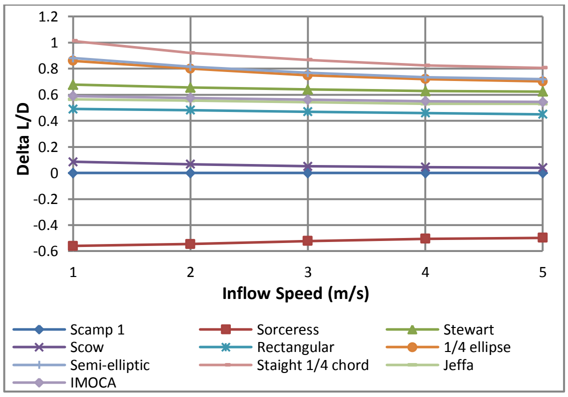

Figure 21: *Rudders delta in Lift/Drag ratio.*

The straight ¼ chord rudder appears to provide more lift and less drag than the other planforms tested, and led to a 10.5% improvement. Those results are supported by tests realised for a rudder angle of 15° (close to stall), where the straight ¼ chord also proved to be the most efficient.

3.3.2.3 Streamlines

The straight ¼ chord rudder provides a significant decrease in tip vortex compared to the original *Scamp* rudder, thanks to a more elliptical distribution of the pressure, as depicted in Figure 22.

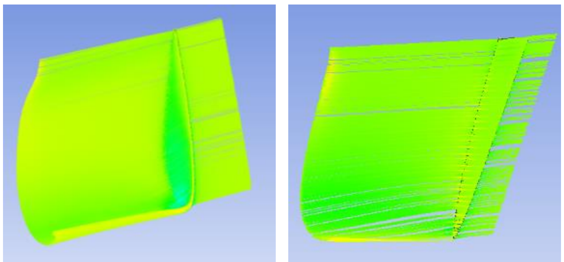

Figure 22: *Original (left) and new (right) rudder.*

3.3.2.3 Conclusions

The CFD analysis conducted on potential rudder planforms recognised the straight ¼ chord as the most suited design, which will therefore be the new rudder.

3.3.3 Section

A NACA 00 series will be selected (as justified in Section 3.2.3), the higher stall angle compared to other NACA series being of primary importance. Rudders are commonly NACA 0012: a thinner foil would have less drag but a lower stall angle. Conversely, a thicker foil would delay stall, but increase the drag. A 12% thickness/chord ratio is often seen as the best compromise, with however three additional factors to take into account.

First of all, the thickness of a rudder is primarily dictated by the need to accommodate the rudder stock inside. The rudders of original A Raters are flat metal plates, to which the rudder stock is welded on the outside. This configuration, while very practical to construct, is not efficient in terms of hydrodynamics, hence the choice of a NACA foil section for the rudder, with an inner rudder stock. At this stage, a preliminary estimate of the stock diameter relying on the American Bureau of Shipping regulation [2], chosen for its simplicity, revealed that a minimum thickness/chord ratio of 9% is necessary. The intended 12% is therefore structurally viable.

Secondly, manufacturing must be taken into account; the complexity of building an accurate NACA section and fitting the rudder stock must not be neglected.

Finally, the impact of the stall angle on performance must be established. Previous work undertaken on the Stewart 34 class [108] reveal that the performance of the yachts in high winds was restricted by the rudder stalling, and the class has recently developed a new rudder design with a 20% thickness/chord ratio to remedy this issue. The velocity prediction program (VPP) that will be created for the A Rater in Chapter 10 will aim at identifying whether a similar issue is likely to occur.

3.3.4 Conclusions

Following a comparative CFD analysis, a straight ¼ chord line rudder configuration has been selected. The intended NACA 0012 section is structurally suitable, but is to be confirmed based respectively on the structural requirements, construction and performance prediction.

3.4 Conclusions

A basic CFD setup has be used to contrast a range of planforms for both the centreboard and rudder, aiming at a maximum lift developed for a minimum drag. The results showed tremendous improvements; a semi-elliptic planform was therefore chosen for the centreboard, while a straight ¼ chord proved to be the most efficient rudder. The new centreplate and rudder improved the lift/drag ratio by 1.8% and 10.5% respectively compared to the original designs. In terms of sections, a NACA 00 series is to be preferred and is advised at this stage. However, further considerations such as the structural and manufacturing requirements will have to be assessed before the final detailed design. Furthermore, the location of the appendages may change to achieve a better balance between the aerodynamic centre of effort of the sails and the hydrodynamic centre of lateral resistance of the appendages, discussed in Section 4.4. .

Chapter 4: Sails and Balance

The sails provide the propulsive power, and are therefore critical for a performance yacht. In the case of the A Raters, sails are available on the market, and should be preferred due to their much lower cost compared to custom made ones. However, to illustrate the principles, a set of sails will be designed for the new A Rater. Vortex Lattice Method (VLM) will be employed to optimise the shape and dimensions. The aerodynamic centre of effort and the hydrodynamic centre of lateral resistance will be estimated in order to achieve a reasonable lead so that the boat is balanced.

4.1 Preliminary Considerations

4.1.1 Definitions

Sail dimensions are described using the standard nomenclature [75] presented in Table 11.

Nomenclature	Dimension
I	Height of fore triangle
J	Base of fore triangle
P	Luff height of mainsail
E	Foot length of mainsail

Table 11: Sail nomenclature.

Furthermore, the sail aspect ratio is often prone to confusion, and needs to be properly defined. Indeed, the aspect ratio is not to be confused with the height/base ratio, given by P/E and I/J for the mainsail and jib respectively. The sail aspect ratio is based on the general definition of aspect ratio:

$$AR = \frac{b^2}{S} \qquad \textbf{Eq. 16}$$

In which:

AR	Sail aspect ratio.	-
b	Span.	m
S	Area.	m^2

This definition will be used throughout this chapter.

4.1.2 Class Rule

The main aspects of the Thames A Rater class rule [111] that impact on the sail plan are the number of sails, the maximum sail area, and the mast restrictions.

Firstly, only a mainsail and a jib are allowed by the rule (Rule E4 (a)), spinnakers being prohibited. As a result, only those two sails will be designed, the mainsail will however have reefing points introduced to meet the expectations of the client and sailors.

Secondly, the total sail area is restricted to a maximum of 350 square feet (Rule E4 (b)), or $32.51m^2$. The maximum allowed will be adopted to maximise light wind performance.

Finally, the mast height is restricted to 43 feet (13.11m) from the sheer (Rule E2 (a)), with the gooseneck no lower than 3 feet (0.91m) above sheer (Rule E2 (d)).

This gives a maximum main height P of 40 feet, or 12.19m, minus potential fittings to be taken into account at a more advanced stage of the design.

4.1.3 Operation

Most sails are aimed at maximising the velocity made good (VMG), because the yachts will mostly race at their optimum VMG angle. This results in a first design optimised for upwind, to which is then added a large asymmetric spinnaker that will maximise the downwind VMG. This is not applicable in the case of the A Raters.

On the one hand, no spinnaker is allowed, which greatly limits the downwind performance. On the other hand, the races occur in narrow inland waterways, a configuration that does not enable the boat to always race at its optimum VMG angle: the wind angle being primarily dictated by the orientation of the wind with respect to the waterway the yacht is sailing in. This calls for a more polyvalent sail plan, beyond the usual VMG targets.

4.2 Vortex Lattice Method

4.2.1 Introduction

Vortex Lattice Method (VLM) has been utilised for the aerodynamics of sails since the early days of computational fluid dynamics, and is still employed for top end racing yachts by the leading sail manufacturers.

4.2.2 Theory

VLM models the surface of the wing (or sail in this instance) by a vortex sheet on its surface, based on potential flow theory. Some of the assumptions made are the incompressible, inviscid and irrotational nature of the flow. Furthermore, the Kutta condition (flow leaving the trailing edge smoothly [86]) is enforced. The method analyses the sail forces such as lift and drag, and models the wake created, thus visualising the tip vortices.

4.2.3 Sail7

In this instance, VLM will not be used to quantify the performance of a sail plan, but to provide a qualitative comparison and help refine the design of the sails thanks to the Sail7 [100] code.

The code first underwent a similar procedure as described in Section 3.1, where a convergence study and error estimation are carried out to ensure its reliability, as well as validation against published data [115]. On completion of this procedure, the current A Rater sails available on the market have been modelled, as illustrated in Figure 23.

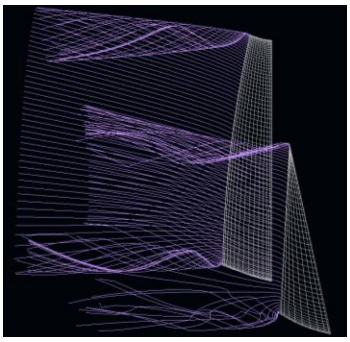

Figure 23: *A Rater sail plan modelled in Sail7 [100].*

The tip vortices appear clearly visible at both the head and foot of the mainsail and jib, leading to a lower efficiency of the sails. The new design will aim to diminish this phenomenon where possible.

4.3 Sail Plan

4.3.1 Rig Configuration

The current A Rater's fleet is based on a fractional rig type (as opposed to a masthead one); this configuration has been retained for its significant advantages.

On the one hand, a fractional rig allows a more flexible mast top, which can efficiently decrease the camber of the mainsail in high wind. This is particularly desirable considering the high sail area of the A Raters.

On the other hand, a fractional rig cuts down the structural constraints of the top of the mast which can therefore be tapered. As a result, a lighter mast is achieved and the weight saved has a very positive impact on lowering the centre of gravity.

4.3.2 Jib

4.3.2.1 Jib Design

In order to improve the aerodynamic performance of the jib, its aspect ratio has been increased from 6 to 6.78, which translated into a 4% increase in lift/drag ratio [85]. This has been realised by shortening the foot length and increasing the height of the jib along the forestay, also closing the gap between the jib and the main. Indeed, VLM demonstrated that the slot effect occurring between the main and the jib could be increased in this instance by bringing the jib leech closer to the mast.

But the main design change that will improve the jib performance is the flat foredeck. Indeed, the tip vortex occurring at the bottom of the jib due to the gap between the foot of the sail and deck results in a loss of performance. A mirror boundary effect can be obtained by sealing this gap, which artificially doubles the effective aspect ratio of the sail.

The will to achieve a mirror boundary effect has also been introduced in the America's Cup, where the mainsail now fits flush on the central platform, eliminating the gap. Note that the minimum height of the gooseneck 3 feet above sheerline prevents the use of this method for the A Rater.

A flat foredeck will however be adopted for the jib, and will also provide a safer environment for the foredeck crew to evolve on, which was one of the main sailors' expectations mentioned in 1.2.5.

By closing the gap between the jib and foredeck, the upwind performance will benefit from a 6% reduction in drag and a 4% increase in lift [75], as shown in Figure 24.

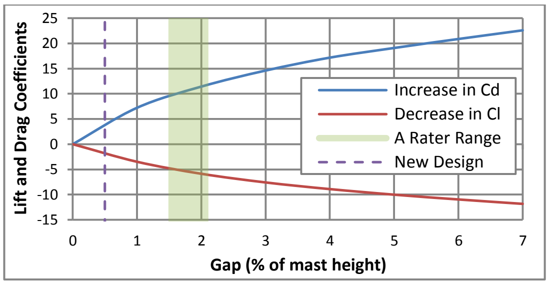

Figure 24: *Effect of gap between sail and deck [75].*

If the jib geometric aspect ratio was increased in the first place, and the effective aspect ratio then doubled thanks to the mirror boundary effect resulting from a flat foredeck, the mainsail follows a much different design philosophy, as later seen in Section 4.3.3.

4.3.2.2 Sheeting Angle

The position of the jib track defines the range of possible sail trims. Longitudinally, the jib track is positioned to be aligned with the clew and intersect the forestay at 40% of its height [94]. In terms of trim angle, 12° at the foot is usually preferred [116]. In this instance, the transversal jib track leads to foot trim angles varying from 8° to 19°, thus offering a wide range of sail trims.

4.3.3 Mainsail

4.3.3.1 Mainsail Design

First of all, the planform of the main must be chosen. Although an elliptical profile would help reduce the tip vortex, it must be remembered that the A Raters will race inland. The impact of the Earth boundary layer on the wind velocity gradient (see Figure 25) will therefore be quite severe, and maximising the sail area higher up, where the wind is stronger, appears to be a priority. This dictated the choice of a square top mainsail.

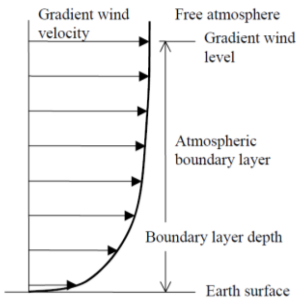

Figure 25: *Boundary layer and velocity profile [38].*

The second consideration is the aspect ratio. Conversely to the jib, a higher mainsail aspect ratio is not necessarily better. In fact, there is increasing evidence that overall, a main aspect ratio of 4.6 is optimum, due to mast interaction effects on high aspect ratio rigs [75, 81]. The square top main artificially decreases the aspect ratio (previously characterised in Eq. 16 as the span squared divided by the area). Furthermore, the sail foot length has been extended, while the boom was slightly raised.

Consequently, the main aspect ratio was deceased from 7.1 to 6.04. While this is still very far from the optimum aspect ratio, it constitutes a non-negligible improvement.

Finally, utilising the whole mast span available appears to be more important to maximise performance than achieving a lower aspect ratio by significantly reducing the mast height.

4.3.3.2 Reefs

The use of reefing points diminishes the sail area in higher wind speeds, where the full sail area could not be carried efficiently. Adding reefing points to the mainsail is among the requirements specified in Section 1.1. However, the proportions of the reefs will only be decided at a later stage, based on the velocity prediction program presented in Chapter 10, and detailed in Drawing 08.

4.3.4 Sail Shape

The shape of a sail is defined by a number of parameters, namely: the chord length, the depth of the camber (or '*belly*') as a percentage of the chord length, the location of maximum camber along the chord line, and the twist angle. Those parameters are set at various stations along the height of the sail.

In terms of belly, very little is provided at the bottom to minimise the tip vortex and induced drag. In the middle of the sail a fair amount leads to a powerful sail. Finally, a reasonable amount at the top maximises the power and makes the vertical load distribution closer to the ideal elliptical loading.

The twist on the other hand is higher as the height increases, thus preventing stall and minimising the induced drag by providing a smoother transition between the high lift in the middle of the sail and the zero lift at the very top. The twist in the sail is necessary due to the change in apparent wind velocity with height, resulting from the wind gradient previously introduced; this phenomenon is illustrated in Figure 26.

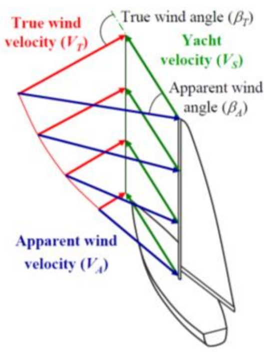

Figure 26: *Apparent wind angle twist [38].*

The sail shape was optimised using VLM to maximise the amount of lift while minimising the drag. Note that, in this instance, the shape analysed is the flying shape, which is the moulding shape deformed by the pressure of the wind. Further work into the required moulding shape to obtain the designed flying shape would be advised.

4.3.5 Sails Development

Once the sails profile and shape have been adopted, the sails must be developed, i.e. flat panels have to be designed so that once joined together the desired sail shape is achieved. Simple radial development has been performed with the SailCut software [101]; the results are to be found in Drawing 08.

4.3.6 Conclusions

Thanks to VLM, the design of the sails has been improved, leading to the principal dimensions given in Table 12.

Parameter	Dimension
Jib area (m^2)	9.30
Mainsail area (m^2)	23.21
Total sail area (m^2)	32.51
I (m)	7.95
J (m)	2.30
P (m)	11.75
E (m)	2.25
Jib aspect ratio	6.78
Mainsail aspect ratio	6.04

Table 12: *Sails dimensions.*

4.4 Balance

4.4.1 Balance

The balance is the equilibrium between the total hydrodynamic force acting at the centre of lateral resistance (CLR) of the underwater body, and the total aerodynamic force acting on the centre of effort (CE) of the sails. Note that good balance does not mean a perfect equilibrium where no rudder angle is needed; a slight weather helm is preferred. Indeed, a small amount of weather helm makes the yacht safe in gusts as it lifts up into the wind, thus depowering the sails. Furthermore, it provides a good feedback to the helmsman. Finally, weather helm means that the rudder side force acts with the centreplate side force and not against it (as it is the case for lee helm).

Balance is a particularly complex problem in yacht design, because neither the CLR nor the CE is known, and no theoretical solution has been found. The CLR and CE can only be located via towing tank and wind tunnel testing respectively, which is not economically viable for most projects. The problem is made harder with heel: the boat rotates about the fore-and-aft axis, but the aerodynamic and hydrodynamic forces do not act at right angles. The motion of the two centres therefore varies greatly with heel, and even more for wide and flat yachts such as the A Raters [75]. As a result, rule of thumbs have been developed to locate the CLR and CE, and define their relative position, known as the lead.

This is however not always accurate enough so room has been given so that the mast position can be modified after the first sea trials. It is not uncommon to have multiple possible mast positions to experimentally assess the best lead once the boat is built [116].

4.4.2 Centre of Lateral Resistance

Some of the methods available to estimate the CLR location include those of Nomoto [89] and Gerristma [30, 31], the later usually being preferred. Gerrtisma considers both the keel and rudder, those are however extended to the waterline (to artificially account for the hull effects), and the rudder contribution is multiplied by a factor of 0.4 (since it operates in the downwash of the keel, and the inflow speed and angle of attack are reduced). This method however has a tendency to predict the CLR too far aft, as it neglects the contribution of the hull forebody [75].

A simpler, yet more precise method consists in taking the CLR on the ¼ chord line, at 45% of the draft [75]. While the ¼ chord line is a good assumption, 45% of the draft is very dependent on the shape of the appendage. As a result, the CLR is better taken on the ¼ chord line at the depth of the geometrical centre of area of the foil [117]. This is the method that has been retained and employed.

4.4.3 Centre of Effort

The centre of effort of the sails is simply taken as the geometrical centre of area [75, 24]. This assumption has been experimentally proven valid for upright and small angles of heel [109], but is not suitable at larger heel angles. Furthermore, the leeward displacement of the CE is particularly extreme for high aspect ratio rigs, such as those found on the A Rater. While this cannot be accurately located without wind tunnel testing, it will be account for when deciding on the relative position of the CE and CLR, namely the lead.

4.4.4 Lead

The lead is expressed as a percentage of the waterline length, thus giving the distance by how much the CE must be forward of the CLR. For fractional sloops, the literature suggests a range from either 3 to 7% [75], and 5 to 7% [116].

Fossati [24] presents a correlation between the lead and the beam/length ratio (Bwl/Lwl) of the boat, the values ranging from 10 to 18% of the waterline. Those values appear to be quite large, which suggest they might be more suited to masthead rigs (requiring a larger lead) than the fractional rig of the A Raters.

In this case, the upper end value of 7% of the waterline has been selected. This is justified by the beamy design coupled with the high aspect ratio rig. Furthermore, should the lead prove to be unsuitable during sea trials, it is always easier to move the CE back (by raking the mast for instance), than bringing it forward. Consequently, greater lead values are seen as safer [116].

4.4.5 Conclusions

Relying on common empirical rule of thumbs, the CLR and CE have been located, and a 7% lead has been chosen. Note that the design will allow the mast position to be changed should the balance prove not to be satisfactory. This is also required since the commercially available rig and sails might be preferred for economic reasons: the yacht must therefore be able to accommodate a range of mast positions.

4.5 Conclusions

Vortex Lattice Method has been used to implement the design of the sails. The jib aspect ratio has been increased while the mainsail one has been decreased. In addition, a flat foredeck has been suggested to benefit from the mirror boundary effect of the jib upwind.

By defining the lead, the relative position of the rig and sails compared to the appendages has been fixed. Their absolute positions along the boat are however not known yet, and will be decided when performing the weight estimate so that the A Rater floats on its intended waterline.

The final sailplan is illustrated in Figure 27, and further detailed in Drawing 08.

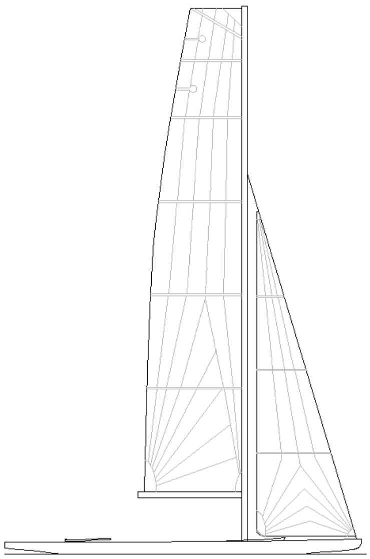

Figure 27: *Sailplan.*

Having designed the sails, the loads on the rig can now be calculated, leading to the development of a new rig.

Chapter 5: Rig

As per the sails, a rig package is available on the market, and will be more cost efficient compared to the tremendous expense of a custom made carbon fibre one. A new rig will however be proposed and the principles involved detailed. The Nordic Boat Standard (NBS) will be used as it is the only small craft regulation inherent to rig design. The aim is to achieve a rig as light as possible to minimise the rise in centre of gravity. Furthermore, the mast is not accounted for in the minimum displacement specified by the A Rater class rule; as a result, important weight savings can be realised.

5.1 Introduction

The design of rigs remains a very complex and specialised area, into which classification societies do not feel confident enough to publish standards. While Germanischer Lloyds (GL) provides guidelines for yacht larger than 24 m [28], the only current regulation applicable to small crafts is the Nordic Boat Standard (NBS) [90], dated 1990.

The long expected ISO standard inherent to sail loads and rig design (ISO 12215 – Part 10), has now been in development for over a decade, demonstrating the difficulties faced in this particular area. The NBS is therefore the only suitable standard applicable, and most mast manufacturer will either rely on this standard, or perform finite element analysis (FEA); the latter option being very pricy, and typically reserved to larger yachts and extreme offshore racing campaigns.

The main target will be to achieve a mast as light as possible. Indeed, feedback from the sailors highlighted the need for a light mast, particularly when lowering and raising the mast is required. Then, the lighter the mast the minimum the inherent rise in VGC is, thus improving the stability of the yacht. Finally, the minimum lightship displacement imposed by the class rule (Rule D5) does not include the mast and rigging, which makes it a critical component where weight savings can be performed.

The rig will therefore be design according to the NBS [90]; the underpinning theory will first be presented, and then applied.

5.2 Nordic Boat Standard

5.2.1 Scope

The scope of the NBS [90] is restricted to sailing yachts (defined as boats for which the sail area is greater than the righting moment divided by 128), up to 15m length, and for foresails having an area not greater than 1.6 times the area of the mainsail. All those criteria are met by the A Rater.

The NBS is based on 2 load cases, discussed hereafter.

5.2.2 Load Cases

5.2.2.1 NBS Load Case 1

The first load case considered is a rig at 30° of heel, loaded by a single headsail, i.e. a point load acting at the top of the forestay. Since only a single point load is applied, it can be related to the righting moment, hence:

$$F_1 \times HA_1 = RM_{30^\circ} \qquad \textit{Eq. 17}$$

Rearranging:

$$F_1 = \frac{RM_{30^\circ}}{HA_1} \qquad \textit{Eq. 18}$$

In which:

F_1	Foresail point load.	N
HA_1	Heeling arm from the Dwl.	m
RM_{30°	Righting moment at 30°.	N.m

Note that the heeling arm neglects the position of the CLR under the waterline, a conservative approach which increases the load F_1.

5.2.2.2 NBS Load Case 2

The second load case assumes a deep reefed mainsail of luff height 60% of P. The resulting force F_2 is assumed to act at the centre of effort of the sail: 1/3 of the luff height. By considering the freeboard and height of the boom above deck, the heeling arm HA_2 from the Dwl is:

$$HA_2 = F + BAD + \frac{0.6P}{3} \qquad \textit{Eq. 19}$$

In which:

HA_2	Heeling arm from the Dwl.	m
F	Freeboard.	m
BAD	Height of the top of the boom above deck.	m
P	Luff height.	m

The force F_2 acting at the centre of effort is therefore given by:

$$F_2 = \frac{RM_{30^\circ}}{HA_2} \qquad \textit{Eq. 20}$$

In which:

F_2	Reefed mainsail point load.	N
HA_2	Heeling arm from the Dwl.	m
RM_{30°	Righting moment at 30°.	N.m

An additional load F_{boom} is assumed to act at the gooseneck:

$$F_{boom} = \frac{F_2}{3} \quad \textbf{Eq. 21}$$

And an arbitrary head sail force F_h is also considered:

$$F_h = 0.4 \times F_2 \quad \textbf{Eq. 22}$$

5.2.2.3 Load Cases Illustration

The two load cases proposed by the NBS are pictured in Figure 28.

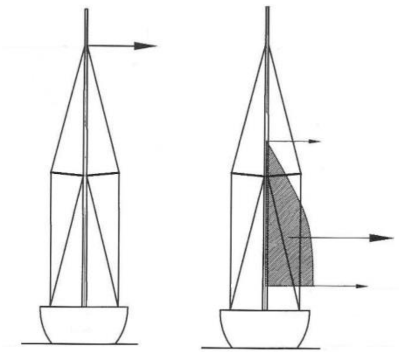

Figure 28: NBS load case 1 (left) and 2 (right) [75].

The NBS standard calculations then only consider the greater of load case 1 or 2.

5.2.3 Shrouds Sizing

5.2.3.1 Nomenclature

For the purpose of the analysis, the vertical shrouds are denominated V1, V2, etc… and the diagonal shrouds D1, D2, etc... where 1 denotes the lowest segment of the rig.

5.2.3.2 Force Resolution

The NBS proposes a simple framework analysis based on classic beam theory to evaluate the tension in the shrouds from the highest of the lateral load cases previously introduced.

5.2.3.3 Factor of Safety

From the tension load calculated for each shroud, the dimensioning is based on the factors of safety provided in Table 13.

Shroud	NBS Factor of Safety
D1	2.8
D2	2.3
D3	3.0
V1	3.2
V2	3.0

Table 13: NBS factors of safety [90].

5.2.4 Stays Sizing

The NBS provides equations to ascertain the minimum breaking strength P of the stays. The fore stay breaking load P_f is given as:

$$P_f = \frac{15 \times RM_{30°}}{I + F} \quad \textbf{Eq. 23}$$

In which:

P_f	Forestay breaking strength.	N
$RM_{30°}$	Righting moment at 30°.	N.m
I	Height of the jib.	m
F	Freeboard.	m

For fractional rigs, the breaking strength of the aft stay P_a can be assessed using:

$$P_a = \frac{2.8 \times RM_{30°}}{I_a \times \sin \alpha_a} \quad \textbf{Eq. 24}$$

In which:

P_a	Aft stay breaking strength.	N
$RM_{30°}$	Righting moment at 30°.	N.m
C	Righting moment at 30°.	N.m
I_a	Mast height from Dwl.	m
α_a	Aft stay angle to the mast.	°

5.2.5 Transverse Mast Stiffness

The required transverse second moment of area I_{xx} is:

$$I_{xx} = k_1 \times m \times PT \times I(n)^2 \quad \textbf{Eq. 25}$$

In which:

I_{xx}	Second moment of area.	mm^4
k_1	Panel factor, see Table 14.	N.m
m	Material factor, $m = 70500/E$.	m^2.N^{-1}
PT	Design load, see Table 15.	N
$I(n)$	Panel length.	m

Rig Type	k_1 for panel 1 Deck Stepped	Keel Stepped	k_1 for panel 2 and 3
1 Spreader	3.24	2.40	3.35
2 Spreaders	3.51	2.60	3.60

Table 14: k_1 factor for fractional rigs [90].

Note the 35% increase for the lower panel when deck stepped; this is due to the boundary condition not been as robust as a keel stepped mast.

Panel	PT
1	$(1.5 \times RM_{30°})/b$
2	$D_1 \times \cos \beta_1$
3	$D_1 \times \cos \beta_1 + D_2 \times \cos \beta_2$

Table 15: Panels design load [90].

In which:

$RM_{30°}$	Righting moment at 30°.	N.m
b	Shroud base.	m
D_n	Diagonal shroud load.	N
β_n	Shroud angle to the mast.	°

5.2.6 Longitudinal Mast Stiffness

The necessary second moment of area of the mast about the y-axis I_{yy} can be found from:

$$I_{YY} = k_2 \times k_3 \times m \times PT \times I^2 \quad \textbf{Eq. 26}$$

In which:

I_{xx}	Second moment of area.	mm^4
k_2	Staying factor (see Table 16).	-
k_3	1.35 for deck stepped masts , 1 for keel stepped masts.	-
m	Material factor, $m = 70500/E$	m^2.N^{-1}
PT	Design load, see Table 15.	N
I	Forestay height above deck.	m

Staying type	Staying factor k_2 for fractional rigs	
	1 Spreader	2 Spreaders
Double lowers	0.80	0.85
Single lowers	0.75	0.80
Runners	0.95	0.90
Swept Spreaders	1.00	0.95

Table 16: k_2 factor for fractional rigs [90].

5.2.7 Fractional Mast Top

The top of the mast experiences much less compression than the bottom, the required section modulus is smaller, and therefore a mast taper can be introduced. The main advantage is weight savings in a decisive area. However, a tapered top mast implies a custom made mast, more expensive than standard extrusions commercially available at a lower cost.

5.2.8 Spreaders

The NBS specifies three criteria to be met for the spreaders, namely the second moment of area at midspan $I_{s/2}$, the section modulus at the mast SM_m and the moment M to be withstood by the spreader attachment. Those are respectively given by:

$$I_{s/2} = \frac{0.8 \times C \times S^2}{E \times \cos\delta} \quad \textit{Eq. 27}$$

$$SM_m = \frac{0.16 \times S \times V \times \cos\delta}{\sigma_{0.2}} \quad \textit{Eq. 28}$$

And:

$$M = 0.16 \times S \times V \times \cos\delta \quad \textit{Eq. 29}$$

In which:

$I_{s/2}$	Midspan second moment of area.	cm^4
SM_m	Section modulus as the mast.	cm^3
M	Moment.	N.m
C	Transverse shroud force.	N
S	Length.	mm
E	Young's modulus.	$N.m^{-2}$
$\varDelta$	Swept back angle.	°
V	V1 for the lower spreader, and D3 for the upper ones.	mm
$\sigma_{0.2}$	Yield strength.	$N.mm^{-2}$

5.2.9 Boom

The minimum vertical section modulus SM_b is given by:

$$SM_b = \frac{600 \times RM_{30°} \times (E - d_1)}{\sigma_{0.2} \times HA} \quad \textit{Eq. 30}$$

In which:

SM_b	Section modulus.	mm^3
$RM_{30°}$	Righting moment at 30°.	N.m
E	Mainsail foot length.	mm
d_1	Horizontal distance from the gooseneck to the vang on the boom.	mm
$\sigma_{0.2}$	Yield strength.	$N.mm^{-2}$
HA	Heeling arm from the Dwl.	mm

5.2.10 Conclusions

The Nordic Boat Standard [90] offers a complete guideline to design a rig. Very little or no technical background is however provided, and a range of arbitrary coefficients are considered.

Investigations into first principles analysis of the rig assuming a pin jointed framework showed a very close correlation [118].

Furthermore, mast manufacturers base their masts on the Nordic Boat Standard: comparing a previous mast design [105] with the manufacturer's quote for the same yacht revealed matching results.

Thanks to its proven reliability for the past 25 years, the NBS has been followed in this instance. The calculation procedure outlined was first spreadsheeted in order to provide a fast computation allowing efficient comparison of various designs.

5.3 Mast Design

5.3.1 Introduction

The primary aim is to produce a mast as light as possible, while providing sufficient stiffness, and a minimum air drag. The design of a two spreaders rig will be undertaken as it is favoured by the sailors: all but one A Rater are two spreaders rig.

5.3.2 Spreaders Location

The lower spreader is located at 55% of the jib height, a typical proportion [118].

The upper spreader (also called '*jumper*') is raked forward and is to be located at the forestay attachment point. This is a standard fractional rig configuration to reinforce the mast in the highly loaded area that the forestay attachment is.

5.3.3 Mast Section

5.3.3.1 Section Selection

In order to keep the costs down, a standard carbon mast section available on the market is advised, such as those proposed by Seldén [104]. The design will therefore try and achieve low loads on the bottom panel (which governs the mast second moment of area) so that a smaller section can be used, thus decreasing weight and cost. From the calculated structural section modulus required (both longitudinally and transversally), the Seldén CC077 section has been selected, and is detailed in Drawing 08.

5.3.3.2 Further Aerodynamic Considerations

An oval shape mast section (as opposed to a circular one) has been preferred for its better aerodynamic performance.

In addition, mast disturbance can be reduced by introducing roughness. Experimental results suggest a reduction in mast aerodynamic drag of the order of 25% for a roughness height of 1% of the mast diameter [75]. Indeed, masts operate at small Reynolds numbers (defined as the product of the diameter and velocity divided by the kinematic viscosity) where the boundary layer never gets turbulent, and separates in the laminar region and before the maximum thickness of the mast, leading to a very wide wake and a high drag.

By introducing roughness, the boundary layer will become turbulent before separation occurs, and the flow will separate after the maximum thickness. The resulting wake is much narrower and the drag is reduced. This principle is depicted in Figure 29.

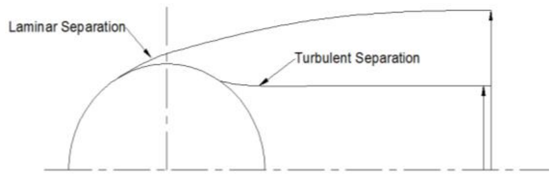

Figure 29: *Flow separation around a cylinder [75].*

A more common example illustrating this phenomenon is a golf ball, where the roughened surface enables the ball to travel a longer distance thanks to the drag diminution.

5.3.4 Shrouds and Stays

The NBS calculations lead to the shrouds and stay sizes presented in Table 17, based on the breaking loads of standard 1x19 wires.

Stay/Shroud	Diameter (mm)
D4 (jumper)	3
D3	4
D2	4
D1	4
V1	4
Forestay	4
Running backstay	6

Table 17: *Shrouds and stays sizing.*

5.3.5 Spreaders

The spreaders cross section has been approximated as a hollow ellipse, for which the second moment on area I_{xx} is given by:

$$I_{xx} = \frac{\pi}{64}(AB^3 - ab^3) \qquad \textbf{Eq. 31}$$

In which:

I_{xx}	Second moment of area.	mm^4
A	Outer long side of the ellipse.	mm
B	Outer short side of the ellipse.	mm
a	Inner long side of the ellipse.	mm
b	Inner short side of the ellipse.	mm

The final dimensions of the spreaders are illustrated in Drawing 08.

5.3.6 Boom

Based on the NBS section modulus, the Seldén BC086 boom section has been selected. This is once again motivated by the will to achieve a lower cost rig by purchasing existing components available on the market, as opposed to a custom made rig.

5.3.7 Conclusions

The structural requirements of the rig components have been described and calculated by applying the Nordic Boat Standard previously introduced, the most appropriate sections from a given manufacturer have then been selected.

It is to be stated that mast design is a highly complex area, and only a basic approach has been utilised in this instance. Mast failures are very common in racing classes, and a reliable mast is therefore critical.

Finally, it would strongly be advised to follow manufacturer’s recommendations. Indeed, although their design methods are largely inspired by the NBS, by agreeing to their specifications, the manufacturer will be liable for any failure, whether due to design or construction issues.

5.4 Conclusions

The only small craft standard regarding rigs, the Nordic Boat Standard, has been detailed and used to evaluate the structural requirements of the mast, boom, spreaders, shrouds and stays. The appropriate sections have then been established, and are depicted in Drawing 08. While the design is backed up by a regulatory body, recommendations for following the mast manufacturer’s specifications have been made, primarily for liability reasons.

Chapter 6: Cockpit Design

The original cockpit design appears outdated and not adapted to efficient racing. A new layout will therefore be proposed, taking into account the downflooding angle, side deck width and length, as well as the internal organisation with compartments more suited to modern racing crew organisation. In addition, ergonomics and anthropometrics have been considered so that the sailing is as comfortable as possible. Finally, the detailed arrangement aimed at keeping the controls as simple as possible, thus saving on hardware cost and weight, while providing all control lines expected on a racing boat.

6.1 Introduction

The design of a practical, polyvalent, and safe cockpit is a major requirement for open boats. Furthermore, due to its low freeboard, the cockpit and deck area are the primary visible areas, and must be aesthetically pleasing, offering an additional opportunity to showcase the level of craftsmanship and the quality and beauty of the wood.

The three main cockpit design philosophies are depicted in Figure 30, and are namely: a narrow rectangular cockpit on the left (original *Scamp*), a slightly wider cockpit running parallel to the sheer (centre), and finally a very wide cockpit (right).

Figure 30: *Cockpit design philosophies [111].*

The pros and cons will be highlighted in order to find an optimum compromise.

6.2 Cockpit Layout

6.2.1 Side Deck Width

6.2.1.1 Downflooding

The primary consideration is the width of the side decks, and inherent width of the cockpit. On original A Raters, such as *Scamp*, the governing factor was avoiding water intake when heeling over or capsizing. The angle at which water gets inside the cockpit is known as the downflooding angle. As presented in Figure 31, the downflooding angle of *Scamp* is just above 90°, thus coherent with a safe design to avoid water intake, and potentially sinking the boat when capsizing.

Nowadays, the buoyancy aid imposed by the A Rater class rule prevents sinkage, leading to much more open cockpits. This allows more space for manoeuvers, and the crew can provide an increased righting moment without having to hike yet since they are sitting further out.

The drawback is an earlier water intake, potentially within operating heeling angles, which would handicap the performance of the boat.

The proposed design offers a good compromise, with a 350mm wide side deck, which allows both a comfortable and efficient position of the crew, while retaining a high downflooding angle of 48°, as seen in Figure 31, which satisfies the relevant ISO regulation [58]

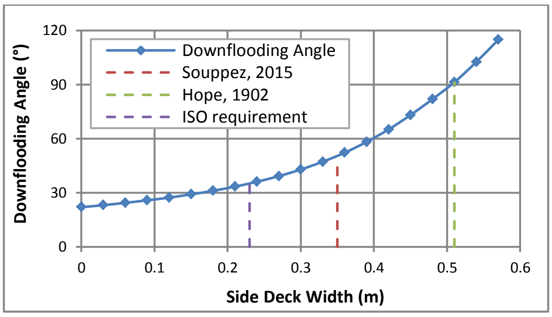

Figure 31: *Downflooding angle.*

6.2.1.2 Ergonomics and Anthropometrics

Another decisive factor, unfortunately rarely incorporated in deciding the width of the side deck is the location of the sailor's back-knee. Consequently, both ergonomics and anthropometrics will be taken into account, respectively defined as the science of designing spaces and environments and the study and measurements of human proportions.

From a comfort point on view, any edge resting on the back-knee when hiking is particularly painful, and the position cannot be sustained for prolonged amount of time. Furthermore, experiments realized on improving hiking positions [77] revealed that the shorter the back-knee/sheer distance, the more efficient and comfortable the hiking is.

With the side width proposed, the sheer lies just above the back-knee when fully hiked, for prolonged efficient contribution to the righting moment. Plus, the inner edge of the cockpit will also lie just above the back-knee of a crew seeking support on the centerplate box.

The width of the cockpit and resulting side decks has therefore been fixed based on both downflooding angle and comfortable hiking. The length of the deck however is governed by a different factor.

6.2.2 Deck Length

As further detailed in Section 7.2.1, longitudinal strength is a likely issue for a yacht such as the A Rater. In this condition, the deck offers a significant structural component not to be neglected. Indeed, considering the entire boat as a beam, the deck is located away from the neutral axis, hence its predominant contribution.

On the one hand, a small open space has been retained in front of the mast in order to provide a convenient location to store excess ropes or gear, without it overcrowding the cockpit.

On the other hand, the aft deck has been extended forward of the rudder stock; this will provide a stronger support point for the top rudder bearing, thus improving the steering comfort.

However, the deck cannot be fully closed, as it must provide sufficient space for the crew to perform manoeuvres. Furthermore, the mass of the crew constitutes a large proportion of the overall weight, a large cockpit offering a wide range of longitudinal positions for the crew will therefore improve the sailing equilibrium. To encourage this, the compartments of the cockpit have been redefined.

6.2.3 Compartments

The cockpit of the original *Scamp* is divided into three main areas, one for each crew. The helmsman has the largest, while the forward crew is confined into a very small space. This is in contradiction with a typical race crew organization, where the helmsman would remain mostly static, while the two other crew would be in charge of the balance. It is crucial to have the ability to move forward and aft so that the longitudinal balance of the yacht can be adjusted.

The new cockpit is only composed of two compartments: the aft one dedicated to the helm, and a spacious forward one for the two crew members. As a result, the sailors can move further forward and further aft, while still having all control lines in close proximity.

The definition of the compartments is primarily dictated by the location of the two main structural frames. The first one, in way of the mast, has to withstand the mast, shrouds, and centreplate loads. The second one, separating the two main cockpit areas, supports the aft end of the centerplate box, the mainsheet, traveller and running backstays.

6.2.4 Detailed Layout

Particular emphasis has been put on a simple arrangement, yet offering all the controls expected on a racing yacht. In addition, a highly functional cockpit will be developed to ease the sailing and improve efficiency. The aim is also for the boat to be easy to use to attract more sailors into the class.

As previously introduced in Section 4.3.3, the boom raised for aerodynamic purposes offers a higher boom above deck, and therefore a larger space to perform manoeuvres in.

As part of the detailed cockpit design, all components of the deck hardware and ropes have been selected. This allows for a more accurate weight and centres and cost estimate, as well as a more precise deck arrangement, presented in Drawing 03.

6.3 Conclusions

Starting from the original cockpit, an improved version has been designed, with a smaller side deck width to provide a more comfortable position and additional righting moment, while retaining a high downflooding angle. In addition, the overall length of the cockpit has been decreased for structural purposes, the actual usable volume has however been greatly increased. Finally, a new layout has been created, offering a larger compartment for the two forward crew members leading to wider range of longitudinal position, a more efficient balance and improved performance.

A graphical comparison of the original and new cockpit design is shown in Figure 32.

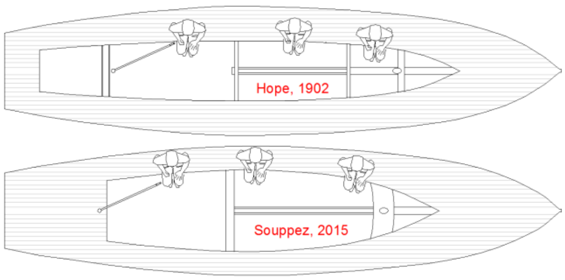

Figure 32: *Cockpit layout comparison.*

Chapter 7: Structural Analysis and Scantlings

The structural analysis not only has to provide a solid and robust yacht at the lightest possible weight, but it is to comply with the relevant regulatory body and standards, the ISO 12215 in this case. The hull structural hierarchy will first be defined and designed in accordance with the ISO, where applicable. Indeed, only the main structural components are covered by regulatory bodies, while smaller and more specialised ones have to be based on rule of thumbs and experience. The centreplate and rudder stock will then be developed. The structural analysis will eventually lead to the scantlings, from which the boat will be built.

7.1 Hull

7.1.1 Structural Hierarchy

The concept of structural hierarchy is omnipresent in design and class rules, and states the different levels of the structural components of a yacht. The hull shell is referred to as the plating, and primarily keeps the water out. The plating is supported by stiffeners (whether longitudinal or transversal) called tertiary members, which help to reduce the panel dimensions and structural requirements. The tertiary members are supported by secondary members, namely frames and bulkheads, which divide their span. Finally, the secondary members are themselves supported by the primary members that are the girders (the keel and hog in the case of a wooden boat), again reducing their span to lower the structural requirements.

7.1.2 The Nature of Wood

Wood as a boatbuilding material is often correlated with a unidirectional composite, as the mechanical properties are particularly strong parallel to the grain, but very weak perpendicular to it. In essence, cold moulding can be compared to a composite layup of unidirectional fibres, with different orientations to even the mechanical properties across the panel.

The major difficulty lies in the actual mechanical properties that are very challenging to quantify. For a given wood species, multiple factors can have an impact, such as the moisture content, and where the tree was grown. Indeed, a tree grown closer to the Pole will grow slower, the annual rings will be closer, and the wooden denser, which contributes to increase the structural strength.

An additional difficulty when designing with wood is the presence of defects, such as knots and sap pockets that cannot always be identified. As a result, the larger the cross section of a piece of wood is, the greater the factor of safety should be, since larger defects could be concealed inside. Luckily, veneers being very thin, defects are easily identifiable, which lowers the factor of safety and lightens the structure.

Without structural testing of the actual wood used for the construction, the mechanical properties have to be estimated. Extensive research in this area has been performed over the years, with very little applicable results [78].

It is worth mentioning that manufacturer's specifications should never be relied upon for design purposes: those have no legal value, and are more likely to be a sell pitch (i.e. the highest value ever achieved) rather than a representative one, such as the average minus two standard deviations, which is a common approach in structural testing [79].

The safest option is to consider the values quoted by regulatory bodies, often seen as pessimistic (i.e. safe), with high factors of safety applied to them. In this case, the Appendix E of the ISO 12215-5 [54] that provides the mechanical properties for woods will be consulted.

7.1.3 Hull Plating

7.1.3.1 Early Design

At an early stage of the design, scantlings estimation can be done using published rule of thumbs. Gerr [29] provides a general idea of the hull thickness based on the product of the length, beam and depth of the yacht. Alternatively, MacNaughton [80] scantlings rely on the cubic root of the displacement only.

Although those methods would not be advised for a detailed structural arrangement, they offer very quick and surprisingly reliable evaluations at a preliminary stage. A recognised class rule should however be adopted to develop the final scantlings, such as the ISO standard [54] in this instance.

Nevertheless, some smaller structural components, such as knees and local reinforcements are neglected by class rules. The basic rule of thumbs can therefore provide a good alternative, as later discussed in Section 7.2.2.

7.1.3.2 ISO Formula

For laminated wood construction, such as cold moulding, the plating thickness t required by the ISO [54] is:

$$t = b \times \sqrt{\frac{P \times k_2}{1000 \times \sigma_d}} \qquad \textbf{\textit{Eq. 32}}$$

In which:

t	Plating thickness.	mm
b	Short side of the panel.	mm
P	Design pressure.	kN.m^{-2}
k_2	Aspect ratio coefficient: 0.5.	-
σ_d	Design stress.	N.mm^{-2}

7.1.3.3 Theoretical Background

The ISO standard does not provide any theoretical background to the regulation. However, the formula previously presented can be derived from first principles and classical beam theory [3].

For a high aspect ratio panel, the problem can be simplified as a beam. For a yacht, the most realistic assumption is a built-in beam under a distributed load. In those conditions, the maximum bending moment M_{max} and minimum section modulus SM_{min} are respectively:

$$M_{max} = \frac{P \times b^2}{12} \quad \textbf{Eq. 33}$$

And:

$$SM_{min} = \frac{t^2}{6} \quad \textbf{Eq. 34}$$

In which:

M_{max}	Maximum bending moment.	N.m
P	Pressure.	kN.m^{-2}
b	Span.	mm
SM_{min}	Minimum section modulus.	mm^3
t	Thickness.	mm

The design stress σ_d is given by:

$$\sigma_d = \frac{M_{max}}{SM_{min}} = \frac{P \times b^2 \times 6}{12 \times t^2} \quad \textbf{Eq. 35}$$

This can be rearranged to give the ISO formula:

$$t = b \times \sqrt{\frac{P \times k_2}{1000 \times \sigma_d}} \quad \textbf{Eq. 36}$$

This provides the theoretical background behind the class rule and justifies the value of 0.5 for k_2.

7.1.3.4 Application

In the case of cold moulding, the number of layers is either 2 (double diagonal) or 3 (outer layer running fore and aft). More than 3 layers would induce a large increase in cost and time, and is therefore uncommon [29].

For laminated wood, the thickness is primarily driven by the available sizes. Since the standard veneer thickness is 2.5mm, the plating thickness is to be 7.5mm. Consequently, Eq. 36 is rearranged to solve for the short side of the panel b i.e. the longitudinal stiffeners spacing from centreline to centreline:

$$b = t \times \sqrt{\frac{1000 \times \sigma_d}{P \times k_2}} \quad \textbf{Eq. 37}$$

In which:

b	Short side of the panel.	mm
σ_d	Design stress.	N.mm^{-2}
t	Thickness.	mm
P	Pressure.	kN.m^{-2}
k_2	Aspect ratio coefficient: 0.5.	-

A value of 179.8mm has been determined, then reduced to 150mm for further reliability and an increased factor of safety.

7.1.3.5 Bottom, Topsides and Deck Plating

The procedure utilised took into consideration the hull bottom pressure. The calculation process is then repeated for the topsides and deck and inherent pressures.

In the case of the A Rater, having extremely low freeboard and heeling a lot, no clear topsides can be identified, and the whole hull has been treated as the bottom.

For the deck, considering a 6mm plywood, the required short side of the panel is 300mm. This thickness also meets the minimum thickness criterion enforced by the ISO standard of:

$$t_{min} = 3.8 + 0.17 \times Lwl \quad \textbf{Eq. 38}$$

In which:

t_{min}	Minimum thickness.	mm
Lwl	Waterline length.	m

Note that, when analysing plywood, the properties are taken perpendicular to the grain (i.e. where the plywood is the weakest) for an added factor of safety. Indeed, it is not always practical (and economical) to have the grain running in the desired direction with plywood, as it could lead to a larger waste factor.

7.1.3.6 Buckling

The ISO standard is based on strength and stiffness analysis only, and ignores other failure behaviours, such as buckling. The critical buckling stress σ_b can be found using [79]:

$$\sigma_b = 0.9 \times k_{ar} \times E \times \left(\frac{t}{s}\right)^2 \quad \textbf{Eq. 39}$$

In which:

σ_b	Critical buckling stress.	N.mm^{-2}
k_{ar}	Aspect ratio coefficient given in Table 18.	-
E	Young's modulus.	N.mm^{-2}
t	Planking thickness.	mm
s	Short side of the panel.	mm

Aspect Ratio	k_{ar}
AR<1	$(1+AR^2)^2$
AR>1	4

Table 18: *K_{ar} coefficient [79].*

In addition to the ISO standard, possible buckling failure has been checked.

7.1.4 Longitudinal Stiffeners

The stiffeners have to satisfy two criteria to meet the ISO regulation, a minimum section modulus SM (bending criterion) and a minimum web area A_w (shear criterion), respectively given by:

$$SM = \frac{83.33 \times k_{CS} \times P \times s \times {l_u}^2}{\sigma_d} \times 10^{-6} \quad \textbf{Eq. 40}$$

And:

$$A_w = \frac{k_{SA} \times P \times s \times l_u}{\tau_d} \times 10^{-9} \quad \textbf{Eq. 41}$$

In which:

SM	Minimum section modulus.	cm^3
k_{CS}	Curvature factor, see Table 19.	-
P	Pressure.	$N.m^{-2}$
s	Stiffeners spacing.	mm
l_u	Stiffener length.	mm
A_w	Shear area.	mm^2
σ_d	Design stress.	$N.mm^{-2}$
k_{SA}	Shear area factor, taken as 5 for a stiffener attached to plating.	-
τ_d	Design shear stress.	$N.mm^{-2}$

Curvature/length (c/l)	k_{CS}
0 to 0.03	1
0.03 to 0.018	$1.1 - 3.33 \times (^c/_l)$
> 0.18	0.5

Table 19: *ISO curvature factors [54].*

As for the plating thickness, the equations provided for the stiffeners appear to be derived from classical beam theory.

Note that the ISO [54] simply considers the frames as transverse stiffeners; frames are therefore treated similarly.

The complexity of the structure of a yacht needs an efficient way to check the structural requirements of each member against the ISO standard. This is performed using the HullScant software [112].

7.1.5 HullScant

HullScant allows to define all panels, stiffeners and frames, and check their scantlings against the ISO 1221-5 [54] to ensure compliance. The software benefits from years of practical validation, and is now regarded as the best way to meet the ISO requirements. Furthermore, HullScant enables to efficiently compare of a range of possible structural designs and materials to determine the lightest option.

The proposed structure for the A Rater has been modelled in HullScant and demonstrated compliance with the ISO standard for the primary structural elements.

7.1.6 Limitations

While additional guidelines can be found on materials and structural arrangements in Part 3 [53] and 6 [55] of the ISO 12215, the guideline for scantlings stops at the plating, stiffeners and frames. Other class rules do not provide any more details for wooden boats.

This reflects the complexity of wooden structural designs, the very little interest (and money) that regulatory bodies are willing to put into wooden construction, as well as the highly empirical and experience based nature of wooden boatbuilding.

As a result, most of the smaller structural components will be designed based on published rule of thumbs (as introduced in 7.1.3.1), as well as first principles analysis where possible.

7.2 Detailed Design

7.2.1 Longitudinal Strength

7.2.1.1 Definition

The longitudinal strength of a yacht refers to its hogging and sagging behaviour. This is particularly relevant for larger craft (40m+), where a detailed analysis is required. There are however special cases where it should be considered for small boats too [79], such as:

- High length/depth ratios (i.e. high bending stress).
- Concentrated loads (such as rig loads).
- Low modulus materials in compression.

The A Rater, with a very low depth, high rig loads and built in wood appears to match all three criteria, it is therefore important to analyse the longitudinal strength.

7.2.1.2 Load Case

The critical load case for the A Rater is sagging: the high rig compression and weight of the centreplate and crew apply a downward force in the centre of the boat, while the forestay and backstay tension pulls the ends up. This is accentuated by the buoyancy distribution when the boat is sailing: the bow and stern waves provide additional upward force, while the midship trough results in a loss of buoyancy where the loads are highest.

7.2.1.3 Structural Requirements

For the purpose of the analysis, the yacht will be considered as a freely supported beam, with a point load acting at the mast. The value of the point load is generally taken as 85% of the total displacement [75]. From beam theory, the maximum bending moment BM_{max} occurring at the mast location is:

$$BM_{max} = \frac{0.85 \times \nabla \times g \times L_1 \times L_2}{L} \quad \textbf{\textit{Eq. 42}}$$

In which:

BM_{max}	Maximum bending moment.	N.m
∇	Loaded displacement.	kg
g	Acceleration due to gravity.	$m.s^{-2}$
L_1	Distance from bow to mast.	m
L_2	Distance from stern to mast.	m
L	Length over all.	m

The section modulus required SM_{req} is therefore:

$$SM_{req} \frac{BM_{max}}{\sigma_u} \quad \textbf{\textit{Eq. 43}}$$

In which:

SM_{req}	Section modulus.	cm^3
BM_{max}	Maximum bending moment.	N.m
σ_u	Lowest of the deck ultimate compression or the bottom ultimate tension.	$N.mm^{-2}$

In addition, the section modulus inherent to the wave pattern can be estimated using the ABS regulation [2]:

$$SM_w = \frac{L^2 \times B \times (12.7 - 0.14L) \times (C_b + 0.7) \times 320}{\sigma_u} \quad \textbf{\textit{Eq. 44}}$$

In which:

SM_w	Section modulus.	cm^3
L	Length over all.	m
B	Beam over all.	m
C_b	Block coefficient.	-
σ_u	Lowest of the deck ultimate compression or the bottom ultimate tension.	$N.mm^{-2}$

The sum of the two section moduli, (respectively SM_{req} and SM_w) gives the total section modulus to be achieved to prevent longitudinal strength failure.

7.2.2 Small Structural Components

As previously introduced in 7.1.3.1, the majority of the small components will be designed in accordance with published rule of thumbs such as the Gerr [29] and McNaughton [80] ones. In those instances, there is no structural or mathematical background, but purely experience based formulas. It is to be noted that traditional boatbuilding benefits for millenniums of practice against a few decades of structural analysis, thus justifying the use of experience based rules.

7.3 Centreplate

7.3.1 Introduction

In the case of the A Rater, that can be seen as a large dinghy, the centreplate does not only has to withstand the hydrodynamic forces, but more importantly the weight of the crew to recover the boat after a capsize.

7.3.2 Load Cases

Under the ISO 12215 Part 9 [57] that regulates the appendages of small crafts, the A Rater is considered as a capsize recoverable dinghy (as opposed to a keel boat), and needs to satisfy the inherent regulation. The design load is to be the greater of the force F_1 due to the crew standing on the centreplate, or the upwind hydrodynamic force F_2, respectively given by:

$$F_1 = 80 \times g \times n_{PR} \qquad \textit{Eq. 45}$$

And:

$$F_2 = 136 \times (0.075 \times \alpha) \times A_{cb} \times V^2 \qquad \textit{Eq. 46}$$

In which:

F_1	Capsize recovery load.	N
g	Acceleration due to gravity.	$m.s^{-2}$
n_{PR}	Minimum number of crew required to recover the boat.	-
F_2	Hydrodynamic load.	N
α	Angle of attack, not less than 5°.	°
A_{cb}	Centreplate area.	m^2
V	Boat speed, see Eq. 47.	kts

Where:

$$V = 2.5 \times \sqrt{Lwl} \times \frac{Lwl}{6.15 \times \sqrt[3]{\frac{m_{LDC}}{1025}}} \qquad \textit{Eq. 47}$$

7.3.3 Analysis

The analysis can be simplified by recognizing that the centreplate is a beam, built-in at one end, and free at the other, i.e. a cantilever, to which a point load is applied. As a result, beam theory applies: the bending moment and transverse section modulus SM_T can be ascertained. From the ISO guidelines, the transverse section modulus provided by a foil is:

$$SM_T = 1.67 \times 10^{-4} \times 0.664^2 \times c \times t^2 \qquad \textit{Eq. 48}$$

In which:

SM_T	Transverse section modulus.	cm^3
c	Foil chord length.	mm
t	Foil thickness.	mm

While the minimum structurally required transverse section modulus for a cantilever beam experiencing a point load at the tip is:

$$SM_{T\,min} = \frac{F \times x}{\sigma_d} \qquad \textit{Eq. 49}$$

In which:

$SM_{T\,min}$	Transverse section modulus.	cm^3
F	Point load force.	N
x	Distance along the span.	m
σ_d	Allowable design stress.	$N.mm^{-2}$

Remembering the semi-elliptic planform of the centreplate, the section modulus is therefore maximum at the root, and decreases towards the tip. This matches the bending moment distribution: maximum at the root and decreasing to 0 at the tip. Rearranging Eq. 48 to solve for the minimum foil thickness, the ISO section modulus requirement can be satisfied, as depicted in Figure 33. Note the addition of a 12% margin on the ISO factor of safety.

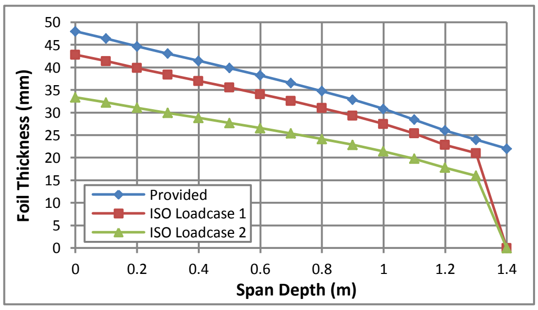

Figure 33: Centreplate thickness.

This results in an average 7.2% thickness/chord ratio, which reduces the hydrodynamic resistance while being structurally sound. The drawback of thin foils is the earlier stall angle, however not an issue for centreplates since they operate at low angles of attack (as opposed to rudders). The detailed centreplate is presented in Drawings 04 and 06.

7.3.4 Conclusions

The design of the centreplate has been conducted in accordance with the ISO standard. Recognising its importance in case of capsize, an increased factor of safety has been adopted. The final foil section is a NACA 00 series, with an average 7.2% thickness/chord ratio.

7.4 Rudder Stock

7.4.1 Introduction

The structural design of the rudder stock was based on the ISO 12115 Part 8 [56]. The importance of the rudder in narrow waterways is paramount, as it does not allow any reaction time: the boat will instantly be hitting the shore or another yacht if steering is lost.

7.4.2 Load Case

The rudder stock load case is a typical example of the main controversy regarding the ISO standard: the absence of theoretical background and the introduction of arbitrary coefficients. The design load F is given as:

$$F = 23 \times Lwl \times A \times {k_{LD}}^2 \times k_{SEA} \times k_{GAP} \times k_{USE} \qquad \textbf{Eq. 50}$$

In which:

F	Design load.	N
Lwl	Waterline length.	m
A	Rudder area.	m²
k_{LD}	Length/displacement coefficient, as given in Eq. 56.	-
k_{SEA}	Sea design condition coefficient, 1.0 for a category C craft.	-
k_{GAP}	Hull/rudder gap coefficient, 1.0 for a gap less than 5% of the rudder mean chord.	-
k_{USE}	Craft use coefficient, 0.9 for category C.	-
Δ	Displacement.	kg

With:

$$k_{LD} = \frac{Lwl}{\left(\frac{\Delta}{1025}\right)^{1/3}} \qquad \textbf{Eq. 51}$$

7.4.3 Analysis

In the case of a spade rudder, the stock will be subject to both bending and torsion, respectively having a lever z_b and r. From first principle, the ISO proposes the pure bending equivalent lever z_{eq} as:

$$z_{eq} = \sqrt{{z_b}^2 + 0.75 \times r^2} \qquad \textbf{Eq. 52}$$

In which:

z_{eq}	Pure bending equivalent lever.	m
z_b	Bending lever.	m
r	Torsion lever.	m

Finally, the diameter d for a solid circular section is:

$$d = 21.65 \times \left(\frac{F \times z_{eq}}{\sigma_d}\right)^{1/3} \qquad \textbf{Eq. 53}$$

In which:

d	Rudder stock diameter.	mm
F	Design load, see Eq. 55.	N
z_{eq}	Pure bending equivalent lever.	m
σ_d	Stock design stress.	MPa

In this case, a bronze stock with a factor of safety doubled compared to the ISO standard has been considered. The choice of bronze, as opposed to the usual stainless steel, is to allow in house manufacturing of the stock. Note that, for a stainless steel stock, the structural requirements would have to be recalculated.

As the stock reaches further down the rudder blade, the required diameter decreases, and rudder stocks are generally absent in the bottom third of the rudder blade. As a result, the stock diameter is tapered. This has been developed in accordance with the ISO regulation [56].

On the other hand, the stock diameter dictates the blade thickness. By adding an extra 7mm on each side of the rudder stock, the blade thickness has been determined, resulting in an average 13% thickness/chord ratio along the length of the span. The stock diameter and blade thickness are shown in Figure 34, while the rudder design is detailed in Drawings 05, 06 and 07.

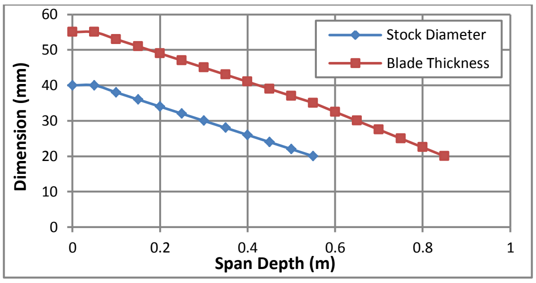

Figure 34: *Rudder stock and blade sizing.*

7.4.4 Conclusions

The rudder stock has been designed in accordance with the ISO standard, considering the manufacturing technique. The required stock diameter dictated the appropriate thickness/chord ratio, 13% in this instance, very close to the 12% intended, thus providing a good compromise between the low drag of thin foils and higher stall angle of thick ones.

7.5 Conclusions

Thanks to the different parts of the ISO 12215, reference standard for the structure of small crafts, the hull, centreplate and rudder stock have been designed. The calculation procedures have been described, and additional factors of safety have been added where necessary for an increased reliability. For the hull structural design, the use of the HullScant software demonstrated compliance while providing a fast and efficient computation method.

Many components of traditional wooden boats are not covered in modern class regulations. Consequently, scantlings based on recognised rule of thumbs and experience have been considered for those.

The structural design of the centreplate, rudder and hull are detailed and illustrated in Drawings 06, 09 and 10.

At this stage, the structure permits to refine the weight estimate and location of the centre of gravity, as discussed in the following chapter.

Chapter 8: Weight and Centres

Critical parts of the design, the weight and centres have a significant impact on multiple aspects of the project, but unfortunately cannot be accurately known at this stage. Indeed, only a best estimate can be realised since the actual values can only be ascertained experimentally once the boat has been built. In order to maximise the accuracy, each item will be considered individually, and appropriate safety margins will be added.

8.1 Design Spiral

As introduced in Section 1.3.2, the design process is a spiral, where each modification will impact another area; the most significant one being without a doubt the displacement of the boat, and inherent location of the centre of gravity. This information impacts on the entire design: the hydrostatics and stability, the scantlings and structural arrangement, the rig, and compliance with regulatory bodies. It is therefore critical to provide a correct weight and centre of gravity. This is a particularly complex problem, and the displacement will not be known until the yacht is built, as the location of the centre of gravity cannot be found until an inclining experiment is performed. At this stage, only an estimate can be achieved through a detailed weight and centres estimation.

8.2 Weight Estimate

8.2.1 Introduction

In the case on the A Rater, being relatively small, it is still manageable to determine the weight and location of every single item. This is the approach taken in this instance. Although more accurate than simpler methods, the main drawback is the very time consuming process.

To make the process more structured, the items are organised in categories. For instance, the centreplate and rudder are gathered into the '*appendages*' category. The '*structure*' category is quite challenging. If the scantlings give the volume of wood, the density can vary greatly, even among the same wood species. Furthermore, the necessary amounts of glue and resin are particularly hard to evaluate, and despite being based on practical experience, a safety margin of 10% has been applied [120].

Mathematically, the total weight is simply the sum of all individual items, and inherent safety margins when relevant.

Note that two displacements are of particular interest in this case: the lightship and fully loaded.

8.2.2 Lightship

The definition of lightship varies from one class society to another. In the case of the A Rater, the lightship is defined by the class rule [111] as:

"The weight to be measured shall include all fixed fittings, which include the bowsprit and fittings if fitted, tabernacle and pin, centreboard and pin, complete rudder assembly including tiller and extension, floor boards, buoyancy bags and fixings if fitted, toe straps and fixings, painters, all blocks and cleats normally attached to the hull for whatever purpose, kicking straps and control lines for sails and backstay but excluding sheets, sails, mast, stays halyards, boom, whisker pole or jib boom. The hull shall be weighed dry, the hull having been out of the water for at least 28 days."

In the case of the A Rater, this definition is particularly important since a minimum hull displacement is imposed. Exciding it would result in an overweight boat, leading to a loss of performance. The design will therefore aim to achieve a yacht lighter than the minimum lightship, without the structural integrity being in jeopardy. Any weight saved will then be added in the form of ballast in the centreplate to lower the centre of gravity and improve the stability and performance. This will ensure the exact minimum displacement is reached: once the boat is built and weighed, any allowable ballast can simply be retro-fitted to the centreplate.

8.2.3 Fully Loaded

If the class rule is only interested in the lightship displacement, for the purpose of the design, the fully loaded one is the most important one. Indeed, the yacht will sail at a given displacement, for which it must be specifically conceived.

As a result, the weight in racing conditions must be established. In this matter, the crew will have a large impact.

8.2.4 Crew Weight

While the yacht weight will remain fixed, the crew will vary, and predicting its exact weight is simply impossible. It is nevertheless a paramount component of the design, and must be estimated as best as possible.

The two consequences are respectively estimating the average crew weight, and accounting for its changes as part of the VPP.

Long taken as 75kg, the value has been modified in recent years to account for the physical human evolution and the tendency for the average weight to increase. The latest ISO standard [57] inherent to appendages design specifies 80kg per crew (as introduced earlier in Eq. 45).

This value will therefore be considered for the purpose of the weight estimate, as 240kg for three crew members appears a reasonable value.

However, in some cases, lighter or heavier crew may be racing. In order to be competitive and maximise the performance, the VPP developed in Chapter 10 will incorporate the weight of each sailor; the aim being to provide a refined VPP for every crew configuration.

8.2.5 Conclusions

From each individual item, the weight estimate was performed, including safety margins to account for the degree of uncertainty in some instances. The addition of the crew weight following the ISO standard assessed both the lightship and fully loaded displacement, as well as the location of the centre of gravity.

8.3 Centres Estimate

The location of the centre of gravity comprises three components: a longitudinal centre of gravity (LCG), a transverse centre of gravity (TCG), and a vertical centre of gravity (VGC).

The LCG should lie as close as possible to the longitudinal centre of buoyancy (LCB), to avoid any trimming moment. Once again, this is particularly relevant to larger crafts. Indeed, the mass of the crew being significant on an A Rater, it will impact on the longitudinal balance. Depending on the sailing conditions, the crew may want to shift the weight forward to trim the boat bow down; conversely, moving aft will trim it bow up and encourage planning behaviour.

In static condition, the TCG is to be on the centreline. For larger crafts, with asymmetric accommodation, this can be a challenge. But for a small sailing yacht such as the A Rater, being perfectly symmetrical, the TCG is not an issue. When sailing, the crew sitting to windward will shift the TCG, thus creating a righting moment.

Finally, the VGC is a vital component since stability is primary governed by its height, as further detailed in Chapter 9. The lower the VCG, the more stable and therefore the more powerful the yacht is. Note that the location of the VCG cannot be precisely known until an inclining experiment is conducted, as later described in Section 9.3.

All three components of the centre of gravity are respectively given by:

$$LGC = \frac{\sum(M_i \times X_{i)})}{\sum(M_i)} \quad \textbf{\textit{Eq. 54}}$$

$$TGC = \frac{\sum(M_i \times Y_{i)})}{\sum(M_i)} \quad \textbf{\textit{Eq. 55}}$$

$$VGC = \frac{\sum(M_i \times Z_{i)})}{\sum(M_i)} \quad \textbf{\textit{Eq. 56}}$$

In which:

LCG	Longitudinal centre of gravity.	m
TCG	Transverse centre of gravity.	m
VCG	Vertical centre of gravity.	m
M_i	Mass of an item.	kg
X_i	Longitudinal position of an item.	m
Y_i	Transverse position of an item.	m
Z_i	Vertical position of an item.	m

8.4 Results

The final weight estimate revealed a loaded displacement of 652 kg, with the breakdown shown in Figure 35.

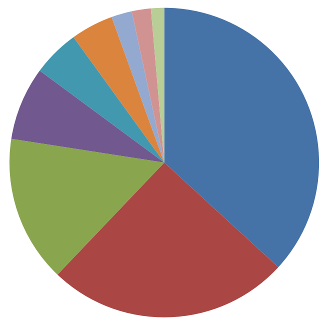

Figure 35: *Weight estimate breakdown.*

The three dimensional location of the centre of gravity from the reference point located at the forward perpendicular on waterline is presented in Table 20.

Component	Location (m aft of FP)
LCG	3.94
TCG	0.00
VCG	0.85

Table 20: *Centre of gravity location.*

8.5 Conclusions

By considering each individual item, the weight and centres have been evaluated. Despite the use of margins, this remains an estimate, to be confirmed by an inclining experiment to ensure sufficient stability is provided.

The weight and centres are the key stone of a yacht's conception; once those have been accurately established the project enters the design evaluation phase, which includes stability assessment and velocity prediction, as well as ensuring compliance with the design brief and relevant regulation.

Chapter 9: Transverse Stability

For safety, performance, and regulation reasons, a stability assessment is to be conducted. The principles of small angle stability will be outlined as they provide the theoretical background to inclining experiments. Indeed, the critical location of the vertical centre of gravity can only be ascertained through the experimental procedure presented. In addition, large angle stability will be introduced, and the various criteria inherent to stability set by the regulatory body will be detailed. A safety margin has been considered on the location of the centre of gravity to provide a conservative approach. At this stage, compliance with the ISO category C has been demonstrated.

9.1 Introduction

As part of the design evaluation, transverse stability is relevant to both the safety aspect, ensuring compliance with the ISO 12217 Part 2 [58], and the performance prediction program. At this stage, the stability is based on the weight and centres estimate previously realised. This being an estimate, a conservative approach will be taken, and a 5% safety margin will be considered [36]. Since the actual values can only be found through an inclining experiment, the process will be outlined after introducing the underpinning theory. Finally, a large angle stability analysis will be performed.

9.2 Small Angle Stability

Small angle theory provides the basis of stability evaluation, and the key principles to undertake an inclining experiment. Four key points are to be defined:

- B, the vertical centre of buoyancy.
- G, the vertical centre of gravity.
- M, the transverse metacentre.
- K, the baseline reference.

Furthermore, the most important distances include:

- $\overline{BM}$, the metacentric radius.
- $\overline{GM}$, the metacentric height.
- $\overline{Gz}$, the righting lever.

For small angle of heel φ, typically less than 3°, the location of the metacentre can be assumed fixed [58]. The key points and distances are depicted in Figure 36.

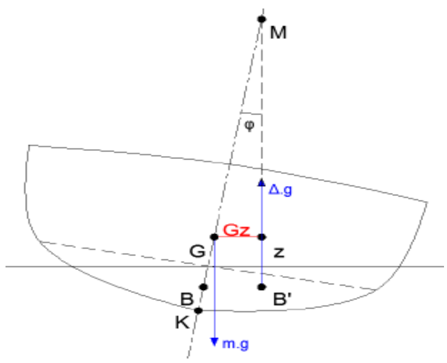

Figure 36: Small angle stability.

The shift in centre of buoyancy position due to heel leads to the upward buoyancy force to be applied through the new centre of buoyancy B', while the downward mass of the vessel remains applied through the centre of gravity G. The righting moment RM_φ is therefore:

$$RM_\varphi = \Delta \times g \times \overline{Gz} \qquad \textbf{Eq. 57}$$

In which:

RM_φ	Heeled righting moment.	N.m
Δ	Yacht displacement.	kg
g	Acceleration due to gravity.	m.s^{-2}
$\overline{Gz}$	Righting lever, given in Eq. 58.	m

For small angles of heel:

$$\overline{Gz} = \overline{GM} \times \sin\varphi \qquad \textbf{Eq. 58}$$

In which:

$\overline{Gz}$	Righting lever.	m
$\overline{GM}$	Metacentric height.	m
φ	Heel angle.	°

The metacentric height can only be found indirectly by knowing the location of the centre of buoyancy and gravity.

$$\overline{GM} = \overline{KB} + \overline{BM} - \overline{KG} \qquad \textbf{Eq. 59}$$

In which:

$\overline{GM}$	Metacentric height.	m
$\overline{KB}$	Distance of the centre of buoyancy from the base.	m
$\overline{BM}$	Metacentric radius, see Eq. 60.	m
$\overline{KG}$	Distance of the centre of gravity from the base.	m

The metacentric radius $\overline{BM}$ is found using:

$$\overline{BM} = \frac{I_{xx}}{\nabla_c} \qquad \textbf{Eq. 60}$$

In which:

$\overline{BM}$	Metacentric radius.	m
I_{xx}	Second moment of area of the waterplane.	m^4
∇_c	Canoe body volume.	m^3

The VCG is to be precisely located once the boat is built via an inclining experiment, based on the small angle stability theory introduced, to ensure compliance with the regulation.

9.3 Inclining Experiment

9.3.1 Introduction

The inclining experiment relies on the fact that the metacentre is fixed for angles of heel less than 3°. The aim is to quantify the metacentric height $\overline{GM}$ by creating a known heeling moment using masses shifted across the deck, and measuring the resulting heeling angle with a pendulum. A typical setup is shown at model scale in Figure 37.

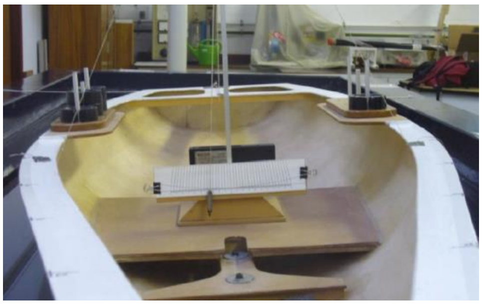

Figure 37: Model inclining experiment.

9.3.2 Calculation Process

For equilibrium, the righting moment is to equal the created heeling moment:

$$RM = HM \quad \textbf{Eq. 61}$$

Or:

$$\Delta \times g \times \overline{Gz} = m \times g \times d \quad \textbf{Eq. 62}$$

Remembering that $\overline{Gz} = \overline{GM} \times \sin\varphi$, then:

$$\Delta \times g \times \overline{GM} \times \sin\varphi = m \times g \times d \quad \textbf{Eq. 63}$$

Solving for $\overline{GM}$:

$$\overline{GM} = \frac{m \times d}{\Delta \times \sin\varphi} \quad \textbf{Eq. 64}$$

For small angles, $\sin\varphi \approx \tan\varphi$, which yields:

$$\overline{GM} = \frac{m \times d}{\Delta \times \tan\varphi} \quad \textbf{Eq. 65}$$

Since $\tan\varphi = x/l$, then:

$$\overline{GM} = \frac{m \times d \times l}{\Delta \times x} \quad \textbf{Eq. 66}$$

In which:

RM	Righting moment.	N.m
HM	Heeling moment.	N.m
Δ	Yacht displacement.	kg
g	Acceleration due to gravity.	$m.s^{-2}$
$\overline{Gz}$	Righting lever, given in Eq. 58.	m
m	Inclining mass.	kg
d	Shifting distance from centreline.	m
$\overline{GM}$	Metacentric height.	m
φ	Heel angle.	°
x	Pendulum deflection.	m
l	Pendulum length.	m

Note that this gives the $\overline{GM}$ with the inclining weights onboard, in order to measure the actual $\overline{GM}$ of the boat, the height of the centre of gravity must be corrected for the inclining weights, based on a $\overline{GG'}$ shift:

$$\overline{GG'} = -\frac{\overline{Gg} \times m}{\Delta - m} \quad \textbf{Eq. 67}$$

In which:

$\overline{GG'}$	Shift in centre of gravity.	m
$\overline{Gg}$	Distance between the yacht and inclining weights centre of gravity.	m
Δ	Yacht displacement.	kg
m	Inclining mass.	kg

Consequently, the final $\overline{GM}_{final}$ is given by:

$$\overline{GM}_{final} = \overline{GM} - \overline{GG'} \quad \textbf{Eq. 68}$$

In which:

$\overline{GM}_{final}$	Yacht metacentric height.	m
$\overline{GM}$	Initial metacentric height.	m
$\overline{GG'}$	Shift in centre of gravity.	m

9.3.3 Accuracy

In order to achieve reliable results, a wide range of precautions should be taken, as detailed hereafter:

- The experiment shall be conducted in water as calm as possible, avoiding waves, tide and wind.
- Mooring must be slack enough not to restrict the heeling.
- The bilge should be dry to avoid free surface effect, and all items should be secured.
- The number of people onboard should be minimised, and ideally performed without anyone onboard.
- The weight and position of each inclining weight should be carefully recorded.
- The pendulum should be as long as possible, not less than 1800mm, and preferably a multiple of 57.3 (to equate radians to millimetres).

Furthermore, careful measurements of the draft forward and aft should be realised to measure the precise waterline the yacht is floating on, and thus the associated hydrostatics. Finally, recording the density of the water in which the experiment has been conducted will be required to accurately ascertain the hydrostatics.

9.3.4 Conclusions

The inclining experiment is the only way to locate the VCG. Based on small angle stability theory, the procedure to be carried out has been outlined. Once built, an inclining experiment is to be performed to prove compliance with the regulatory body (ISO 12217-2 [58]), and refine the velocity prediction program, which will consider stability at larger angles of heel.

9.4 Large Angle Stability

While small angle stability is relevant to the inclining experiment, it is not representative of a sailing yacht behaviour. Large angle stability is however not only restricted to normal sailing angles, but covers the whole spectrum from upright (0°) to fully capsized (180°). As a result, the vanishing angle of stability (angle past which the righting lever becomes negative, and thus the boat will inevitably capsize) and the upside down stability can be determined.

The stability is expressed as a function of the righting lever $\overline{Gz}$, which cannot be easily calculated for large heel angles; hence the development of specialised software, such as Hydromax [8], used in this instance. The A Rater analysis is depicted in Figure 38.

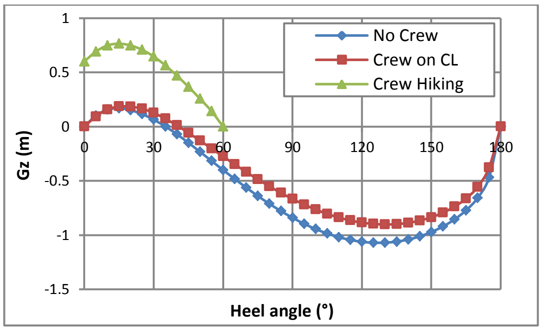

Figure 38: *$\overline{Gz}$ curve.*

Due to the large weight proportion of the crew, the ISO standard requires both the lightship and fully loaded conditions to be analyses. In both cases, the initial $\overline{Gz}$ is very low, and the inverted stability region is tremendous. This highlights the low stability of dinghies and inherent tendency to capsize. With the three crew members on the rail, a much higher righting lever is achieved, leading to a delayed angle of vanishing stability.

For the purpose of the stability evaluation, the most pessimistic $\overline{Gz}$ curve will be considered. However, in a worst case scenario for structural purposes, such as the maximum righting moment for the mast design, the $\overline{Gz}$ curve with all crew hiking is to be used.

9.5 Stability Assessment

9.5.1 Introduction

For category C and D boats, as defined in [95], the ISO 12217-2 [58] offers a range of options to demonstrate compliance, each with various criteria to satisfy, as summarised in Table 21.

Option	1	2	3	4	5	6
Downflooding openings	x	x	x	x	x	
Downflooding height	x	x		x		
Downflooding angle	x					
Angle of vanishing stability	x					
Stability Index	x					
Knockdown-recovery test		x	x			
Wind stiffness test				x	x	
Flotation requirements			x		x	
Capsize recovery test						x

Table 21: *ISO stability requirements [58].*

Understandably, option 6 is generally favoured since only a single practical test is necessary, which is particularly attractive.

However, for design interest as well as added safety and reliability, all criteria have been considered and applied where possible, and are detailed in the following subsections.

9.5.2 Downflooding Openings

Downflooding openings are particularly relevant to offshore yachts (category A and B), as it focuses on hatches, doors and exhaust openings. The only criterion applicable to the A Rater is the absence of downflooding points within 200mm of the waterline, which is met in this instance.

9.5.3 Downflooding Height

For category C and D, the minimum downflooding height of the centreboard case is shown in Figure 39.

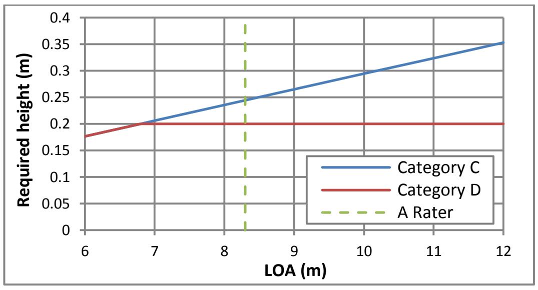

Figure 39: *Minimum downflooding height.*

For the A Rater, the 250mm height will be retained.

9.5.4 Downflooding Angle

The downflooding angle, previously identified as 48° in Section 6.2.1 largely meets the ISO criterion of 35° and 30° for category C and D respectively.

9.5.5 Angle of Vanishing Stability

The angle of vanishing stability is not particularly relevant to dinghies, where most of the righting moment is provided by the crew hiking. It is therefore no surprise that the minimum value of 75° for a category D boat is not met. This is however not an issue as the angle of vanishing stability is only required in one out of the six classification options.

9.5.6 Stability Index

The stability index, better known as STIX, is only relevant to larger crafts with fixed ballast, and is not satisfied by the A Rater.

Note that classification option 1 is the only one to require the downflooding angle, the angle of vanishing stability, and the stability index, and is clearly targeting larger yachts, more specifically keel boats. All other classification options are more suited to dinghies and capsize recoverable crafts.

9.5.7 Knockdown Recovery Test

The knockdown recovery test is a practical experiment aiming to demonstrate the ability of the boat to be recovered after a 90° knock down; the setup is illustrated in Figure 40.

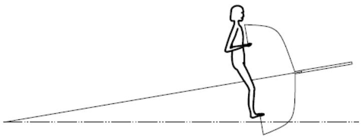

Figure 40: *Knockdown recovery test [58].*

After 60 seconds for a category C boat (or 10 seconds for category D), the yacht must still be afloat and the crew must be able to bring it back upright.

9.5.8 Wind Stiffness Test

The wind stiffness test experimentally demonstrates the appropriate wind speed so that the boat does not start flooding. This is done by artificially applying a known force at a given height, and converting it into an equivalent wind speed using the ISO calculation procedure [58]. Note that, should the A Rater fail this criterion, it can still be classified as a category C or D, provided appropriate warnings are featured in the user manual. This criterion is therefore not an issue in the case of the A Rater, aiming for Category C.

9.5.9 Flotation Requirements

To ensure the boat will not sink, a volume of flotation greater than the mass of the yacht is to be provided. Remembering the Thames A Rater class rule introduced in 1.2.6, a buoyancy volume greater than the lightship displacement is to be provided. As a result, this criterion has already been satisfied.

9.5.10 Capsize Recovery Test

The capsize recovery test consists in fully capsizing the yacht (upside down). The crew must be able to recover the boat, which should remain afloat at all times. The recovery must be realised in less than five minutes by the three crew members. This is the preferred method as classification as a category C boat can be obtained with this single test. Furthermore, this appears a very important test to be carried out to ensure the safety of the sailors.

9.5.11 Conclusions

Out of the six options for the classification of the A Rater, all but option 1 are easily accessible. Those experiments however represent a non-negligible amount of time, and the outcomes will impact on the content of the owner's manual. An appropriate amount of time will therefore be allocated for classification and testing after the end of the construction and before delivery to the owner.

Note that, in the very unlikely event where the A Rater should fail either the knockdown and capsize recovery test, and if retro-fitted ballast in the centreplate did not prove to be sufficient, the boat could still be classified. Indeed, option 4 and 5 could be used to successfully obtain a category C classification since the downflooding openings have been designed to comply, appropriate buoyancy is provided, and the wind stiffness test cannot be failled. This is however not recommended as the crew must be able to recover the boat, but offers a classification guarantee.

9.6 Conclusions

In order to be classified as an ISO category C craft, the A Rater is to comply with the ISO 12217-2.

Firstly, an inclining experiment based on small angle stability principles is to be conducted. As a result, the precise location of the centre of gravity will be located, and the stability assessment refined. At this stage, a pessimistic 5% margin has been added to the centre of gravity established via the weight estimate to be on the conservative side.

Large angle stability has then been tackled, which will play an important role as part of the velocity prediction program.

Finally, the criteria to be satisfied to meet the regulation have been outlined. A mathematical compliance proof cannot be provided for capsize recoverable dinghies, as it mostly relies on practical tests aiming to demonstrate the feasibility of the recovering. However, all design requirements have been incorporated, and it was proven that the boat could be classified even in the event of not passing the capsize recovery test, thus providing a guarantee to the builder and client that the yacht will receive the expected classification.

Chapter 10: Velocity Prediction Program

The velocity prediction is a significant part of the design, especially for racing yachts, as it quantifies the sailing performance and behaviour, as well as contrast different options. It also contributes to strategic choices when racing. The underpinning theory of the six degrees of freedom velocity prediction program created will be detailed. The importance of the program as part of the design process is clearly visible in the length of this chapter compared to previous ones.

10.1 Background Theory

10.1.1 Degrees of Freedom

10.1.1.1 Six Degrees of Freedom

The motion of a yacht in space can be described by six degrees of freedom, divided into three forces and three moments. The longitudinal, transverse and vertical forces are respectively known as surge (x), sway (y) and heave (z). The moments about the longitudinal, transverse and vertical axis are respectively named roll (φ), pitch (θ) and yaw (β). The degrees of freedom are depicted in Figure 41.

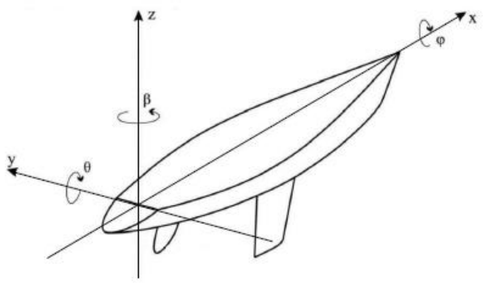

Figure 41: *Degrees of freedom [67].*

10.1.1.2 Coordinate System

For the purpose of the VPP realised in this instance, the coordinate systems illustrated in Figure 41 for the forces F and moments M applies:

- F_x (surge) positive forward.
- F_y (sway) positive to port.
- F_z (heave) positive upwards.
- M_x (roll) positive to starboard.
- M_y (pitch) positive downwards.
- M_z (yaw) positive to port.

As highlighted in previous work [108], the coordinate system is a decisive part of the VPP.

10.1.1.3 Relative Hierarchy

The degrees of freedom do not all have the same importance as part of a VPP.

Surge, which corresponds to the boat speed, is the paramount component to be ascertained. Roll and sway, respectively better known as heel and leeway angles, are the next most important components of the VPP.

In fact, most VPP are limited to boat speed, heel and leeway, and are therefore labelled as three degrees of freedom VPP.

In some cases, yaw, which relates to the rudder angle, will be incorporated, thus resulting in a four degrees of freedom VPP.

Heave and pitch are generally neglected for monohulls: the former being self-adjusted, and the latter being very small due to the large longitudinal stability of monohulls.

However, in the case of the A Rater, exhibiting planning behaviour and considering the ability of the crew to heavily trim the boat, the development of a six degrees of freedom VPP appears to be relevant to maximise accuracy.

10.1.2 Velocity Prediction Program

10.1.2.1 Aims

Velocity prediction programs aim at determining the optimum sailing conditions for a given true wind speed and true wind angle, such as the best sails combination, best VMG angle, best heel angle, etc… While this is particularly desirable for the sailors when racing to maximise performance, the VPP is also a major component of the design phase. Indeed, the primary aim of a racing boat is to be fast, and the theoretical speed can only be quantified through the VPP. This therefore allows for comparison and optimisation by studying the impact of multiple parameters on performance.

In addition to traditional VPP outputs, the program created in this instance will be more focussed on dinghies, with particular emphasis on the varying crew size and weight and planning.

The VPP constitutes the core of the design process and following evaluation in the case of the new A Rater.

10.1.2.2 Principle

The VPP relies on the equilibrium principle, i.e. the balance of forces and moments. For instance, the maximum boat speed is reached when the drag force equals the drive force. Moreover, the heel angle is the result of the equilibrium between the heeling and righting moment. The equilibrium equations for each degree of freedom are summarised in Table 22 and will be further discussed in the subsequent sections of this chapter.

DoF	Equilibrium equation
Surge	Drag force = Drive force
Sway	Aero side force = Hydro side force
Heave	Displacement force = Buoyancy force
Roll	Heeling moment = Righting moment
Pitch	Pitching moment = Righting moment
Yaw	Yaw moment = Restoring moment

Table 22: VPP equilibrium equations.

10.1.2.3 Program Development

The first decision regarding the VPP was the choice of the software to develop the program, the two candidates being Microsoft Excel [84] and Matlab [82] (or open source versions, respectively OpenOffice Math and Octave); the former is a cell-based spreadsheet whereas the latter is a multi-paradigm numerical coding application.

While Matlab would provide better graphics and easier coding since it is fully explicit, the arguments in favour of Excel outweigh those in favour of Matlab.

First of all, Excel is available and efficiently run by any device; this makes for an easier use of the program.

Furthermore, most people are familiar with Excel, which makes the program more accessible to owner and sailors.

Finally, the cell structure of an Excel spreadsheet clearly identifies the range of inputs, thus making the program more user-friendly. Conversely, the creation of a guide user interface (GUI) would be required in Matlab, leading to additional programing time without significant improvements to the VPP itself.

The proposed VPP will therefore be developed in Excel. The different modules involved will independently be introduced, to finally be brought together to achieve the balance of all six degrees of freedom.

10.2 Hydrodynamic Model

10.2.1 Resistance Models

The hydrodynamic resistance of sailing yachts can be broken down based on two different resistance concepts: the Froude model [25, 26] and the International Towing Tank Conference (ITTC) model [50, 51].

10.2.1.1 Froude Model

Presented in 1872 by the hydrodynamic pioneer William Froude [25], the resistance is stripped down into two components: the friction resistance R_f and the residuary resistance R_r, giving the total resistance R_t as:

$$R_t = R_f + R_r \qquad \textbf{Eq. 69}$$

In which:

R_t	Total hydrodynamic resistance.	N
R_f	Frictional resistance.	N
R_r	Residuary resistance.	N

Froude defines the frictional resistance as the drag of a flat plate having the same area as the yacht's wetted surface area; all other components of the resistance being encapsulated in the residuary resistance.

10.2.1.2 ITTC model

The more modern ITTC model divides the resistance into the viscous and wave components, respectively R_v and R_w. Hence the total resistance R_t:

$$R_t = R_v + R_w \qquad \textbf{Eq. 70}$$

In which:

R_t	Total hydrodynamic resistance.	N
R_v	Viscous resistance.	N
R_w	Wave resistance.	N

Note that the viscous resistance is the effect of the three dimensional shape of the hull on the friction resistance.

10.2.1.3 Conclusions

Both resistance models are still common nowadays, the ITTC being preferred for experimental analysis, while the Froude one is employed in empirical methods such as the Delft Systematic Yacht Hull Series (DSYHS) [66], further discussed in Section 10.2.3.

10.2.2 Methods

10.2.2.1 Resistance Prediction

Four main methods are available at a design stage to establish the resistance of a yacht: towing tank testing, RANSE CFD, Panel Code CFD, and semi-empirical methods such as the DSYHS.

In this case, both towing tank testing and panel code CFD are not available. The tremendous expense of towing tank testing cannot be justified, and no panel code CFD was available. The choice therefore lies between RANSE CFD and the DSYHS in this case.

10.2.2.2 RANSE vs DSYHS

The semi-empirical method proposed by the DSYHS has been preferred to RANSE CFD due to two main factors.

On the one hand, the DSYHS is more flexible, which allows to compute a large range of designs, making the optimisation process much faster. In addition, the DSYSH is instantly applicable to a wide spectrum of crafts, whereas CFD would have to be repeated for each one. The DSHYS will allow the VPP to analyse any boat and provide an instantaneous analysis.

On the other hand, with the computational resources available, a RANSE analysis is not feasible. For a VPP, a squared out matrix is needed. Considering eight speeds, four heel angles, three yaw angles, three rudder angles, two trim angles and two displacements, a total of 1152 simulations would be required to achieve six degrees of freedom. To obtain results, the expected solving time per simulation is of the order of 10 hours [107]. In this case, 480 days of simulation would be necessary, four times the time allocated for the entire design. This method appears not feasible without a large cluster available.

Finally, previous work undertaken by the author [108] demonstrated that the DSYHS should be preferred to CFD for its greater reliability and its better suited application as part of a VPP hydrodynamic model. The DSYHS has therefore been retained to model the hydrodynamic resistance as part of the VPP realised.

10.2.2.3 DSYHS Calculation Method

The DSYHS is a semi-empirical resistance prediction method dating back to the 1970s. Over 70 model yachts have been tested, and regression equations have been developed to predict the resistance. The method is extremely popular, and fully documented thanks to a vast literature, first published by Gerritsma [32, 33, 34] and more recently Keuning [61, 62, 63, 64, 65, 66, 67, 68].

10.2.3 DSYHS

10.2.3.1 Range of Parameters

For the DSYHS to apply, i.e. for the regression method to be valid, the yacht must fit within a given range of parameters, presented in Table 23 and demonstrating the compliance of the A Rater.

Parameter	Range			A Rater	Comply?
Lwl/Bwl	2.73	to	5.00	3.37	Yes
Bwl/Tc	2.46	to	19.38	10.24	Yes
$Lwl/\nabla_c^{1/3}$	4.34	to	8.50	6.49	Yes
LCB_{fpp}	0.00%	to	-8.20%	-1.30%	Yes
LCF_{fpp}	-1.80%	to	-9.50%	-1.87%	Yes
Cp	0.52	to	0.60	0.546	Yes
Cm	0.65	to	0.78	0.762	Yes
$Aw/\nabla_c^{2/3}$	3.78	to	12.67	9.77	Yes

Table 23: DSYHS range of parameters.

Since the new A Rater fits within the permitted range of design ratios, the method will be applied. Note that, since the VPP is also aimed at future use on other yachts, a DSYHS module has been set up to check those parameters, and provide appropriate warnings should the boat not meet the requirements.

10.2.3.2 Bare Hull: Upright

The upright frictional resistance R_{fh} is given by:

$$R_{fh} = \frac{1}{2} \times \rho \times V^2 \times Sc \times C_f \quad \textit{Eq. 71}$$

If unknown, the wetted area Sc can be estimated as:

$$Sc = \left(1.97 + 0.171 \times \frac{Bwl}{Tc}\right) \times \sqrt[3]{\frac{0.65}{Cm}} \times \sqrt{\nabla c \times Lwl} \quad \textit{Eq. 72}$$

And:

$$C_f = \frac{0.075}{(log_{10} Rn - 2)^2} \quad \textit{Eq. 73}$$

With:

$$Rn = \frac{\rho \times V \times 0.7 \times Lwl}{\mu} \quad \textit{Eq. 74}$$

In which:

R_{fh}	Upright hull friction resistance.	N
ρ	Water density.	$kg.m^{-3}$
V	Boat speed.	$m.s^{-1}$
Sc	Hull wetted surface area.	m^2
C_f	ITTC 1957 friction coefficient.	-
Bwl	Waterline beam.	m
Tc	Canoe body draft.	m
Cm	Midship coefficient.	-
∇c	Canoe body volume.	m^3
Lwl	Waterline length.	m
Rn	Reynolds number.	-
μ	Water viscosity.	$kg.(s.m)^{-1}$

The DSYHS suggests that only 70% of the Lwl is utilised for the Reynolds number, to account for the fact that the ITTC 1957 friction coefficient [37] was elaborated for ships that feature a parallel mid-body absent on yachts. Although debatable, this approach is commonly used.

On the other hand, the upright hull residuary resistance Rrh is given by:

$$\frac{R_{rh}}{\nabla c \times \rho \times g} = a_0 + \left(a_1 \times \frac{LCB_{fpp}}{Lwl} + a_2 \times Cp + a_3 \times \frac{\nabla c^{2/3}}{Aw} + a_4 \times \frac{Bwl}{Lwl} + a_5 \times \frac{LCB_{fpp}}{LCF_{fpp}} + a_6 \times \frac{Bwl}{Tc} + a_7 \times Cm\right) \times \frac{\nabla c^{1/3}}{Lwl} \quad \textit{Eq. 75}$$

In which:

Rrh	Residiary resistance.	N
∇c	Hull displacement.	m^3
ρ	Water density.	$kg.m^{-3}$
g	Acceleration due to gravity.	$m.s^{-2}$
LCB_{fpp}	LCB location from the FPP.	m
Lwl	Waterline length.	m
Cp	Prismatic coefficient.	-
Aw	Waterplane area.	m^2
Bwl	Waterline beam.	m
LCF_{fpp}	LCF location from the FPP.	m
Tc	Canoe body draft.	m
Cm	Midship area coefficient.	-
a_0 to a_7	Regression coefficients given in Table 24.	-

Fn	a_0	a_1	a_2	a_3	a_4	a_5	a_6	a_7
0.15	-0.0005	0.0023	-0.0086	-0.0015	0.0061	0.0010	0.0001	0.0052
0.20	-0.0003	0.0059	-0.0064	0.0070	0.0014	0.0013	0.0005	-0.0020
0.25	-0.0002	-0.0156	0.0031	-0.0021	-0.0070	0.0148	0.0010	-0.0043
0.30	-0.0009	0.0016	0.0337	-0.0285	-0.0367	0.0218	0.0015	-0.0172
0.35	-0.0026	-0.0567	0.0446	-0.1091	-0.0707	0.0914	0.0021	-0.0078
0.40	-0.0064	-0.4034	-0.1250	0.0273	-0.1341	0.3578	0.0045	0.1150
0.45	-0.0218	-0.5261	-0.2945	0.2486	-0.2428	0.6293	0.0081	0.2086
0.50	-0.0388	-0.5986	-0.3038	0.6033	-0.0430	0.8332	0.0106	0.1336
0.55	-0.0347	-0.4764	-0.2361	0.8726	0.4219	0.8990	0.0096	-0.2272
0.60	-0.0361	0.0037	-0.2960	0.9661	0.6123	0.7534	0.0100	-0.3352
0.65	0.0008	0.3728	-0.3667	1.3957	1.0343	0.3230	0.0072	-0.4632
0.70	0.0108	-0.1238	-0.2026	1.1282	1.1836	0.4973	0.0038	-0.4477
0.75	0.1023	0.7726	0.5040	1.7867	2.1934	-1.5479	-0.0115	-0.0977

Table 24: DSYHS a_i coefficients.

The sum of the frictional and residuary resistance gives the total bare hull upright resistance, to which the appendages can be added.

Note that the DSYHS does not include a resistance component that is actually not negligible: the roughness resistance. Indeed, the surface of the hull and appendages will suffer from imperfections, unfairness, wear and tear and weeds growing, which leads to a certain amount of roughness resistance R_a that is calculated as follows:

$$R_a = \frac{1}{2} \times \rho \times S \times V^2 \times C_a \qquad \textit{Eq. 76}$$

In which:

R_a	Roughness resistance.	N
ρ	Water density.	kg.m^{-3}
S	Overall wetted area (hull and appendages).	m^2
V	Inflow speed.	m.s^{-1}
C_a	Roughness coefficient.	-

The value of the roughness coefficient is taken as the standard ship value of 0.0004 [71], which is commonly assumed for yachts in the absence of better suited data.

10.2.3.3 Appendages: Upright

For the appendages, the viscous resistance $R_{v\,app}$ is:

$$R_{v\,app} = R_f \times (1 + k) \qquad \textit{Eq. 77}$$

With the form factor based on Hoerner's formula [48]:

$$(1 + k) = 1 + 2 \times \frac{t}{c} + 60 \times \left(\frac{t}{c}\right)^4 \qquad \textit{Eq. 78}$$

In which:

$R_{v\,app}$	Viscous appendage resistance.	N
R_f	Based on Eq. 71, using the appendage wetted area and Reynolds number.	N
$1 + k$	Form factor.	-
t	Mean thickness.	m
c	Mean chord length.	m

While this is applicable to both the centreplate and rudder, the residuary resistance of the rudder is neglected; hence the keel residuary resistance $R_{r\,k}$:

$$\frac{R_{r\,k}}{\nabla_k \times \rho \times g} = A_0 + A_1 \times \frac{T}{Bwl} + A_2 \times \frac{Tc + Zcb_k}{{\nabla_k}^{1/3}} + A_3 \times \frac{\nabla_c}{\nabla_k} \qquad \textit{Eq. 79}$$

In which:

$R_{r\,k}$	Upright keel residuary resistance.	N
∇_k	Keel volume.	m^3
ρ	Water density.	kg.m^{-3}
g	Acceleration due to gravity.	m.s^{-2}
T	Total draft.	m
Bwl	Waterline beam.	m
Tc	Canoe body draft.	m
Zcb_k	Keel vertical centre of buoyancy.	m
∇_c	Canoe body volume.	m^3
A_0 to A_3	Regression coefficients given in Table 25.	-

Fn	A_0	A_1	A_2	A_3
0.20	-0.00104	0.00172	0.00117	-0.00008
0.25	-0.00550	0.00597	0.00390	-0.00009
0.30	-0.01110	0.01421	0.00069	0.00021
0.35	-0.00713	0.02632	-0.00232	0.00039
0.40	-0.03581	0.08649	0.00999	0.00017
0.45	-0.00470	0.11592	-0.00064	0.00035
0.50	0.00553	0.07371	0.05991	-0.00114
0.55	0.04822	0.00660	0.07048	-0.00035
0.60	0.01021	0.14173	0.06409	-0.00192
Coefficients are multiplied by 1000				

Table 25: *DSYHS keel coefficients.*

From the upright, the heeled and yawed conditions can be considered, thus covering the actual sailing behaviour of yachts.

10.2.3.4 Bare hull: Heeled

The heeled frictional resistance is calculated as presented in Eq. 71 for the upright condition, but incorporating the heeled wetted surface area Sc_φ, which can be approximated as:

$$Sc_\varphi = Sc_{\varphi=0} \times \left(1 + \frac{1}{100}\left(s_0 + s_1 \times \frac{Bwl}{Tc} + s_2 \times \left(\frac{Bwl}{Tc}\right)^2 + s_3 \times Cm\right)\right) \qquad \textit{Eq. 80}$$

In which:

Sc_φ	Heeled wetted surface area.	m^2
$Sc_{\varphi=0}$	Upright wetted surface area.	m^2
Bwl	Waterline beam.	m
Tc	Canoe body draft.	m
Cm	Midship coefficient.	-
s_0 to s_3	Regression coefficient, given in Table 26.	-

φ	s_0	s_1	s_2	s_3
5°	-4.112	0.054	-0.027	6.329
10°	-4.522	-0.132	-0.077	8.738
15°	-3.291	-0.389	-0.118	8.949
20°	1.850	-1.200	-0.109	5.364
25°	6.510	-2.305	-0.066	3.443
30°	12.334	-3.911	0.024	1.767
35°	14.648	-5.182	0.102	3.497

Table 26: *DSYHS s_i coefficients.*

The method is applicable up to 35° of heel, which covers the vast majority of the normal sail conditions.

The residuary resistance is determined in a different manner. First, the difference (delta) in residuary resistance at 20° of heel $\Delta R_{r\,\varphi=20°}$ compared to upright is calculated, and then corrected for any heel angle up to 30°.

$$\frac{\Delta R_{rh\,\varphi=20°}}{\nabla c \times \rho \times g} = u_0 + u_1 \times \frac{Lwl}{Bwl} + u_2 \times \frac{Bwl}{Tc} + u_3 \times \left(\frac{Bwl}{Tc}\right)^2 + u_4 \times LCB + u_5 \times LCB^2 \qquad \textit{Eq. 81}$$

For any heel angle φ:

$$\Delta R_{rh\,\varphi} = \Delta R_{rh\,\varphi=20°} \times 6 \times \varphi^{1.7} \qquad \textit{Eq. 82}$$

Hence the residuary resistance at any heel angle:

$$R_{rh\,\varphi} = R_{rh\,\varphi=0°} + \Delta R_{rh\,\varphi} \qquad \textit{Eq. 83}$$

In which:

$\Delta R_{rh\,\varphi=20°}$	Delta residuary resistance at 20° of heel.	N
∇c	Canoe body volume.	m^3
ρ	Water density.	$kg.m^{-3}$
g	Acceleration due to gravity.	$m.s^{-2}$
Lwl	Waterline length.	m
Bwl	Waterline beam.	m
Tc	Canoe body draft.	m
LCB	Longitudinal centre of buoyancy.	m
u_0 to u_5	Regression coefficient, given in Table 27.	-
$\Delta R_{rh\,\varphi}$	Delta residuary resistance at any heel angle (up to 30°).	N
φ	Heel angle.	°
$R_{rh\,\varphi}$	Heeled hull residuary resistance.	N
$R_{rh\,\varphi=0°}$	Upright hull residuary resistance.	N

Fn	u_0	u_1	u_2	u_3	u_4	u_5
0.25	-0.0268	-0.0014	-0.0057	0.0016	-0.0070	-0.0017
0.30	0.6628	-0.0632	-0.0699	0.0069	0.0459	-0.0004
0.35	1.6433	-0.2144	-0.1640	0.0199	-0.0540	-0.0268
0.40	-0.8659	-0.0354	0.226	0.0188	-0.5800	-0.1133
0.45	-3.2715	0.1372	0.5547	0.0268	-1.0064	-0.2026
0.50	-0.1976	-0.1480	-0.6593	0.1862	-0.7489	-0.1648
0.55	1.5873	-0.3749	-0.7105	0.2146	-0.4818	-0.1174
Coefficients are multiplied by 1000						

Table 27: *DSYHS u_i coefficients.*

The sum of the heeled frictional and residuary resistance gives the total hull resistance, to which the heeled appendages resistance can be added.

10.2.3.5 Appendages: Heeled

The viscous resistance of the appendages remains unchanged as the yacht heels; a valid assumption provided the centreboard and rudder remain fully immersed.

The rudder residuary resistance is still unaccounted for by the DSYHS, while the change (delta) in keel residuary resistance at any heel angle $\Delta R_{rk\,\varphi}$ is given by:

$$\frac{\Delta R_{rk\,\varphi}}{\nabla_k \times \rho \times g} = \left(H_1 \times \frac{Tc}{T} + H_2 \times \frac{Bwl}{Tc} + H_3 \times \frac{Tc}{T} \times \frac{Bwl}{Tc} + H_4 \times \frac{Lwl}{\nabla_k^{\frac{1}{3}}}\right) \times Fn^2 \times \varphi \quad \textbf{Eq. 84}$$

In which:

$\Delta R_{rk\,\varphi}$	Heeled keel delta residuary resistance.	N
∇_k	Keel volume.	m^3
ρ	Water density.	$kg.m^{-3}$
g	Acceleration due to gravity.	$m.s^{-2}$
Tc	Canoe body draft.	m
T	Overall draft.	m
Bwl	Waterline beam.	m
Lwl	Waterline length.	m
Fn	Froude number.	-
φ	Heel angle.	°
H_1 to H_4	Regression coefficients given in Table 28.	-

H_1	H_2	H_3	H_4
-3.5837	-0.0518	0.5958	0.2055

Table 28: *DSYHS H_i coefficients.*

Finally, the appendages are to operate at an angle of yaw to develop lift, a case considered by the DSYHS. But first, the extended keel method assumption must be detailed.

10.2.3.6 Extended Keel Method

Yacht foils such as keels and rudders experience tip losses at one end only since the other one is in contact with the hull. This leads to the mirror boundary effect, introduced for the jib in Section 4.3.2, that effectively doubles the aspect ratio of the foil. In order to account for the effect of the rudder and asymmetry of the waterplane as the yacht heels, the calculations are performed using an extended keel, or centreplate in this case, which is projected to and mirrored about the waterline, as shown in Figure 42.

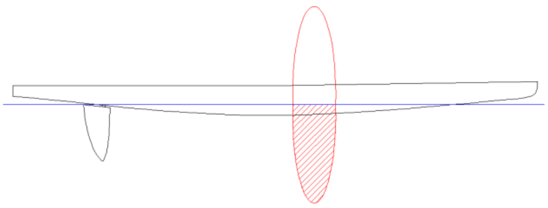

Figure 42: *Extended keel method.*

The yawed calculations rely on this assumption.

10.2.3.7 Appendages: Yawed

By generating lift, the appendages also create side force, and an induced drag component.

Firstly, the effective draft Te is assessed:

$$\frac{Te}{T} = \left(A_1 \times \frac{Tc}{T} + A_2 \times \left(\frac{Tc}{T}\right)^2 + A_3 \times \frac{Bwl}{Tc} + A_4 \times TR\right) \times (B_0 + B_1 \times Fn) \quad \textbf{Eq. 85}$$

In which:

Te	Effective draft.	m
T	Overall draft.	m
Tc	Canoe body draft.	m
Bwl	Waterline beam.	m
TR	Taper ratio.	-
Fn	Froude number.	-
A_1 to A_4	Regression coefficients given in Table 29.	-
B_0 and B_1	Regression coefficients given in Table 30.	-

φ	A_1	A_2	A_3	A_4
0°	3.7455	-3.6246	0.0589	-0.0296
10°	4.4892	-4.8454	0.0294	-0.0176
20°	3.9592	-3.9804	0.0283	-0.0075
30°	3.4891	-2.9577	0.0250	-0.0272

Table 29: *DSYHS A_i coefficients.*

φ	B_0	B_1
0°	1.2306	-0.7256
10°	1.4231	-1.2971
20°	1.5450	-1.5622
30°	1.4744	-1.3499

Table 30: *DSYHS B_i coefficients.*

Applying the extended keel method, the lateral area of the appendages is:

$$A_{lat} = \bar{c} \times T \quad \textbf{Eq. 86}$$

Hence the effective ratio:

$$AR_e = \frac{Te^2}{A_{lat}} \quad \textbf{Eq. 87}$$

In which:

A_{lat}	Appendage lateral area.	m²
$\bar{c}$	Appendage mean chord.	m
T	Overall draft.	m
AR_e	Effective aspect ratio.	-
Te	Effective draft.	m

Based on the effective aspect ratio, the lift and induced drag coefficient are respectively:

$$C_L = \frac{2\pi \times \lambda}{1 + \frac{2}{AR_e}} \qquad \textit{Eq. 88}$$

And:

$$C_{Di} = \frac{C_L^2}{\pi \times AR_e} \qquad \textit{Eq. 89}$$

In which:

C_L	Lift coefficient.	-
λ	Angle of attack.	°
AR_e	Effective aspect ratio.	-
C_{Di}	Induced drag coefficient.	-

Finally, the side force Fh and induced drag Ri can be found:

$$Fh = C_L \times \frac{1}{2} \times \rho \times A_{lat} \times V^2 \qquad \textit{Eq. 90}$$

And

$$Ri = C_{Di} \times \frac{1}{2} \times \rho \times A_{lat} \times V^2 \qquad \textit{Eq. 91}$$

In which:

Fh	Side force.	N
C_L	Lift coefficient.	-
ρ	Water density.	kg.m^{-3}
A_{lat}	Appendage lateral area.	m²
V	Inflow speed.	m.s^{-1}
Ri	Induced drag.	N
C_{Di}	Induced drag coefficient.	-

Note that, at this stage, the rudder is assumed to be fixed on centreline; the lift and induced drag due to a rudder position off centreline will be tackled in Section 10.5.2.2.

10.2.3.7 Conclusions

The hydrodynamic resistance of a sailing yacht can be quantified over a range of sailing conditions thanks to the DSYHS.

10.2.4 Conclusions

The hydrodynamics of the A Rater will be modelled using the DSYHS for it greater flexibility and faster solving time compared to a RANSE CFD analysis. The calculation process has been thoroughly detailed, and will be part of the VPP.

Thanks to decades of research and the popularity of the method, its validity is agreed and has been demonstrated in previous work [108], provided the vessel fits within the range of parameter, which the A Rater does.

Note that added resistance due to waves has been neglected in this instance since the A Raters are racing on inland waterways, and therefore do not encounter waves.

To achieve equilibrium of the resistance and drive force, the sails forces must be determined in the aerodynamic model, which comprises further drag components to be added to the resistance.

10.3 Aerodynamic Model

10.3.1 Velocity Triangle

The inputs for the velocity prediction program are the true wind speed (TWS) and true wind angle (TWA), these conditions are however not those experienced by the yacht. Due to the boat speed, the sails operate at an apparent wind speed (AWS) and apparent wind angle (AWA), illustrated in Figure 43 and mathematically given by:

$$V_a \times \cos\beta_a = V_s + V_t \times \cos\beta_t \qquad \textit{Eq. 92}$$

And:

$$V_a \times \sin\beta_a = V_t \times \sin\beta_t \qquad \textit{Eq. 93}$$

In which:

V_a	Apparent wind speed.	m.s^{-1}
β_a	Apparent wind angle.	°
V_s	Boat speed.	m.s^{-1}
V_t	True wind speed.	m.s^{-1}
β_t	True wind angle.	°

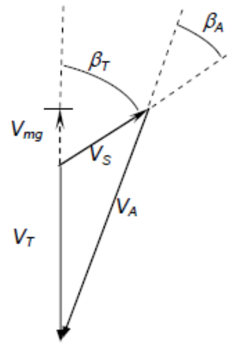

Figure 43: *Velocity triangle [38].*

Neglecting the effect of pitch, the impact of heel on the apparent wind speed and angle can be established based on the effective angle theory [38] that gives:

$$\beta_{eff} = tan^{-1}(\tan\beta_a \times \cos\varphi) \qquad \textit{Eq. 94}$$

And:

$$V_{eff} = V_a\sqrt{1 - sin^2\,\beta_a \times sin^2\,\varphi} \qquad \textit{Eq. 95}$$

In which:

β_{eff}	Effective wind angle.	°
β_a	Apparent wind angle.	°
φ	Heel angle.	°
V_{eff}	Effective wind speed.	m.s^{-1}
V_a	Apparent wind speed.	m.s^{-1}

Effective angle theory will only be applied up to a 90° of true wind angle, as it is not suited to downwind sailing [38].

Finally, a very important concept in yacht performance is the velocity made good (VMG), which is the boat speed in the direction of the wind:

$$VMG = V_s \times \cos \beta_t \qquad \textit{Eq. 96}$$

In which:

VGM	Velocity made good.	$m.s^{-1}$
V_s	Boat speed.	$m.s^{-1}$
β_t	True wind angle.	°

The wind triangle depends on the true wind speed, which varies with height in a specific velocity profile, as introduced earlier in Section 4.3.4.

10.3.2 Velocity Profile

The true wind speed varies with height according to:

$$V_t(z) = V_{t\,ref} \times \frac{\ln\left(z/z_0\right)}{\ln\left(z_{ref}/z\right)} \qquad \textit{Eq. 97}$$

In which:

$V_t(z)$	True wind speed at a height z.	$m.s^{-1}$
$V_{t\,ref}$	Reference true wind speed.	$m.s^{-1}$
z	Height.	m
z_0	Roughness length, given in Eq. 98.	m
z_{ref}	Reference height.	m

Since the surface of the water becomes rougher as the wind speed increases, the following equation for the roughness length has been suggested [22]:

$$z_0 = 5 \times 10^{-5} \times \frac{V_{t\,10}^2}{g} \qquad \textit{Eq. 98}$$

In which:

z_0	Roughness length.	m
$V_{t\,10}$	True wind speed at z=10m.	m
g	Acceleration due to gravity.	$m.s^{-2}$

The resulting wind gradient for a 5 m/s true wind speed at a 10m height is presented in Figure 44.

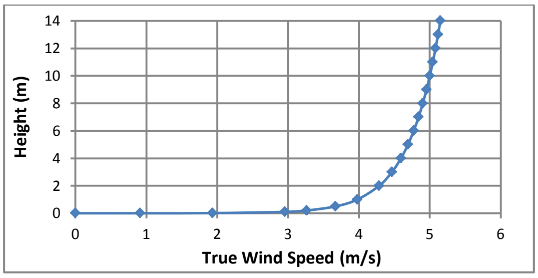

Figure 44: Wind gradient for 5 m/s TWS.

The sail forces will be assessed for this wind gradient.

10.3.3 Sail Forces

10.3.3.1 Introduction

As any foil, the sails develop lift and drag; once those are known, the aerodynamic drive force and sail side force can be resolved. The sail drag can be broken down into 3 main components: parasitic, induced and separation drag. The method detailed in this section is based on Hazen's aerodynamic model [47]; however, the sail coefficients used are those of the Offshore Racing Congress (ORC) [91].

10.3.3.2 Lift and Parasitic Drag Coefficients

Lift and parasitic drag coefficients are available to evaluate the sail forces. Those of Hazen [47] are still very popular as part of VPP. Nevertheless, the ORC coefficients have been preferred in this instance. First of all, they consider a wider range of true wind angle, with more data points. Secondly, those coefficients are more representative of modern sail design. Finally, the ORC sail coefficients are part of the ORC VPP based handicap system, and therefore have a proven validity. Those coefficients are given in Table 31.

Mainsail			Jib		
B_a (°)	C_L	C_{Dp}	B_a (°)	C_L	C_{Dp}
0	0.000	0.043	7	0.000	0.050
7	0.948	0.026	15	1.100	0.032
9	1.138	0.023	20	1.475	0.031
12	1.250	0.023	27	1.500	0.037
28	1.427	0.033	50	1.430	0.250
60	1.269	0.113	60	1.250	0.350
90	1.125	0.383	100	0.400	0.730
120	0.838	0.969	150	0.000	0.950
150	0.296	1.316	180	-0.100	0.900
180	-0.112	1.345			

Table 31: ORC sail coefficients.

The lift and parasitic drag coefficient for the combined jib and mainsail are respectively:

$$C_L = \frac{C_{L\,main} \times A_{main} + C_{L\,jib} \times A_{jib}}{A_{main} + A_{N\,jib}} \qquad \textit{Eq. 99}$$

And:

$$C_{Dp} = \frac{C_{Dp\,main} \times A_{main} + C_{Dp\,jib} \times A_{jib}}{A_{main} + A_{N\,jib}} \qquad \textit{Eq. 100}$$

Where:

$$A_{main} = 0.5 \times P \times E \qquad \textit{Eq. 101}$$

$$A_{jib} = 0.5 \times \sqrt{I^2 + J^2} \times LP \qquad \textit{Eq. 102}$$

$$A_{N\,jib} = 0.5 \times I \times J \qquad \textit{Eq. 103}$$

In which:

C_L	Combined lift coefficient.	-
$C_{L\,main}$	Mainsail lift coefficient.	-
A_{main}	Mainsail area, see Eq. 101.	m²
$C_{L\,jib}$	Jib lift coefficient.	-
A_{jib}	Jib area, see Eq. 102.	m²
$A_{N\,jib}$	Jib nominal area, see Eq. 103.	m²
C_{Dp}	Combined parasitic drag coefficient.	-
$C_{Dp\,main}$	Mainsail combined parasitic drag coefficient.	-
$C_{Dp\,jib}$	Jib combined parasitic drag coefficient.	-
P	Mailsail luff.	m
E	Mainsail foot.	m
I	Jib luff.	m
J	Jib foot.	m
LP	Jib luff perpendicular.	m

In addition to the parasitic component of drag, the induced and separation ones must be considered.

10.3.3.3 Induced and Separation Drag Coefficient

Both the induced and separation drag are gathered together in a single equation:

$$C_{Di} = {C_L}^2 \times \left(\frac{1}{\pi \times AR} + 0.005\right) \qquad \textbf{\textit{Eq. 104}}$$

In which:

C_{Di}	Induced and separation drag coefficient.	-
C_L	Sails lift coefficient.	-
AR	Aspect ratio.	-

Note that the constant 0.005 accounts for separation drag. As expected for induced drag, the aspect ratio has a large impact, and is determined in a different manner for close hauled courses (up to 30° AWA) which models the jib mirror boundary effect, and other courses. Those two different aspects ratios are respectively given by:

$$AR_{ch} = \frac{(1.1 \times (E_{MH} + FA))^2}{A_{main} + A_{N\,jib}} \qquad \textbf{\textit{Eq. 105}}$$

And:

$$AR_o = \frac{(1.1 \times E_{MH})^2}{A_{main} + A_{N\,jib}} \qquad \textbf{\textit{Eq. 106}}$$

In which:

AR_{ch}	Close hauled aspect ratio.	-
E_{MH}	Mast height from sheer.	m
FA	Average freeboard.	m
A_{main}	Mainsail area.	m²
$A_{N\,jib}$	Jib nominal area.	m²
AR_o	Other course aspect ratio.	-

Now having all components of the drag coefficient, the lift and drag of the sails can be found.

10.3.3.4 Total Drag

The total drag coefficient C_D is the sum of the parasitic and induced (comprising separation) coefficients; mathematically:

$$C_D = C_{Dp} + C_{Di} \qquad \textbf{\textit{Eq. 107}}$$

In which:

C_D	Sails drag coefficient.	-
C_{Dp}	Parasitic drag coefficient.	-
C_{Di}	Induced and separation drag coefficient.	-

The sails lift L and drag D can then be calculated using:

$$L = C_L \times \frac{1}{2} \times \rho \times SA \times {V_{eff}}^2 \qquad \textbf{\textit{Eq. 108}}$$

And:

$$D = C_D \times \frac{1}{2} \times \rho \times SA \times {V_{eff}}^2 \qquad \textbf{\textit{Eq. 109}}$$

In which:

L	Sails lift.	N
C_L	Lift coefficient.	-
ρ	Water density.	kg.m^{-3}
SA	Sail area.	m²
V_{eff}	Effective wind speed.	m.s^{-1}
D	Sails drag.	N
C_D	Drag coefficient.	-

Lift acts perpendicular to the flow, while drag acts parallel to it. In the case of a yacht, the forces have to be resolved in terms of drive and side force.

10.3.3.5 Force Resolution

A schematic of the force resolution from the lift and drag of the sails into the drive and side force is proposed in Figure 45.

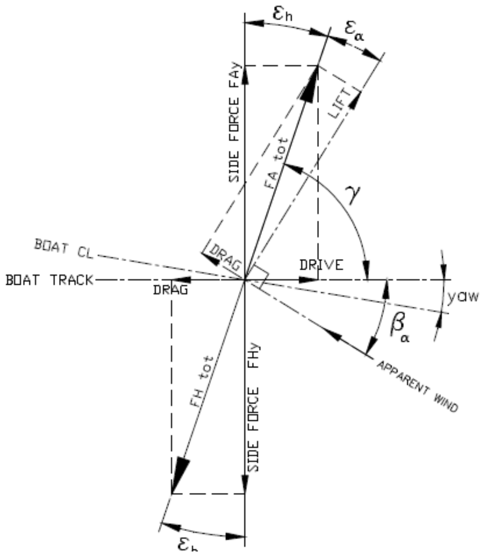

Figure 45: *Sail forces resolution [116].*

The drive force Dr and sail side force SFF are respectively:

$$Dr = L \times \sin\,(\beta_{eff} - \lambda) - D \times \cos\,(\beta_{eff} - \lambda) \qquad \textbf{\textit{Eq. 110}}$$

And:

$$SSF = L \times \cos\,(\beta_{eff} - \lambda) - D \times \sin\,(\beta_{eff} - \lambda) \qquad \textbf{\textit{Eq. 111}}$$

In which:

Dr	Drive force.	N
L	Sails lift.	N
β_{eff}	Effective wind angle at the centre of effort height.	°
λ	Leeway angle.	°
D	Sails drag.	N
SSF	Sail side force.	N

Note that the sail side force is actually the heeling force, which can be transposed into the actual side force in the horizontal plane by multiplying by the cosine of the heel angle.

10.3.3.6 Conclusions

From the lift and drag coefficients of the sails, the forces have been resolved into the components of main interest for a VPP, namely the drive and side force.

10.3.4 Depowering

In certain circumstances, a higher speed can be achieved by depowering the sails. A good example is reefing in higher wind speeds: the full sail area would create too much heeling moment and could not be handled by the crew, whereas a reefed mainsail will actually provide a higher drive force and therefore a faster boat.

Experimental research highlighted that depowering parameters such as ease and twist are more representative of actual yacht depowering behaviour [39]. However, the traditional reef and flat have been used in this instance for there well established role in VPP, as well as the easier mathematical modelling.

The reef parameter reduces the sail area while conserving the aspect ratio, leading to a lessened lift and drag as well as a lower centre of effort, which decreases the heeling arm. One of the issues with the reef function is that the values are somewhat unrealistic. Indeed, the VPP will detect the optimum reef among the infinite number of possibilities, while an actual sail will only have a limited number of reefing points, corresponding to a set proportion of the original sail area. As part of the design phase, this allows to assess the most appropriate reefing factors, and thus influence the mainsail development.

On the other hand, the flat parameter allows to flatten the sail, reducing the lift and induced drag; the parasitic drag, sail area and centre of effort however remain unchanged.

Mathematically, reef r and flat f impact on the lift and induced drag coefficients as follows:

$$C_L = C_{L\,opt} \times r^2 \times f \qquad \textbf{Eq. 112}$$

And:

$$C_{Di} = \frac{{C_{L\,opt}}^2 \times r^2 \times f^2}{\pi \times e \times AR} \qquad \textbf{Eq. 113}$$

In which:

C_L	Lift coefficient.	-
$C_{L\,opt}$	Optimum lift coefficient.	-
r	Reef function.	-
f	Flat function.	-
C_{Di}	Induced drag coefficient.	-
e	Efficiency factor.	-
AR	Aspect ratio.	-

The reduction in centre of effort height due to reefing is:

$$z_{CE} = z_{boom} + (z_{CE\,opt} - z_{boom}) \times r \qquad \textbf{Eq. 114}$$

In which:

z_{CE}	Centre of effort height.	m
z_{boom}	Boom height.	m
$z_{CE\,opt}$	Optimum centre of effort height.	m
r	Reef function.	-

In order to optimise the performance in higher wind speeds, depowering will be included as part of the VPP.

10.3.5 Windage

10.3.5.1 Introduction

So far, the aerodynamic analysis has been focused on the sail forces. There is however a whole other dimension to the aerodynamic model, which is the windage, i.e. the aerodynamic drag of the hull, crew and rigging, to be added to the hydrodynamic resistance.

10.3.5.2 Calculation

Various windage calculation procedures have been developed for VPP purposes, such as those of Hazen [47] and Van Oossanen [114]. They however do not offer the possibility to model the windage of multiple components: only the hull and rig being considered. As a result, the first principles approach proposed by Wallis [116] and illustrated in Figure 46 has been adopted.

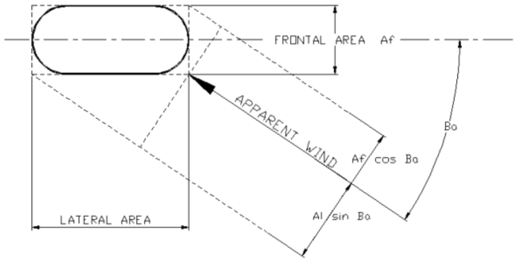

Figure 46: *Windage drag [116].*

Mathematically, the windage drag of an element is:

$$D_w = \frac{1}{2} \times \rho \times {V_{eff}}^2 \times (A_L \times \sin\beta_{eff} \times C_{D\,L} + A_F \times \cos\beta_{eff} \times C_{D\,F}) \qquad \textbf{Eq. 115}$$

In which:

D_w	Windage drag.	N
ρ	Air density.	kg.m^{-3}
V_{eff}	Effective wind speed at the centre of area.	m.s^{-1}
A_L	Lateral area of the object.	m²
β_{eff}	Effective wind speed at the centre of area.	°
$C_{D\,L}$	Lateral drag coefficient.	-
A_F	Frontal area of the object.	m²
$C_{D\,L}$	Frontal drag coefficient.	-

Typical values for the lateral and frontal drag coefficients are provided in Table 32 for the windage components taken into account, namely the hull, crew members, mast and rigging.

Object	$C_{D\,L}$	$C_{D\,F}$
Hull	0.9	0.4
Crew	0.9	1.1
Mast	0.8	1.1
Rigging	1.0	1.0

Table 32: *Windage drag coefficient [116].*

The windage drag can then be resolved in terms of heel and drive components.

10.3.5.3 Heel and Drive Components

Windage results in an increased heeling moment and reduced drive, which makes it a significant part of a performance prediction analysis. The heel and negative drive component are respectively:

$$Fh_w = D_w \times \sin\beta_{eff} \qquad \textbf{Eq. 116}$$

And:

$$Dr_w = D_w \times \cos\beta_{eff} \qquad \textbf{Eq. 117}$$

In which:

Fh_w	Heel force due to windage.	N
Dr_w	Drive force reduction due to windage.	N
D_w	Windage drag.	N
β_{eff}	Effective wind speed at the centre of area.	°

10.3.5.4 Conclusions

The added resistance and heeling moment due to windage have been considered in a first principles analysis to refine the velocity prediction program and provide a more realistic and accurate modelling of the yacht.

10.3.6 Conclusions

The aerodynamics, relying on wind triangles and effective angle theory has been introduced. Hazen's aerodynamic model has been utilised for the sail forces, incorporating the modern ORC sail coefficients to resolve the drive and heeling force components. Further aspects such as depowering and windage have been tackled to provide a model as complete and precise as possible.

10.4 Stability

10.4.1 Introduction

The transverse stability analysis performed in Chapter 9 was focused on the background theory, stability principles, and compliance with the regulation. As part of the VPP, the stability assessment will be focussed on the righting moment, taking into account the crew hiking, as well as the heeling moment and dynamic factors.

10.4.2 Weight and Centres

The driving factors in stability are the weight and location of the centre of gravity, or rather centres of gravity. Indeed, the displacement of the boat dictates the hydrostatics, and has a paramount impact on resistance. On the other hand, the centres of gravity (LCG, TCG and VCG) will respectively influence the trim, righting moment and transverse stability of the yacht. In the case of the A Rater, the crew mass is over a third of the total displacement, and thus the crew position will have a large impact.

The VPP therefore incorporates a weight and centres module, divided into the lightship and crew.

The lightship displacement is first set, either from estimates, or from an inclining experiment once conducted for greater accuracy.

Furthermore, the weight and height of the three crew members and role onboard can be added. This is clearly aimed at optimising racing performance, so that the boat is always raced to the maximum of its abilities. The displacement will be adjusted thanks to the weight, while the height will impact on the effectiveness of hiking and transverse centre of gravity location.

As a result, the VPP will provide an updated velocity prediction for any crew configuration. This offers the ability for the VPP to be used as part of the Thames A Rater Class so that each crew can exploit the best sailing configuration.

While the hiking righting moment is included in the VPP crew module, the form stability due to the hull shape is to be considered.

10.4.3 Righting Moment

10.4.3.1 $\overline{Gz}$ Estimation

The righting lever $\overline{Gz}$ is the required input for transverse stability. While it can be roughly estimated up to around 20° for larger yachts, it is not applicable to lighter crafts, and does not cover the overall range of heel angles.

This is in fact a major issue with many VPP. More advanced software such as FS-Equilibrium [27] include a lines processing module that performs a stability analysis similar to Hydromax. However, more common software such as the Wolfson's Unit WinDesign [123] expect manual inputs of $\overline{Gz}$ values at various angles of heel; values that involve a detailed stability analysis. It is therefore very challenging to provide an accurate and reliable stability estimation. As a result, the outputs of Hydromax stability will be programmed in the VPP; the $\overline{Gz}$ values will however be replaced by $\overline{KN}$.

10.4.3.2 $\overline{KN}$

The $\overline{KN}$ concept is little known in the yachting industry that prefers $\overline{Gz}$. Conversely, the shipping industry ignores $\overline{Gz}$ in favour of $\overline{KN}$, the reason being that ships experience tremendous changes in displacement and VCG. This would require a specific $\overline{Gz}$ analysis for every weight and VCG configuration, when a single $\overline{KN}$ analysis is sufficient.

$\overline{KN}$ is the base-line righting lever. It is a measure of the righting lever, but from the fixed base-line reference point K, as opposed to the varying VCG. The concept is illustrated in Figure 47.

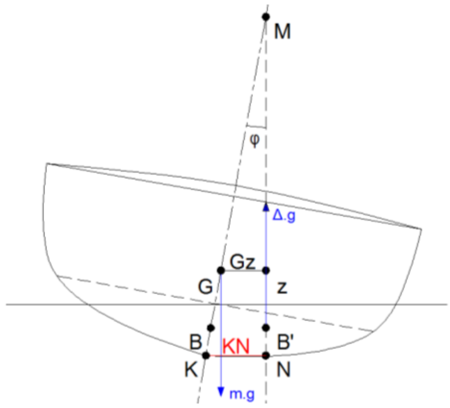

Figure 47: *Base-line righting lever.*

Using a $\overline{KN}$ curve enables to only input a single righting lever curve, from which $\overline{Gz}$ can be calculated for any VCG in the following manner:

$$\overline{Gz} = \overline{KN} - \overline{KG} \times \sin\varphi \qquad \textbf{Eq. 118}$$

In which:

$\overline{Gz}$	Righting lever.	m
$\overline{KN}$	Base-line righting lever.	m
$\overline{KG}$	Height of the VCG from base.	m
φ	Heel angle.	°

This constitutes the form righting moment to which will be added the righting moment provided by the crew hiking, thus giving the total righting moment, which is to equal the heeling moment for equilibrium.

10.4.4 Heeling Moment

10.4.4.1 Introduction

The heeling moment is the product of the heeling force (known thanks to the aerodynamic analysis presented in Section 10.3.3) and the heeling harm, i.e. the vertical distance from the centre of lateral resistance to the centre of effort.

10.4.4.2 Centre of Effort

As introduced in Section 4.4.3, the centre of effort of the sails is simply taken as the geometric centre of area. It is easily calculated and updated for a reefed mainsail, and illustrated in Drawing 08.

10.4.4.3 Centre of Lateral Resistance

The centre of lateral resistance, previously discussed in Section 4.4.2, will neglect the hull and only consider the two major components: the centreplate and rudder. Their respective centre of lateral resistance will be located on the quarter chord line at the centre of area height. The combined CLR location will be determined based on how much lift each appendage is producing, depending on the leeway angle and angle of attack of the rudder. The mathematical implications of the method are to be found in Section 10.5.2.

10.4.4.4 Heeling Moment

The heeling arm and moment are therefore given by:

$$HA = z_{CE} + z_{CLR} \qquad \textit{Eq. 119}$$

And:

$$HM = Fh \times HA \qquad \textit{Eq. 120}$$

In which:

HA	Heeling arm.	m
z_{CE}	Centre of effort height above Dwl.	m
z_{CLR}	Centre of lateral resistance height below Dwl.	m
Fh	Heeling force.	N
HA	Heeling arm.	m

Equating the heeling and righting moments to achieve equilibrium solves for the heel angle.

10.4.5 Conclusions

With a live weight estimate, the yacht performance can be maximised for any given crew. By employing the $\overline{KN}$ concept instead of the traditional $\overline{Gz}$, the number of input is minimised, and better suited to the varying displacement of light crafts. Finally, calculating the heeling arm and resulting heeling moment leads to a solution for the heel angle.

10.5 Appendages

10.5.1 Introduction

The appendages provide and hydrodynamic side force that counteracts the aerodynamic one. Furthermore, the rudder allows to steer the boat, a critical function. Those aspects will therefore be analysed.

10.5.2 Rudder Lift

10.5.2.1 Lift

While the centreplate experiences a relatively undisturbed flow, the rudder operates in its downwash. The DSYHS [62] suggests that this behaviour can be modelled by reducing the inflow speed to 90%, and halve the leeway angle. Based on those assumptions, the lift generated by the rudder L_R on centreline is:

$$L_r = \frac{1}{2} \times \rho \times A_r \times (0.9 \times V)^2 \times \frac{2\pi \times \frac{\lambda}{2}}{1 + \frac{2}{AR_e}} \qquad \textit{Eq. 121}$$

Assuming weather helm, if a rudder angle of attack α is applied by the helmsman, the equation becomes:

$$L_r = \frac{1}{2} \times \rho \times A_r \times (0.9 \times V)^2 \times \frac{2\pi \times \left(\frac{\lambda}{2} + \alpha\right)}{1 + \frac{2}{AR_e}} \qquad \textit{Eq. 122}$$

In which:

L_r	Rudder lift.	N
ρ	Water density.	kg.m^{-3}
A_r	Rudder lateral area.	m^2
V	Inflow speed.	m.s^{-1}
λ	Angle of attack.	°
α	Rudder angle.	°
AR_e	Effective aspect ratio.	-

With the corresponding induced drag:

$$R_{Di\,r} = \frac{1}{2} \times \rho \times A_r \times (0.9 \times V)^2 \times \frac{1}{\pi \times AR_e} \times \left(\frac{2\pi \times \left(\frac{\lambda}{2} + \alpha\right)}{1 + \frac{2}{AR_e}} \right)^2 \qquad \textit{Eq. 123}$$

In which:

$R_{Di\,r}$	Rudder induced drag.	N
ρ	Water density.	kg.m^{-3}
A_r	Rudder lateral area.	m^2
V	Inflow speed.	m.s^{-1}
λ	Angle of attack.	°
α	Rudder angle.	°
AR_e	Effective aspect ratio.	-

10.5.2.2 CLR

The location of the longitudinal and vertical CLR, respectively x_{CLR} and z_{CLR} is then found using:

$$x_{CLR} = \frac{L_k \times x_{CLR\,k} + L_r \times x_{CLR\,r}}{L_k + L_r} \qquad \textit{Eq. 124}$$

And:

$$z_{CLR} = \frac{L_k \times z_{CLR\,k} + L_r \times z_{CLR\,r}}{L_k + L_r} \qquad \textit{Eq. 125}$$

In which:

x_{CLR}	Combined longitudinal CLR.	m
L_k	Centreplate lift.	N
$x_{CLR\,k}$	Centreplate longitudinal CLR.	m
L_r	Rudder lift.	N
$x_{CLR\,r}$	Rudder longitudinal CLR.	m

z_{CLR}	Combined vertical CLR.	m
$z_{CLR\,k}$	Centreplate vertical CLR.	m
$z_{CLR\,r}$	Rudder vertical CLR.	m

Based on the centreplate and rudder lift, the CLR can be located. The next unknown is the amount of rudder angle necessary to stay on a steady course.

10.5.3 Equilibrium

As suggested in Section 4.4.1, balance is an important part of sailing, and is achieved by aligning the centre of effort of the sails with the centre of lateral resistance of the appendages. This is practically very hard to conserve over a range of conditions, and is therefore dynamically corrected by introducing rudder angle to shift the CLR in line with the CE. This solves for the yaw moment equilibrium, and quantifies the rudder angle. Mathematically, equilibrium is reached for:

$$x_{CE} = x_{CLR} \qquad \textbf{Eq. 126}$$

Substituting for x_{CLR} as given in Eq. 124:

$$x_{CE} = \frac{L_k \times x_{CLR\,k} + L_r \times x_{CLR\,r}}{L_k + L_r} \qquad \textbf{Eq. 127}$$

Solving for the rudder lift L_r:

$$L_r = \frac{L_k \times (x_{CLR\,k} - x_{CE})}{x_{CE} - x_{CLR\,r}} \qquad \textbf{Eq. 128}$$

Hence the rudder angle α:

$$\alpha = \frac{L_r \times \left(1 + \frac{2}{AR_e}\right)}{\frac{1}{2} \times \rho \times A_r \times (0.9 \times V)^2 \times 2\pi} - \frac{\lambda}{2} \qquad \textbf{Eq. 129}$$

In which:

x_{CE}	Longitudinal centre of effort.	m
x_{CLR}	Combined longitudinal CLR.	m
L_k	Centreplate lift.	N
$x_{CLR\,k}$	Centreplate longitudinal CLR.	m
L_r	Rudder lift.	N
$x_{CLR\,r}$	Rudder longitudinal CLR.	m
α	Rudder angle.	°
AR_e	Effective aspect ratio.	-
ρ	Water density.	kg.m^{-3}
A_r	Rudder lateral area.	m^2
V	Inflow speed.	m.s^{-1}
λ	Leeway angle.	°

The rudder angle to keep the boat on a steady course has been ascertained, therefore achieving balance.

10.5.4 Conclusions

The lift of the appendages has been modelled to establish the longitudinal and vertical location of the CLR. In addition, the amount of lift generated to balance the sail side force solves for the sway force, i.e. the leeway angle. Finally, the rudder angle required to cancel the yaw moment has been calculated, thus solving for an additional degree of freedom.

10.6 Planning

10.6.1 Introduction

10.6.1.1 Savitsky Planning Theory

The planning theory developed by Savitsky, originally published in 1964 [102] and implemented in 1976 [103] is one of the most influential publications in modern naval architecture. Savitsky theory offers a numerical method of proven reliability and widely applicable throughout the industry to assess planning motor crafts, whether V-shaped of flat bottomed, and relative design factors such as the lift generated, trim angle, resistance and behaviours such as porpoising.

10.6.1.2 Adaptation to Yachts

Modelling the planning behaviour of sailing yachts remains a hard task. Methods such as the DSYHS are unable to do so, and CFD codes proved to have difficulties as higher Froude numbers, once the yacht reaches semi-displacement mode [108].

The A Rater exhibits planning behaviour at low Froude numbers, and planning cannot be neglected as part of the VPP as it normally is in the large majority of the commercial programs.

The aim is to introduce Savitsky planning theory as part of the VPP for the A Rater. As a result, the lift generated when planning and associated trim angle will be calculated, leading to a refined performance prediction.

The underwater body of the A Rater can be approximated as a flat plate, and will be treated as such when applying a simplified approach of Savitsky planning theory.

10.6.2 Calculation Process

10.6.2.1 Speed Coefficient

Boat speed is normally characterised by the Froude number Fn:

$$Fn = \frac{V}{\sqrt{gL}} \qquad \textbf{Eq. 130}$$

In which:

Fn	Froude number.	-
V	Boat speed.	m.s^{-1}
g	Acceleration due to gravity.	m.s^{-2}
L	Waterline length.	m

In the case of a planning craft, the waterline length will greatly reduce once planning, making the Froude number irrelevant. A beam based Froude number, known as the speed coefficient C_V is therefore preferred:

$$C_V = \frac{V}{\sqrt{gb}} \qquad \textbf{Eq. 131}$$

In which:

C_V	Speed coefficient	-
V	Boat speed.	m.s^{-1}
g	Acceleration due to gravity.	m.s^{-2}
b	Waterline beam.	m

10.6.2.2 Length-Beam Ratio

Savitsky defined the planning length-beam ratio λ as:

$$\lambda = \lambda_1 - 0.30 \qquad \textit{Eq. 132}$$

In which:

λ	Length-beam ratio for $\lambda_1 \in [1, 4]$	-
λ_1	Static length-beam ratio.	-

This value is predominantly in the calculation process.

10.6.2.3 Trim Angle

The trim angle τ at which the yacht operates will impact on the planning lift coefficient. The trim angle will be ascertained as part of the VPP based on the pitch moment provided by both the sails and the crew.

10.6.2.4 Lift Coefficient

The flat plate lift coefficient C_{L0} is given by Savitsky as:

$$C_{L0} = \tau^{1.1} \times \left(0.012 \times \sqrt{\lambda} + \frac{0.0055 \times \lambda^{\frac{5}{2}}}{C_V^2}\right) \qquad \textit{Eq. 133}$$

In which:

C_{L0}	Planning lift coefficient.	-
τ	Running trim angle.	°
λ	Length-beam ratio.	-
C_V	Speed coefficient.	-

The lift will lessen the displacement of the yacht, leading to new hydrostatics. The lift is acting at the centre of pressure, considered as part of the theoretical method.

10.6.2.5 Centre of Pressure

The centre of pressure C_{oP} is where the lift and drag forces are applied, and is located using:

$$C_{oP} = 0.75 - \frac{1}{2.39 + 5.21 \times {C_V^2}/{\lambda^2}} \qquad \textit{Eq. 134}$$

In which:

C_{oP}	Centre of pressure.	m
C_V	Speed coefficient.	-
λ	Length-beam ratio.	-

It is worth mentioning that Savitsky suggests the use of the Schoenherr friction coefficient [6] as opposed to the standard ITTC 1957. However, the later proved not to have any significant impact on the results [121] and will therefore be used as it is already part of the DSYHS.

10.6.3 Equilibrium of Planning Crafts

Bringing together the forces and moments acting on a planning craft, the vertical and horizontal force balance can respectively be resolved as [121]:

$$\Delta \times g = L \times \cos\tau + Dr \times \sin(\tau + \varepsilon) - D_f \times \tan\tau \qquad \textit{Eq. 135}$$

And:

$$Dr \times \cos(\tau + \varepsilon) = \Delta \times \tan\tau + \frac{D_f}{\cos\tau} \qquad \textit{Eq. 136}$$

While the pitching moment balance is:

$$L \times (x_{CG} - x_{CP}) + D_f \times (z_{CG} - z_{CP}) = Dr \times Dr_l \qquad \textit{Eq. 137}$$

In which:

Δ	Yacht displacement.	kg
g	Acceleration due to gravity.	m.s^{-2}
L	Planning lift.	N
τ	Running trim angle.	°
Dr	Drive force.	N
ε	Drive force angle to keel like.	°
D_f	Frictional drag.	N
x_{CG}	Longitudinal centre of gravity.	m
x_{CP}	Longitudinal centre of pressure.	m
z_{CG}	Vertical centre of gravity.	m
z_{CP}	Longitudinal centre of pressure.	m
Dr	Drive force.	N
Dr_l	Drive force lever.	m

10.6.4 Conclusions

Applying the basic principles of Savitsky planning craft theory to the A Rater, approximated as a flat plate, the heave and pitch can now be considered.

The adaptation of the theory for planning sailing yachts therefore creates a more complete and realistic VPP. This aspect is to be validated via speed trials, as further developed in Section 14.2.4.

10.7 Equilibrium

10.7.1 Introduction

The various aspects of the prediction program have been separately introduced in the previous sections. They can now be brought together to solver for the six degrees of freedom of yachts.

10.7.2 Surge (Boat Speed)

When sailing, the boat will accelerate until the drive force equals the total resistance. This includes all the components of the resistance, both hydrodynamic and aerodynamic. Mathematically:

$$Dr = R_T \qquad \textit{Eq. 138}$$

Detailing the total resistance:

$$Dr = R_{rh\,\varphi} + R_{fh\,\varphi} + R_{rh\,\varphi} + R_{fk} + R_{fr} + R_a + R_{ik} + R_{ir} + D + D_w \qquad \textit{Eq. 139}$$

In which:

Dr	Drive force.	N
R_T	Total resistance.	N
$R_{rh\,\varphi}$	Heeled hull residuary resistance.	N
$R_{fh\,\varphi}$	Heeled hull frictional resistance.	N
$R_{rk\,\varphi}$	Heeled centreplate residuary resistance.	N
R_{fk}	Centreplate friction resistance.	N
R_{fr}	Rudder frictional resistance.	N
R_a	Roughness resistance.	N
R_{ik}	Centreplate induced drag.	N
R_{ir}	Rudder induced drag.	N
D	Sails drag.	N
D_w	Windage drag.	N

The boat speed at which the total resistance is achieved gives the yacht velocity.

10.7.3 Sway (Leeway)

The leeway angle required for the appendages to generate the same amount of side force as the sails is found by equating the aerodynamic and hydrodynamic side forces:

$$SSF = KSF \qquad \textit{Eq. 140}$$

The leeway angle λ is therefore:

$$\lambda = \frac{SSF}{\frac{1}{2} \times \rho \times A_l \times V_s{}^2 \times \frac{2\pi}{1 + \frac{2}{AR_e}}} \qquad \textit{Eq. 141}$$

In which:

SSF	Sail (aero) side force.	N
KSF	Keel (hydro) side force.	N
λ	Leeway angle.	°
ρ	Water density.	kg.m^{-3}
A_l	Appendage lateral area.	M²
V_s	Boat speed	m.s^{-1}
AR_e	Effective aspect ratio.	-

10.7.4 Heave (Displacement)

The vertical equilibrium equation given by Savitsky in Eq. 135 solves for the reduction in displacement. The new displacement is to equal the buoyancy, leading to a new set of hydrostatics automatically updated into the DSYHS hydrodynamic module of the VPP.

10.7.5 Roll (Heel Angle)

For equilibrium, the heeling moment must equal the righting moment:

$$HM = RM \qquad \textit{Eq. 142}$$

Which yields:

$$Fh \times HA = \Delta \times g \times (\overline{KN} - \overline{KG} \times \sin\varphi) + RM_c \qquad \textit{Eq. 143}$$

In which:

HM	Heeling moment.	N.m
RM	Righting moment.	N.m
Fh	Heeling force.	N
HA	Heeling arm.	m
$\overline{Gz}$	Righting lever.	m
$\overline{KN}$	Base-line righting lever.	m
$\overline{KG}$	Height of the VCG from base.	m
φ	Heel angle.	°
RM_c	Crew righting moment	N.m

Note that the righting moment comprises both the form righting moment (from the $\overline{KN}$ curve), as well as the righting moment provided by the crew.

10.7.6 Pitch (Trim Angle)

The pitch angle is based on the longitudinal moment balance given in Eq. 137, in which the longitudinal crew location will play a significant part. The result is the running trim angle of the boat, thus updating the amount of lift generated as well as the hydrostatics.

10.7.7 Yaw (Rudder Angle)

The rudder angle required can be ascertained using Eq. 129. This corresponds to the amount of lift to be provided by the rudder to keep the boat balanced. The resulting drag will penalise the yacht performance, and has been accounted for.

10.7.8 Conclusions

A six degrees of freedom VPP has been created for the A Rater. The VPP is an important tool as part of the design spiral, hence its high flexibility to efficiently compute and compare various options. Furthermore, the VPP aimed at maximising the racing performance of the boat, accounting for the variations in crew for instance.

The proposed VPP differs from standard programs by considering all six degrees of freedom (when pitch and heave are generally neglected). Moreover, the use of $\overline{KN}$ proved to be more suited than the traditional $\overline{Gz}$ for the stability assessment. Finally, the planning behaviour and the importance of the crew location onboard have been implemented, resulting in a VPP focussed on lighter crafts.

An accurate prediction of the performance of the new A Rater can therefore be achieved, with a VPP specifically conceived for light planning crafts.

10.8 Velocity Prediction

10.8.1 Results

The primary output of the VPP is the boat speed over a range of true wind speed and true wind angle, allowing to find the optimum VMG angle. The polar plot is presented in Figure 48, other degrees of freedom can be found in Appendix B.

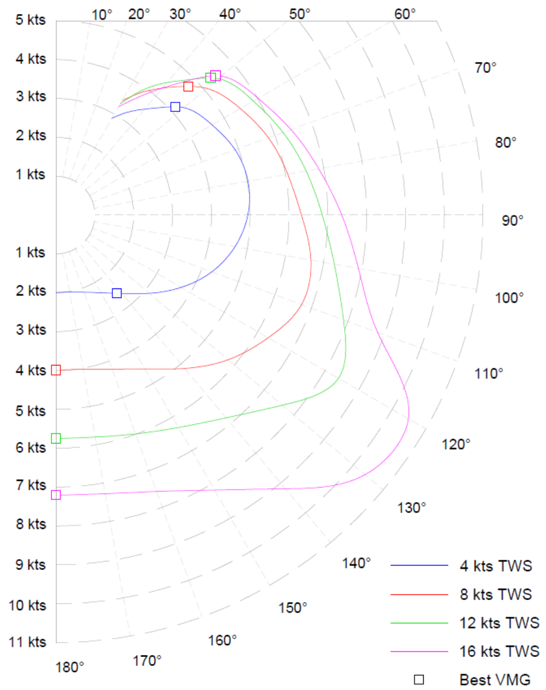

Figure 48: *Boat speed.*

First, it can be seen that close hauled performance in strong wind is primarily restricted by the stability of the yacht, and a large amount of depowering is required, leading to a lower boat speed in 16 knots of true wind speed compared to 12 or even 8 knots. As illustrated on the polar plot, the VMG angle in 16 knots is however the highest, and the yacht should therefore be sailed at this particular angle rather than close hauled.

In addition, the impact of the planning behaviour and associated resistance is clearly visible in the 110° to 140° true wind angle range, with a much higher speed increase rate as the wind speed rises. Nevertheless, the theoretical prediction indicates that, despite a significantly higher speed at those angles, the optimum VMG lies dead-downwind. This is a very good example of the importance of the VPP: intuitively, a sailor may think that getting on the plane and benefiting from the much higher speed would be an advantage. However, in this instance, the VPP shows that the best strategic option is to sail dead-downwind.

10.8.2 Comparison

A boat speed comparison of the original *Scamp* hull with the current rig and the proposed design has been undertaken to demonstrate and quantify the increase in performance resulting from the work conducted. The results are provided in Figure 49.

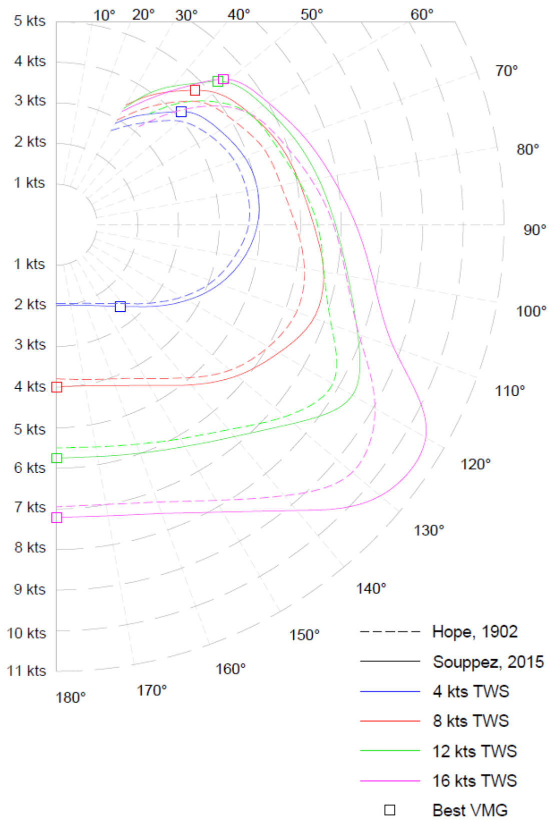

Figure 49: *Boat speed comparison.*

The new design appears to be faster than the original one, both upwind and downwind. In addition to the lower hydrodynamic resistance and higher drive force, additional factors contributed to the large increase in performance.

Firstly, the reefed mainsail, higher CLR location, added form stability and more efficient hiking lead to a faster boat upwind, especially in higher wind speeds as the crew can fully handle the yacht. Downwind, the flatter hull shape combined with the ability for the crew to move longitudinally thanks to the next cockpit layout promotes planning behaviour, which results in greater performance. Finally, the increase in speed is much smaller dead-downwind, where the stability, longitudinal balance and high aspect ratio foils have very little impact on the sailing.

10.9 Conclusions

The principles of a six degrees of freedom velocity prediction program have been outlines in this Chapter, providing the underpinning theory to the program created.

The VPP was developed to be highly flexible. On the one hand, this allows efficient design comparisons. On the other hand, it will later maximise the performance of the yacht once built.

The program is specifically aimed for light planning craft, such as the A Rater, with three major innovations compared to most commercial VPP packages.

First of all, the impact of changes in crew height and weight has been incorporated to accurately model the righting moment due to hiking.

In addition, the use of the righting lever $\overline{Gz}$ was demonstrated not to be the best suited to the VPP of light crafts, leading to the introduction of the $\overline{KN}$ concept as part of the program.

Finally, Savitsky theory was adapted to model the planning abilities of the boat, and inherent increase in performance. The necessary validation via speed trial is discussed in 14.2.4.

A complete six degrees of freedom has been realised for the new A Rater, increasing the confidence in the performance of the yacht, demonstrated to be superior to the current on.

This concludes the preliminary design phase; the production is now to be considered to develop the detailed design.

Chapter 11: Production

The main steps and principles of the construction will be detailed to provide an overview of the intended manufacturing. Often neglected as part of the conception, production can heavily influence design choices, particularly the structural arrangement, and provides the framework for the project scheduling and timing.

11.1 Introduction

Traditionally, the naval architect and builder used to be the same person. However, nowadays, the two disciplines are very distinct and the amount of communication between the two parties is minimum, and in some cases inexistent. Indeed, many commissioned yachts are now designed before the manufacturer is known, and the chosen one will likely be the one who can build a given boat for the lowest price.

This modern separation of the design and production may not always be beneficial: the construction method and facilities have a large impact on the design, and manufacturing constraints are a primary factor to consider. This justifies the overview of the manufacturing proposed in this chapter.

11.2 Shipyard Organisation

11.2.1 Yard Layout

The IBTC yard layout is presented to scale in Figure 50.

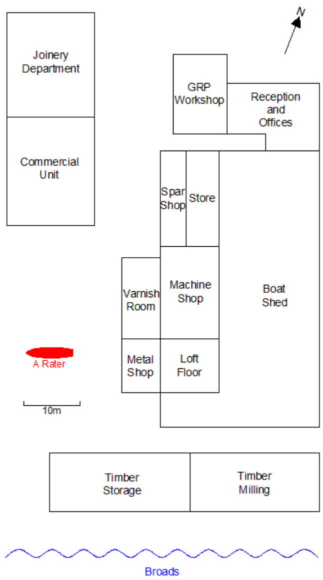

Figure 50: Boatyard schematic.

The yard layout is critical when dealing with a production line where the yacht goes through various specific building stations. In the case of a one-off boat, there is no advantage to such a process; the building will therefore take place in a single static location. In term of equipment, a complete range is available for timber machining and traditional boatbuilding, from a log saw mill to highly specific small hand tools.

11.2.2 Health and Safety

Throughout the premises, health and safety regulation applies. Without detailing the multiple aspects inherent to the various codes of practice to be respected, a non-exhaustive list of the main ones is provided hereafter:

- British Standards [15, 16, 17, 18, 19].
- Control of substances hazardous to health (COSHH) [46].
- Health and safety at work act (HASAWA) [40].
- Lift operation lift equipment regulation (LOLER) [44].
- Management of health and safety at work (MHSW) [41].
- Personal protective equipment (PPE) [42].
- Provision and use of work equipment regulations (PUWER) [45].
- Reporting injuries, diseases and dangerous occurrences regulation (RIDDOR) [43].

In addition, risk assessments are to be conducted as part of the normal yard operation, and personal protective equipment (PPE) are to be worn when required.

11.3 Lofting

11.3.1 Introduction

With the advances in both Computer Aided Design (CAD), and automated manufacturing (laser cutting and 5-axis machines), lofting has been declining, and is now less common. The principles have however remained unchanged for centuries, and there is more to lofting than simply drawing the yacht full size, which is how it is perceived nowadays.

Still favoured by traditional wooden boatbuilders, the principles of lofting can be particularly effective, and will be discussed in the subsequent sections.

11.3.2 Lines Drawing

The very first stage of lofting is to draw the linesplan full size from the table of offsets. On a white painted floor are to be drawn (in order):

1. The grid.
2. The profile outline.
3. The body plan (stations).
4. The half breadth (waterlines).
5. The profile (buttocks).
6. The body plan (diagonals).

At each stage, the fairness of the lines and their correspondance from one view to another is checked. This phase guaranties the accuracy and faireness of the yacht. The majority of 9.41mm building tolerance allocated in Section 2.4.2 is expected to be lost through lofting and the fairing of the lines.

To draw the curves, a flexible batten is held between nails, ensuring the line is fair and going through the offset points. The process is illustrated in Figure 51.

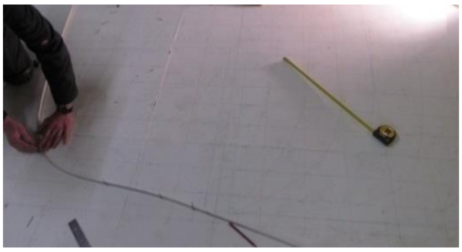

Figure 51: *Lofting.*

Tidiness and cleanliness are of paramount importance. The lofting floor should be kept as clean as possible, which implies removing shoes, and double checking each line before drawing it to avoid rubbing marks. Furthermore, drawing with a hard pencil (H grade) would be advised over a soft pencil (B grade), as it prevents lines fading and tends to remain cleaner.

11.3.3 Station Moulds

Once drawn, the linesplan enables to construct the stations moulds. In this case, the profile stick method should be used: profile sticks are used to transfer the lines onto the wood that will become the station mould. In order to save building time and materials, the stations mould will become the frames of the yacht, they are therefore not temporary but permanent. As a result, great care should be taken during the manufacturing of the plywood frames.

11.3.4 Further Lofting Capabilities

If building the stations mould is the primary output from lofting, there is much more that can be obtained from the lofting floor [99], such as the transom developed shape, the station moulds and floors bevel, rabbet angles, length of bolts, etc…

The full size drawing offers a great opportunity for patterns and jigs making, as well as preventing clash between fasteners and ensuring appropriate assembly. Consequently, additional time will be allocated to the lofting phase to ensure its full potential is exploited.

11.4 Backbone

11.4.1 Introduction

The backbone of the yacht is the primary structure, which include the stations moulds, the keel assembly onto which they will then be set up, and the addition of the longitudinal stringers. The backbone construction includes accurate alignment, ensuring components are level and plumb, as well as strongly braced.

Aspects involved in the keel building such as laminating and scarfing will be discussed, so will the steaming and machining considerations relevant to the longitudinal stringers. Note that the notions tackled hereafter are applicable to other aspects of the production, beyond the backbone setup.

11.4.2 Laminating

Whether it is for the keel, the hull shell or small components such as the breasthook or knees, laminating layer of veneers together is a common practice in wooden boatbuilding. A major decision to be made is the resin system, epoxy and resorcinol (resorcinol-formaldehyde) being the two favourites.

The opposition of the two adhesive systems has long been discussed [92], and with the exception of a few specialised applications that requires one over the other, it appears that personal preference often is the primary driving factor.

In the case of the A Rater, epoxy is advised over resorcinol. Indeed, resorcinol does not exhibit gap filling properties, thus requiring a large amount of clamping pressure, not always easily provided. In addition, the epoxy is more versatile, with a wider range of applications, and various consistencies can be achieved. Furthermore, the transparency of the epoxy ensures more discrete glue lines compared to the black colour of resorcinol. The only drawback is a slight increase in cost and the need for UV protection.

But the deciding factor in this instance is the curing behaviour. Once mixed, epoxy will cure fast in the mixing pot, but much slowly if spread over an area. Conversely, resorcinol will remain usable for long time in the pot, but will cure very fast once spread out. As a result, epoxy will offer a longer working time to position the veneers once glue has been applied. This is also very significant from a quality control point of view: if the epoxy has cured in the pot, this can be monitored, ensuring that only uncured epoxy is applied. This is not possible with resorcinol: the glue might still appear usable in the pot, but could be cured before the laminate is secured in position, leading to very poor interlaminar connections.

Moreover, epoxy will eventually cure: a cold temperature will simply slow down the process. However, if exposed to cold temperatures, resorcinol will look like it has cured, when it actually has not, resulting in very poor properties. Epoxy should therefore be preferred for the keel, hull shell, and other large structural components.

For smaller items, especially those requiring fitting in the boat (such as the breasthook) resorcinol is a better alternative. Indeed, the softer nature of resorcinol will make using hand tools easier and will minimise damage to the tools when shaping the piece to fit.

10.4.3 Scarfing

10.4.3.1 Scarf Types

There are physical (and natural) restrictions to the maximum length of a wooden component. It is therefore often necessary to join two pieces together to achieve the overall length required: this is done via a scarf joint. The 5 main scarf types are illustrated in Figure 52.

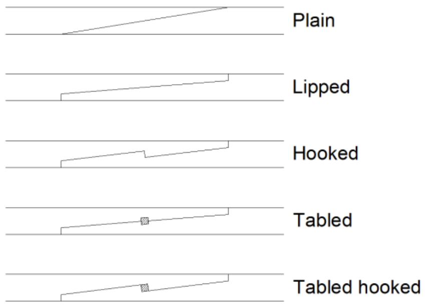

Figure 52: Scarf types.

The first two types (plain and lipped) are better suited to planking, while the last 3 are advised for bolted joints, such as those of the keel.

The hooked joint provides a particularly efficient joint. Then, the tabled one features a key with the grain running perpendicular to the joint, thus acting as a stop water: in case of water ingress, the key expands and locks the joint in place, preventing further water ingress. The hook and tabled joint benefits from the advantages of both.

10.4.3.2 Scarf Length

A scarf is expressed as the ratio of the length to the thickness. The longer the scarf, the stronger and more efficient the joint is [10], as depicted for plain scarfs in Figure 53.

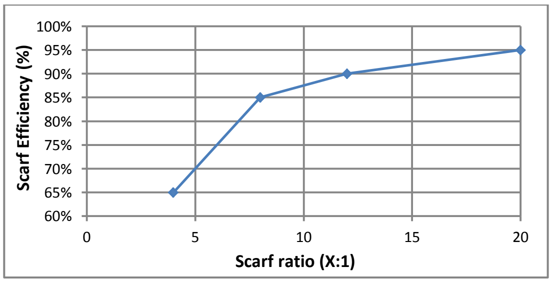

Figure 53: Scarf efficiency [10].

From a structural point of view, the longer the scarf the better. The drawback being the increased waste: a longer scarf will shorten the final overall length; this should therefore be kept in mind when establishing the scarf ratio as it can be a limiting factor.

Most scarfs, particularly for planking, have a 4:1 ratio, while a 6:1 ratio is preferred for keels. Those are generally justified by the old Lloyds rules (respectively rule 4707 and 4302). Although only published once in the late 1970s and not valid anymore, the old Lloyds rules had and still have a large influence in traditional boatbuilding. Furthermore, Lloyds rules specify that keel scarfs should be more than 1.5m away from each other, and not in way of the mats step (rule 4303): such a configuration will be avoided.

A 8:1 ratio is advised for its increase in strength [35], while a 12:1 ratio tends to be restricted to spars.

In the case of the A Rater, the keel scarf will have a 8:1 ratio while other scarfs will be the traditional 4:1 ratio.

10.4.4 Steaming

In cases where the wood is to be curved beyond its breaking point, it can be steamed. When exposed to water vapour, the wood will soften and become more flexible: it can then be bent as desired. This process will for instance be used for the stringers. While the wood will fit the gentle curve at the back of the boat, the curvier forward end will most likely require steaming.

In this case, the traditional rule of thumbs of 1 hour per 1 inch thickness to be bent will be applied. While there is no scientific background, the rule has proven its reliability through the centuries, and is particularly convenient. Indeed, the measurement traditionally being in fractions of an inch, this translates into fractions of an hour to be steams. For instance: a ¼ inch piece of wood would be streamed for a ¼ hour (15min). Too little steaming and the piece will not bend; too much and the wood will become too soft and will be crushed on the inner bend, this is known as a compression fracture.

10.4.5 Cross Section

10.4.5.1 Structural Considerations

From a structural design perspective; a deep thin stringer is the best configuration as it offers the maximum section modulus for a minimal weight. However, this is not practical from a manufacturing point of view: a deep section would be too hard to bend, even when steamed, and would most likely twist. Most steamed timbers are therefore wider than deep, which makes the bending very easy, but is not structurally efficient.

A square cross section would offer a good compromise, and more importantly a machining advantage.

10.4.5.2 Machining Considerations

The wood bends much better in the direction of the grain, this is however not always practical to achieve, and so the grain should be oriented as close as possible to the ideal. Considering a slab sawn plank from which the stringers are to be machined, rectangular and square stringers would have a very different manufacturing process, as shown in Figure 54.

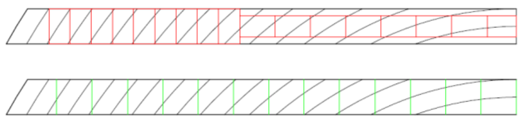

Figure 54: Stringer manufacturing options.

A rectangular cross section will have to be made in two batches to optimise the grain orientation, which means two different settings for the planning thickness and sawing width, which may introduce inconsistency in the dimensions. Conversely, a square section can be machined in a single batch, with a single planning thickness and sawing width, ensuring consistency and a faster manufacturing rate. The square stringers can then simply be rotated so that the grain is in the right direction.

This is a perfect example of the influence of production on the design specifications, and how to reduce the manufacturing time.

10.4.6 Backbone Assembly

10.4.6.1 Orientation

The orientation of the backbone is to be considered prior to the setup. As previously mentioned in Section 1.2.3, traditional wooden boats are to be built back to the water. However, the major orientation factor is which way up it will be constructed. European boatbuilding favours upright: this is dictated by the use of copper nails and roves, which have to be fastened from the inside. In the case of cold moulding, the hull lamination is more easily done with the yacht upside down; the backbone will therefore be set up in such as way.

10.4.6.2 Setup

The typical setup is illustrated in Figure 55.

Figure 55: *Typical backbone setup.*

The stations moulds are installed, levelled (fore and aft and athwartships), plumbed and then fixed into position. Since the yacht is built upside down, the steam and keel assembly will then be dropped onto the stations moulds and fastened into place. Finally, evenly spaced longitudinal stringers are to be fastened to the station moulds, thus providing the primary structure.

10.4.6.3 Conclusions

Once set up, the backbone should be accurately checked to ensure fairness and symmetry, as well as appropriate dimensions. From the exactitude of the backbone depends the final shape of the yacht.

10.4.7 Conclusions

Following the lofting and manufacturing of the station moulds, the critical backbone assembly can be undertaken. Due to the building technique proposed, the yacht is to be set up upside down. The stations moulds and longitudinal stringers will define the shape of the hull, onto which the hull shell will be laminated, using the cold moulding technique.

11.5 Hull Shell

11.5.1 Cold Moulding

The origins of the could moulding technique date back to the 1930s and the Ashcroft system developed in Britain. With the evolution of adhesives, the method turned into hot moulding around World War II, and was particularly appreciated in aircraft manufacturing for its strength and lightweight. The term hot moulding refers to the high temperature (and pressure) oven involved in curing the glue.

Thanks to the fast development of composite boatbuilding during the 1970s and the generalisation of modern glues, heat was no longer required as part of the curing, hence the term cold moulding.

Sometimes known as double diagonal (2 layers at +/-45°), cold moulding is essentially a lamination process, where multiple skins of thin veneers are glued together at various orientations.

Cold moulding benefits from a wide range of advantages for boatbuilding applications and was preferred to traditional carvel in this case.

11.5.2 Benefits

11.5.2.1 Strength

Cold moulding allows to exploit the uni-directional properties of the wood. By varying the orientation, a composite material is effectively achieved, with a high strength and dimensional stability, which results in a lightweight hull.

In addition, thin veneers facilitate the identification of defects in the wood, making the material properties more reliable. Conversely, a thick plank could hide various types of defects (knot, sap-pocket, etc…) on the inside, which could go unidentified.

A lighter, stronger and more reliable hull is therefore produced, which justifies the racing yacht applications of this construction method.

11.5.2.2 Maintenance

A common issue with wooden boats is the high maintenance required due to the nature of the wood. Indeed, depending on the environmental moisture, wood will expand and contract. When taken out of the water, the hull can dry out, and will only expand again once in the water. Over time, those cycles can damage the wood, and create structural issues. Furthermore, rot and its propagation are a constant threat. In addition, wood is a desirable food source and living space for many marine borers, with potential damages to the hull, particularly in fresh water, where the A Rater is to sail.

For a cold moulded hull however, none of the above is a problem. The thin veneers are fully encapsulated in the resin, the wood is therefore sealed from the environment. As a result, there is no moisture absorption or loss that would lead to expansion and shrinkage, no rot issues, and no access for marine borers.

A cold moulded hull will therefore have minimum maintenance and a very high longevity. Looking at a centenary old class such as the A Rater, building a durable boat is imperative. The lower maintenance will lead to a lower running cost, making the yacht a more attracting investment.

11.5.2.3 Construction

From a production perspective, cold moulding allows for a much faster construction than carvel.

First of all, a veneer is also much lighter than a carvel plank and therefore easier to handle and less tiring for the workforce. The average veneer weight has been assessed at less than 600g, against an average 5.4kg for a carvel plank.

Then, the fitting is very straight forward: each veneer is dry fitted next to the previous one, a parallel edge is marked and planned, and the veneer can be fitted. This is a much faster process than the time consuming fitting of a carvel plank.

Moreover, the fastening is done by stapling the veneers. Once again, this is a much quicker process than roving a carvel plank, which involves drilling a pilot hole and counter bore, hammering the nail in, hammering the rove on, trimming the excess nail length and then roving up the nail; a procedure that demands two workers.

Finally, a larger number of students can work on the hull at the same time. In a carvel construction, the fastest option is to have a worker on each side at the same time. However, for cold-moulding, starting amidships, progress can be made both fore and aft on each side, hence four workers can be involved against two for carvel, effectively halving the man hours. Cold moulding therefore makes for a much faster building time.

11.5.2.4 Waste factor

The last and decisive advantage of cold moulding against carvel is the minimum waste factor, defined as the ratio of the amount of material paid for divided by the amount actually utilised on the boat. In essence, it is a measure of how much material and thus money has been wasted. Since only the materials are to be paid for in this precise instance, reducing material costs appears very relevant.

To understand the importance of waste factor, a practical example will be given, based on an 18 foot plank. Consider a carvel plank. First of all, a wooden board will be selected, which must be large and thick enough so that the final plank can be manufactured. In this case, a 20 feet long by 8 inches wide by 1 inch thick board is selected, and therefore billed to the customer. The final plank however is to be 18 feet long, by 4.5 inches wide, by ¾ inch thick, as illustrated in Figure 56.

Figure 56: *Waste factor illustration.*

For wood, the quantity and inherent price is expressed in cubic feet. In this instance, a 1.11 ft^3 plank has been billed, for only a 0.42 ft^3 one fitted to the boat, i.e. a 62% waste factor, a common figure for carvel.

Now, consider a cold moulding yacht. The veneers are already of the right thickness, only a small strip will be removed for fitting purposes on one side, and once cut to length, the remaining length of veneers can be reused. A waste factor of 15% [56] appears to be a very pessimistic maximum. This results in large savings on wood costs.

Finally, cold moulding being stronger, a thinner hull can be achieved, providing further savings. Note that the expenses inherent to the fastening and gluing are similar for both techniques.

In order to minimise cost and wasted resources in an industry where environmental concerns are growing, cold moulding has been preferred to carvel. For the multiple advantages, only one disadvantage of cold moulding has been identified.

11.5.2.5 Disadvantage

The disadvantage of cold moulding is a more complex repair process. For a carvel yacht, the damage portions of planking can easily be cut out, removed, and new plank segments scarfed in. However, the multiple layers of a cold moulding hull make the repairs harder and more time consuming.

11.5.2.6 Conclusions

The advantages of cold moulding in terms of strength, maintenance, construction and waste clearly outweigh the repair drawback. This justifies the choice of a cold moulded hull.

11.5.3 Construction

A cold moulded hull consists in the lamination of a succession of veneers with a varying orientation. The first layer is fastened to the stringers and station moulds; the subsequent layers are then glued and fastened to the previous one.

A total of three layers have been chosen in this case for aesthetical reasons. The first 2 layers at +/-45° provide the dimentional strength required, while the 3rd and outer layer running for and aft allows for a more visually pleasing hull, matching the original lines of carvel hulls.

To provide an additional layer of protection, the hull will be sheathed with a light E-glass fibre layer. The light cloth results in a see-through finish that does not alter the visual appeal of the wood, while protecting it from scratches and small shocks. As far as the structural analysis is concern, the contribution of the fiberglass is ignored in the ISO [54].

Finally, while a clear finish has been advised, the final aesthetical decision is to be taken by the client, who could decide on a painted hull (and deck), in which case additional building time will be allocated towards the end of the project to complete the relevant tasks.

11.6 Hull Structure

11.6.1 Internal Structure

Once the hull shell has been laminated, the hull is turned over to allow access to the inside, leading to a new support assembly. The hull turn-over is a milestone in the building.

The various structural components can then be installed, as detailed in Drawings 09 and 10.

This stage offers a range of small tasks involving many different techniques, thus providing suitable exercises for the educational purpose of the manufacturing.

The floors and centreplate box structure should be carried out first so that the maximum space is available inside the boat, making the production more comfortable for the workers. The sub-deck structure can then be laid out.

11.6.2 Deck

To reduce cost and building time, a veneered plywood deck has been suggested. This makes for an easy manufacturing, with the visual appeal of the outer veneer. However, the deck has a large aesthetical impact, especially on a yacht such as the A Rater having a very low freeboard. A visually attractive deck is therefore vital, and alternative options should be presented to the customer, such as a solid deck, with the possible variations in wood species and pattern (either parallel to the sheer or straight fore and aft).

The more advanced techniques and materials are likely to result in greater building time and expenses, which are to be clearly explained and agreed to by the customer. Indeed, a veneered plywood deck can be installed in a matter of days at a very low price, whereas a solid teak deck with slats bent along the sheer could extend to months of work and up to 4 times the price of a plywood deck based on current retail prices [98].

11.7 Fit Out

11.7.1 Hardware

Once the deck is in place, the hull building is mostly completed. The fit out will then begin, in order to install the required hardware. This includes deck fittings and controls, as well as rudder bearings and chain plates.

11.7.2 Appendages

As further discussed in Section 12.2.2, the manufacturing of the appendages is located outside of the critical path, i.e. it can be conducted as any time during the building of the hull, therefore optimising the production.

To achieve the complex 3D shape of a hydrofoil, the appendages will be manufactured using a lamination technique, specified for the centreplate and rudder in Drawing 04 and 05 respectively.

11.7.3 Rig

The final stage will be the installation of the mast and rigging components. Since it is a subcontracted item that will be installed by the manufacturer, it is very important to ensure that the delivery and installation date matches the advancement of the building. If the yacht is not completed for the due date, or if the rig is not ready when the boat is finished, unnecessary delays will result.

11.8 Post-Production

Once the final assembly is complete, the production phase is finished, but the yacht is not ready to be delivered yet, and enter the post-production phases.

This final part of the project aims at providing quality control, and fixing any technical issue. This is done via a first launch and sea trials, as well as physical experiments such as the inclining experiment and the capsize recovery test, respectively introduced in Sections 9.3 and 9.5.10. Compliance with the ISO standard is to be demonstrated and obtained, which requires additional time.

Finally, considering the academic nature of the project, an appropriate amount of time will be dedicated to the post-production phase in order to compare the intended design and the finished product; this is thoroughly discussed in Section 14.2.

11.9 Conclusions

A brief outline of the production steps and principles has been provided in this instance; note that further guidelines are detailed in the relevant drawings.

From the lofting, the station moulds will be created and the backbone set up. The hull is to be built using cold moulding, preferred to carvel for it numerous advantages. The internal structure will then be added to eventually allow for the deck to be installed. The fit out of the hardware, appendages and rig can then be performed, thus completing the building phase.

Aesthetical aspects such as the deck type or hull colour will be left at the customer’s discretion to offer the possibility of personalisation, and the production will be updated accordingly. The timing and costing of the project can now be undertaken.

Chapter 12: Planning

Time and money are strategic factors in every project, even more when such aspects may be part of a contract and lead to penalties if not met. They are also decisive for the production planning and financing, and must therefore be estimated as best as possible to provide a cost and time frame for the building of the yacht.

12.1 Introduction

From the production method proposed in Chapter 11, the timing and costing will be developed, based on a conservative approach to ensure the schedule and budget are met. The applications of the critical path analysis to a one-off wooden boat will be studied. The man hours and inherent time frame required for the building will then be evaluated, as well as the cost.

12.2 Critical Path Analysis

12.2.1 Definition

In production planning and management, the notion of critical path is primordial. A critical path analysis (CPA) aims at achieving the most efficient scheduling of a project, and is based on the dependencies linking the various tasks to be completed.

Consider a basic rowing canoe made of three plywood panels stitched and glued together as a simplistic example. First, the plywood panel must be obtained, cut to shape, then positioned on the frames, to finally be glued: this is the critical path. The panels cannot be glued if they have not been cut to shape first, and they cannot be cut to shape if the plywood has not been delivered yet. On the other hand, parts of the production are independent of the critical path. In this instance, the oars could be manufactured at any time: before or after the canoe is built, as it does not impact in any way on the construction of the craft itself. An easy way to improve the efficiency is to identify elements outside the critical path, and schedule them in parallel. As a result, for the canoe example, the oars could be made while the resin is curing, thus reducing the overall construction time.

CPA can be extremely complex for large crafts, especially in the case of production lines with different stations, manufacturing different components, only brought together for the final assembly.

12.2.2 Application to Wooden Boats

For a wooden boat, the CPA appears to be harder to apply. The general principles are still valid, and components such as the appendages or the rig can be manufactured at any time. But a more accurate analysis seems not to be appropriate. Indeed, the majority of the components have to be made to size to fit in the boat. In the case of a composite yacht built from a mould, the hull and deck can be made separately and simultaneously, and then bolted together, achieving a perfect fit every time.

Wood being a natural material, it will expand, contract, and move depending on the temperature and humidity. Thus, components constructed to the design sizes outside of the critical path may not actually fit, and it is a much safer approach to manufacture all components from the actual built size. This is an inevitable process for a wooden boat, effectively preventing from realising a detailed CPA, which makes the planning and timing a harder task.

12.2.3 Planning Approach

The planning of the project will be a step by step process, where each step requires the previous one to be completed. Effectively, all steps are part of a single critical path. The schedule will therefore be broken down into a number of tasks to be completed, to which a set amount of time will be allocated, thus providing a time estimate.

12.3 Timing

12.3.1 Aims and Objectives

The timing of the project consist in detailing the schedule of the main tasks to be accomplished, with set dates to achieve given milestones, the primary one being delivering the boat on time, and in the shortest time frame possible.

Time is intrinsically linked to cost, as further detailed in Section 12.4, the reason being that labour is the largest expense in traditional wooden boatbuilding. However, in this particular case, the labour is undertaken by students, meaning it is free of charge.

A precise timing is still important with regard to the yacht delivery, and vital to the supply flow. The various building materials have to be ordered in advance, the supply chain must therefore be audited to establish the delivery times; materials are consequently only purchased when needed. Ordering too much at once could induce storage issues, while running out of materials would stop the construction and result in delays. An equilibrium is to be found between the supply flow and building schedule via an accurate planning.

12.3.2 Time Estimate

The most significant part of the scheduling process is estimating the required amount of time to complete a given task.

First of all, a breakdown of all the tasks is detailed, as presented in Appendix C.

Then, a number of hours is to be allocated for each task: this is a highly empirical process, with a variety of rule of thumbs. The crudest method, suggested by the Gougeon Brothers [35], consists in tripling the amount of time one would think is needed for each task. At the other end of the spectrum, McNaughton [80] offers a labour and cost estimate based on the yacht's displacement, as shown in Figure 57.

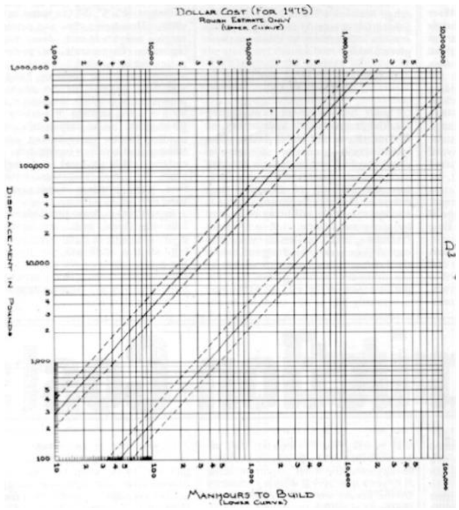

Figure 57: *Labour and cost estimate [80].*

While a labour proportional to the displacement appears a relevant criterion, the table does not account for the building material and method or the skills of the workers. The cost estimate is also very likely to vary depending on the use of the boat (cruising or racing), and is not adjusted for inflation.

Given the infinite number of variables that can affect the construction, an accurate evaluation is generally a work of fiction, even for the smallest crafts. Nevertheless, an approximation, even off by 30%, does still provide a good basis for scheduling the project [35].

As for many areas of traditional wooden boatbuilding, the best method might not be scientific. Experienced shipyards are able to provide a reliable estimate solely relying on their previous work. This is the approach taken in this instance: the timing of each task will be based on the author's record of previous work undertaken at the IBTC, thus accounting for the particularities of the shipyard.

Note that the IBTC involves students, the building time will therefore be higher than for a commercial shipyard. As a result, additional time in the form of safety margins will be included.

Once the total number of hours required has been quantified, it must be translated into a perceptible time frame.

12.3.3 Man Hours

In production, the concept of man hours refers to the workload that can be performed by an average worker in an hour. This can be somewhat abstract, as it does not relate to an actual time frame. A 100 man hours can be performed in 1 hour by 100 men. Whereas it would take a single man more than 100 hours to complete them: assuming 10 hours of work a day, it would take 10 days. Since there are only 5 working days a week, this gives a total of 2 weeks for the 100 man hours to be complete by an individual.

In order to ascertain the time frame from the man hours, the specificities of the IBTC must be considered. A typical week consists of 4.5 working days, with 7.5 hours of work on full days, and 4 hours on the half day, giving a total of 34 hours a week. Being an educational institution, a number of lectures and short courses are dispensed, for which an average of 1 day per week has been set aside, leaving 26.5 hours of work a week. Only 25 hours have eventually been retained to account for general tasks such as timber unloading, cleaning and tool care.

In this instance, 25 man hours per week can be expected for each individual involved in the building.

12.3.4 Results

Considering a 25% additional margin, a total of 2400 man hours have been estimated for the build of the A Rater. The time breakdown for each major phase of the project is presented in Figure 58 and detailed in Appendix C.

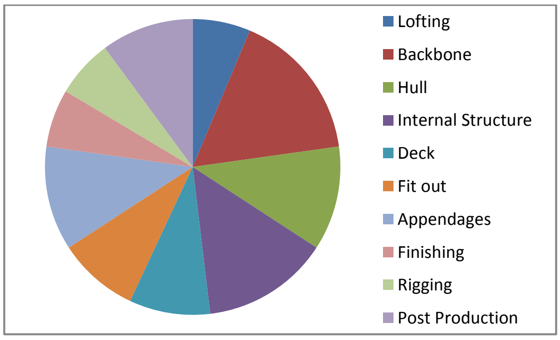

Figure 58: *Time estimate breakdown.*

Based on the 25 man hours per week assumption, a total of just less than two years would be needed for a single worker to complete the building by himself. With two workers, less than a year is now required, and four workers would be able to complete the project in under six months. The actual build time is therefore entirely dependent on the number of workers allocated to the production.

12.3.5 Conclusions

A total of 2400 man hours have been estimated appropriate to complete the project. In terms of actual time frame, this can heavily vary, from six months to over two years depending on the number of workers involved. Finally, the possibility of manufacturing a mould tool for future composite production, suggested in Section 14.4, could impact on the building time.

12.4 Costing

12.4.1 Introduction

From a customer's point of view, '*how much will it cost?*' is probably the first and most important question that will be asked. Typically, an invitation to tender is sent to multiple shipyards, and the one who can build a given boat for the lowest price will usually get the contract. In most cases, the building price will be specified on the contract: if the final cost is higher, the shipyard is effectively losing money, while building the boat competitively will increase its margin.

Labour is the driving and hardest to establish component of a cost estimate, and is in this instance free of charge, thus allowing for an inexpensive and competitive boat, with a more reliable cost evaluation. Do to so, the price of the building materials and consumables are to be accurately quantified.

Note that, since the yacht is to be built in England, the cost estimate has been developed in British Pounds (£); the proposed conversions in New Zealand Dollars ($) considers the average exchange rate for the first quarter of 2015, which can be conveniently rounded to £1 = $2.

12.4.2 Cost Estimate

12.4.2.1 Estimation

The cost estimate can be compared to the weight one, to which it is closely linked. Due to the relative small size of the A Rater, each item and associated price will be recorded individually. In the absence of labour, the cost is based on four main categories, respectively the building materials, consumables, hardware and subcontracted items.

12.4.2.2 Building Materials

This involves products such as the wood, resin and fasteners: all the raw materials from which the boat will be built. Some of the necessary outcomes include a bill of materials as well as a cutting list. Indeed, the sizes of wood to be bought must accommodate for the machining waste factor, so that the desired size can be achieved.

12.4.2.3 Consumables

The consumables refer to products needed for the building, but not part of the final boat, and ranges from paint brushes to saw blades. A pessimistic approach has been adopted with increased safety margins to reflect the inherent uncertainty.

12.4.2.4 Hardware

Those are '*off the shelf*' components that can be directly purchased, such as the deck hardware and control lines. Based on the deck plan presented in Drawing 03, an exact bill of materials can be set up, hence a resulting very reliable cost estimate.

12.4.2.5 Subcontracted Item

Finally, the greatest expenses will be made on large subcontracted items, such as the rig and sails.

12.4.2.6 Conclusions

Thanks to the small size of the boat and the absence of labour, an accurate cost estimate can be realised. A pessimistic approach will be considered for consumables, and a 5% overall margin will be added to cope with potentially defectuous items, building errors, delivery and rise in prices.

Finally, the shipyard and classification fees will be added as well as taxes, thus providing the final cost.

12.4.3 Reducing Expenses

12.4.3.1 Lowering Costs

From both a design and production perspective, decisions can be made in order to minimise the costs. They are respectively discussed for the four cost categories previously introduced.

12.4.3.2 Building Materials

Firstly, as stated in Section 11.6.2.4, cold moulding results in a very small waste factor compared to carvel, which allows for significant savings. Despite its high price, the expenses inherent to the epoxy resin are equivalent to the 4000 copper nails that would be involved for a carvel hull, but at a fraction of the weight.

The concept of waste factor applies to the resin as well. At an early stage of the project, trials should be conducted to ascertain the precise amount of resin (in grams per square meter) needed for the lamination of the veneers. The closer the amount of resin mixed is to the required amount, the minimum the waste factor is.

Finally, the choice of affordable woods allows for a lower cost. For instance, mahogany or teak veneered plywood for the deck will have the same visual appeal as solid wood, for half the price [98].

12.4.3.3 Consumables

The price of consumables can be reduced in two ways.

On the one hand, items that are only to be used once (gloves, brushes, etc…) should be purchased for the smallest possible price (provided the quality is suitable for the work) in order to minimise costs.

On the other hand, careful planning and organisation can help diminish the consumables cost, by performing all similar tasks at the same time. For instance, varnishing all components at once will only require a single set of consumables, as opposed to numerous if all are done individually at different times.

12.4.3.4 Hardware

Remembering the cockpit design philosophy stated in Section 6.2.4, the proposed layout is as simple as possible, which leads to less deck hardware, hence a smaller price. The wide range of hardware manufacturer results in a large scatter in prices, from basic to ultra-light equipment. The decision regarding the hardware should therefore be left to the customer's appreciation, depending on the intended use and budget for the boat.

12.4.3.5 Subcontracted Items

As stated in Chapters 4 and 5, standard mast and sails are available for the A Rater class. These would be more economical than custom made ones. Once again, the decision will be left at the client's discretion depending on the budget.

12.4.3.6 Conclusions

As part of the design and production planning, aspects allowing to reduce the waste and overall costs have been implemented. However the hardware, rig and sails being extremely expensive, the owner's decisions will have a large impact on the final price.

12.4.4 Results

12.4.4.1 Overall Cost

A very conservative approach has been adopted for the cost estimate to avoid unexpected expenses. Large waste factor have been considered, and an overall 20% margin has been added.

A total boatbuilding cost of £16k ($32k) has been determined, onto which is added the shipyard fee. Finally, the costs of the deck hardware, ropes, rig and sails are to be added. In a standard configuration, a further £9k ($18k) will be required, giving the cost breakdown shown in Figure 59.

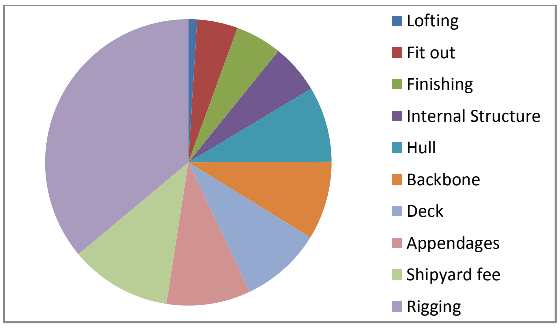

Figure 59: Cost estimate breakdown.

As a result, the overall production price of the yacht has been approximated at £28.2k ($56.4k), with a very conservative approach.

The price will however be extremely dependent on the owner's choices regarding the subcontracted items.

12.4.4.2 Cost Evolution

From a financing perspective, the evolution of the cost during the duration of the project is of particular interest. Figure 60 presents the evolution of the cost during the completion of the project (blue), the same estimate if labour was charged (red), and the actual expenses (green); the latter accounts for the fact that materials must be order before-hand.

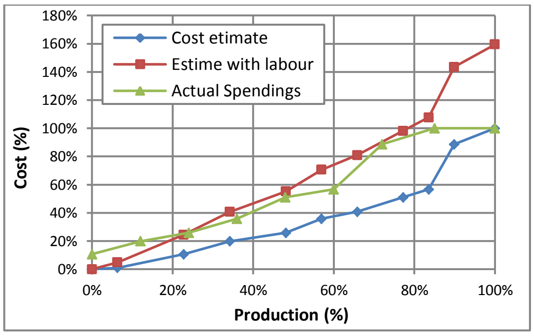

Figure 60: Cost evolution with production.

Firstly, the tremendous savings generated by the absence of labour can be seen.

Secondly, the need to order the building materials imposes an initial investment prior to the construction.

Finally, it is interesting to note that, before the very large expenses due to the subcontracted items occurring at the end of the project, the evolution of the cost with time is linear, whether or not the labour is included. This translates into regular monthly expenses throughout the majority of the project.

12.4.5 Conclusions

A conservative cost estimate has been realised, with a building cost of $16k ($32k), and an overall price ready to sail of £28.2k ($56.4). This cost is however likely to significantly increase should the owner decide to upgrade subcontracted items. The yacht however remains very affordable, mostly thanks to the absence of paid labour.

12.5 Conclusions

While an accurate critical path analysis did not prove applicable in the case of a one off wooden boat, a timing estimate has been produced. Considering appropriate margins of safety, the amount of man hours required has been evaluated to be 2400; the actual building time frame will depend on the number of workers allocated to the project. The final cost has been approximated at £28.2k ($56.4), deemed very affordable, and likely to be lower thanks to the conservative approach. The production planning is to be found in Appendix C.

Further time and cost reduction could be achieved by manufacturing a female mould tool from the wooden hull, aiming at future composite capabilities; this aspect will be tackled in Section 14.4

At this stage of the project, both the design and production planning phases are complete, allowing for the final drawings to be developed, which constitute the finality of this project.

Chapter 13: Drawings

From an academic perspective, a professional report describing the decisions made is the main deliverable. However, from the point of view of the customer and builder, a picture is worth a thousand words, and detailed drawings illustrating the design and providing the manufacturing instructions are of paramount importance. A complete set of drawings has therefore been developed, and are to be found in this chapter.

Although 3D renders are a particularly efficient and attractive way to visually depict the yacht, and would certainly be necessary in a strictly commercial environment, the academic nature of the project dictated the choice not to undertake 3D modelling. Indeed, the tremendous amount of time required was deemed better employed at improving the design. Nonetheless, 3D renders are suggested as future work to be undertaken, particularly to promote and advertise the final product.

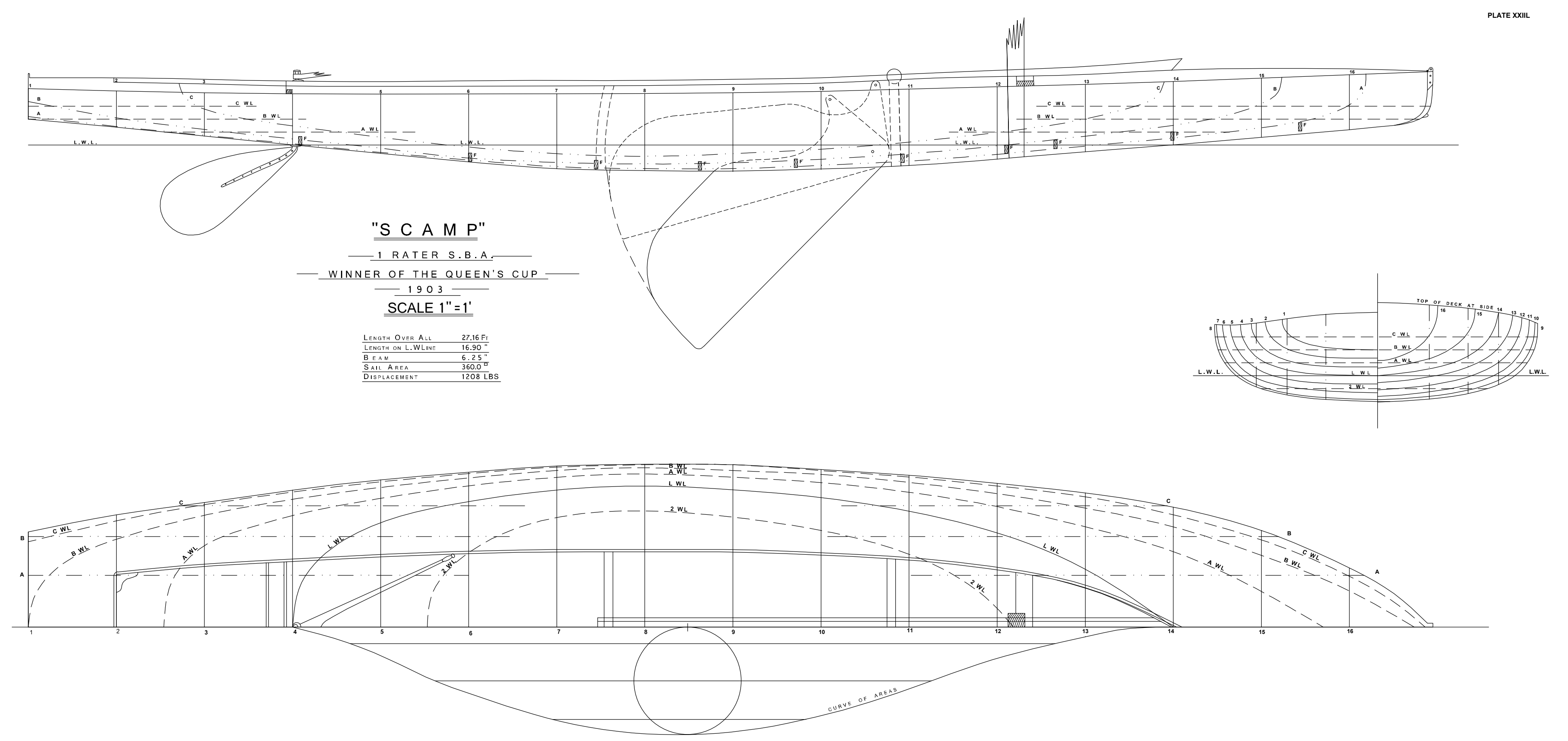

Notes:

1 - Exact replica of the linesplan published in: *Dixon Kemp's Manual of Yacht and Boat Sailing and Yacht Architecture*, new and eleventh edition, edited by Brooke Heckstall-Smith and Linton Hope, London: Horace Cox, 1913.

2 - Original plan conserved at the British Library, London.

3 - Original plan size: 796mm by 434mm.

4 - As it is an exact replica, some of the design discrepancies (such as the centreplate) have been conserved.

JEAN-BAPTISTE ROGER GUILLAUME SOUPPEZ

Scamp (L. Hope Design) - Linesplan Replica

PROJECT: Thames A Rater		FORMAT: A4	UNITS: mm
DATE: 27/06/2015	DRAWN BY: JBS	DRAWING n°: 01	SCALE: 1:36

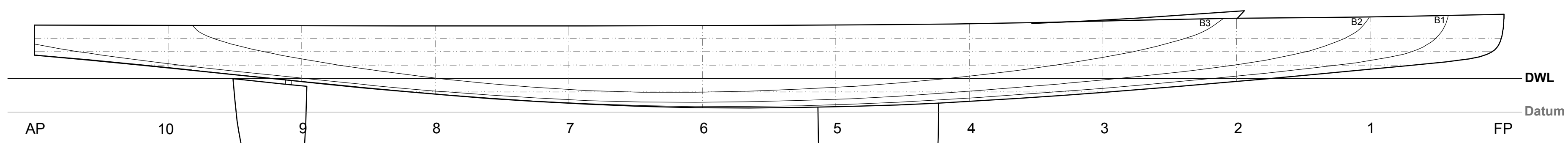

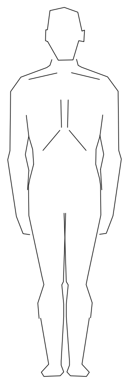

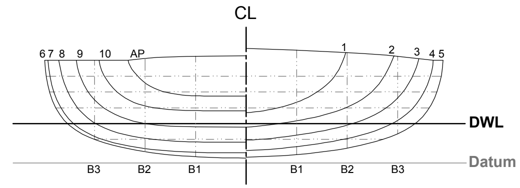

Specifications

Length Over All	8.30 m	27.23 ft
Length on Waterline	5.62 m	18.44 ft
Beam Over All	1.92 m	6.30 ft
Beam on Waterline	1.70 m	5.58 ft
Canoe Body Draft	0.16 m	0.52 ft
Overall Draft	1.55 m	5.09 ft
Displacement	0.652 m^3	23.03 ft^3
Wetted Surface Area	7.55 m^2	81.27 ft^2
Prismatic Coefficient	0.546	0.546

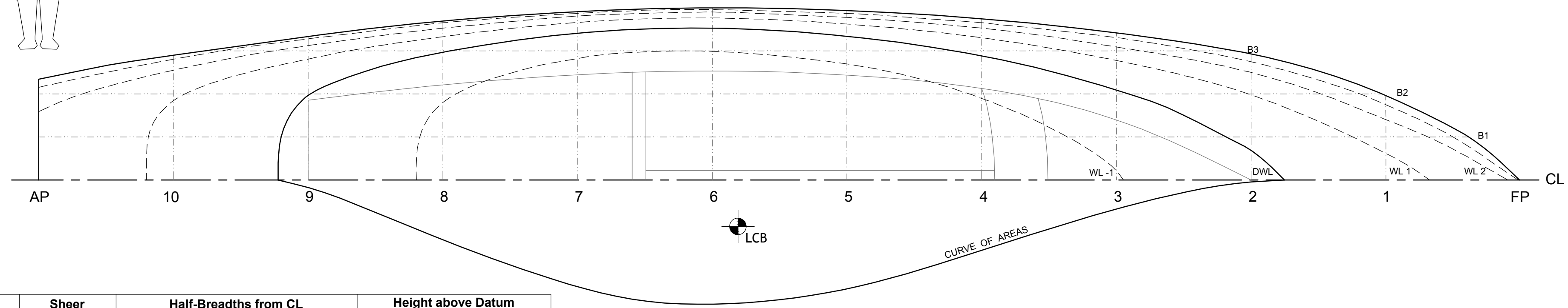

Station	Sheer		Half-Breadths from CL					Height above Datum			
	Height from Datum	B/2 from CL	WL -1	DWL	WL 1	WL 2	WL 3	Keel	B1	B2	B3
FP	73	0						73			
1	71	64			20	45	56	32	38		
2	70	94		22	63	80	88	23	27	35	
3	68	110	8	67	89	99	106	15	18	24	41
4	66	119	61	92	106	113	117	8	10	16	27
5	65	125	87	107	116	121	124	4	5	10	19
6	65	128	96	113	121	125	127	3	4	7	15
7	65	126	91	109	117	122	124	6	7	9	17
8	65	119	57	95	107	113	117	13	13	16	25
9	65	108		63	90	100	105	23	23	25	40
10	65	93			59	82	90	33	33	36	
AP	65	75				51	69	42	42	51	

Notes:

1 - Lines to outside of planking.
2 - Waterlines spaced by 75 mm from DWL.
3 - Datum 188 mm below DWL..
4 - Stations spaced by 753 mm from AP.
5 - Buttock spaced 241 mm from CL.
6 - Transom camber 22 mm.

JEAN-BAPTISTE ROGER GUILLAUME SOUPPEZ			
Linesplan and Table of Offsets			
PROJECT: Thames A Rater		FORMAT: A4	UNITS: mm
DATE: 27/06/2015	DRAWN BY: JBS	DRAWING n°: 02	SCALE: 1:36

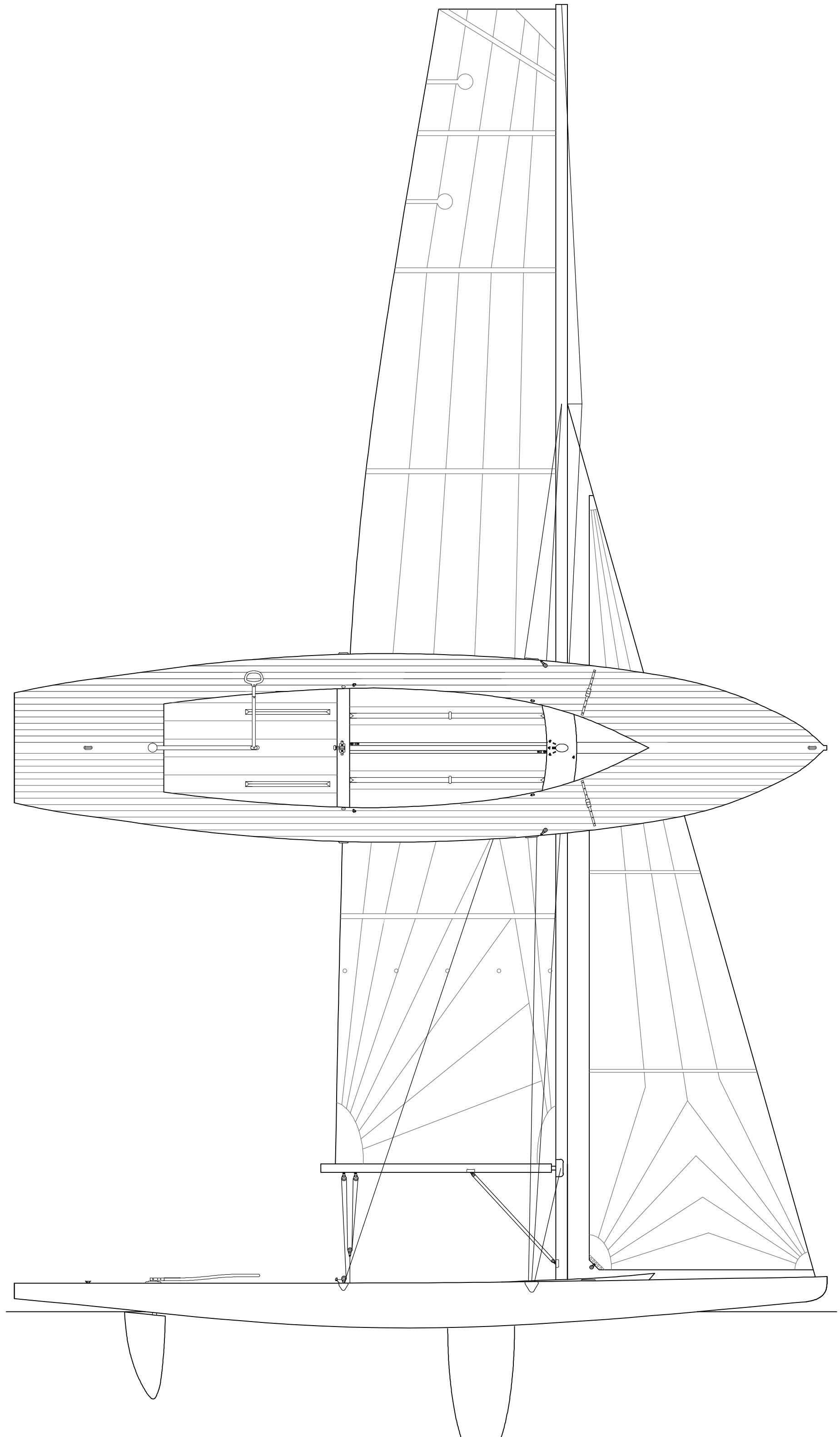

Thames A Rater

Length Over All	8.30 m	27.23 ft
Length on Waterline	5.62 m	18.44 ft
Beam Over All	1.92 m	6.30 ft
Canoe Body Draft	0.16 m	0.52 ft
Overall Draft	1.55 m	5.09 ft
Lightship	340 kg	750 lbs
Full Load	652 kg	1437 lbs
Total Sail Area	32.51 m²	350 ft²

JEAN-BAPTISTE ROGER GUILLAUME SOUPPEZ

Outboard View

PROJECT: Thames A Rater	FORMAT: A4	UNITS: mm
DATE: 27/06/2015	DRAWN BY: JBS	DRAWING n°: 03	SCALE: 1:70

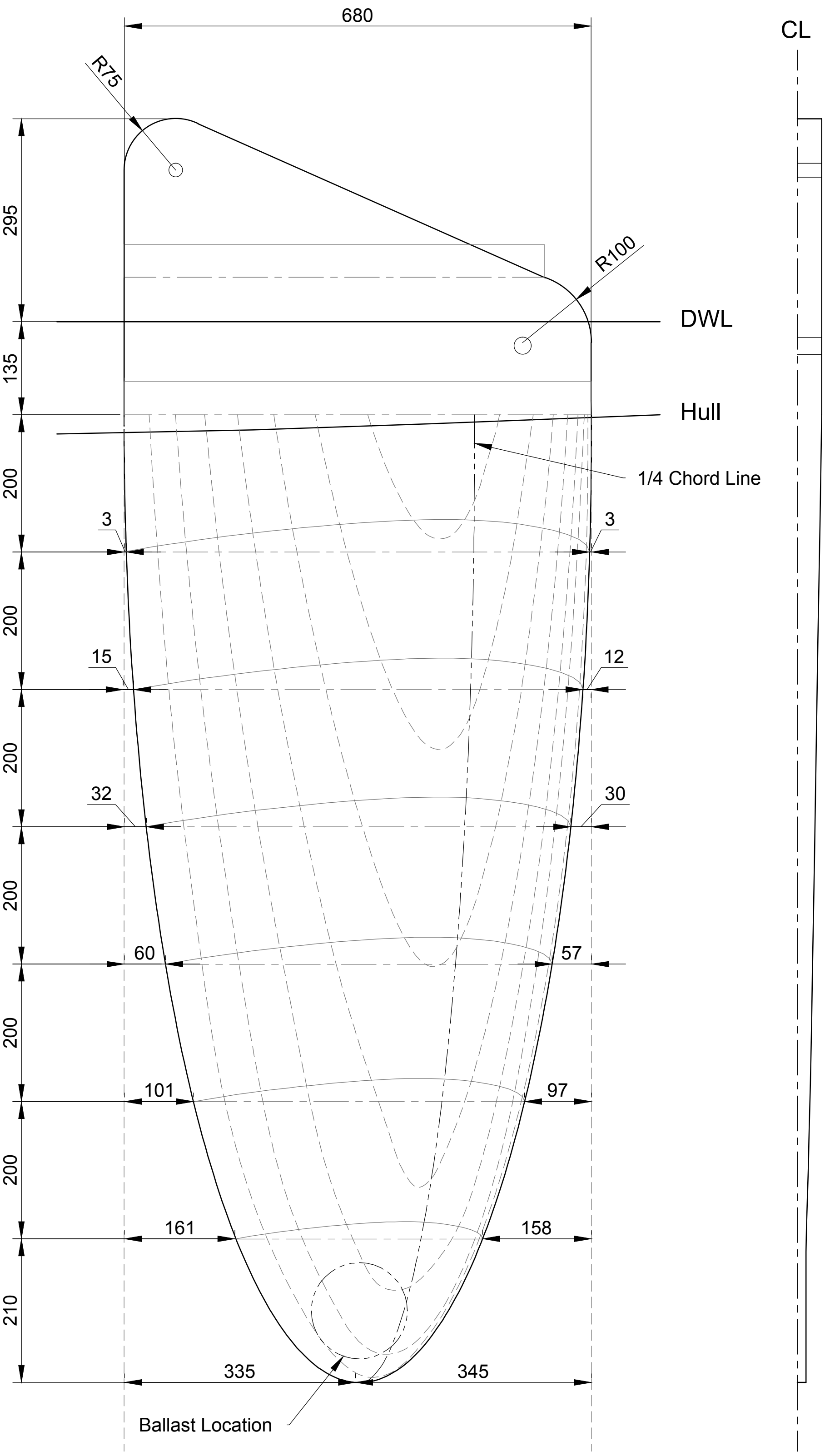

Notes:
1 - Construction details to be found in Drawing 06.
2 - Optional ballast location, amount to be advised after weighing of the yacht and/or unsatisfactory stability.

JEAN-BAPTISTE ROGER GUILLAUME SOUPPEZ

Centreplate Geometry

PROJECT: Thames A Rater		FORMAT: A4	UNITS: mm
DATE: 27/06/2015	DRAWN BY: JBS	DRAWING n°: 04	SCALE: 1:10

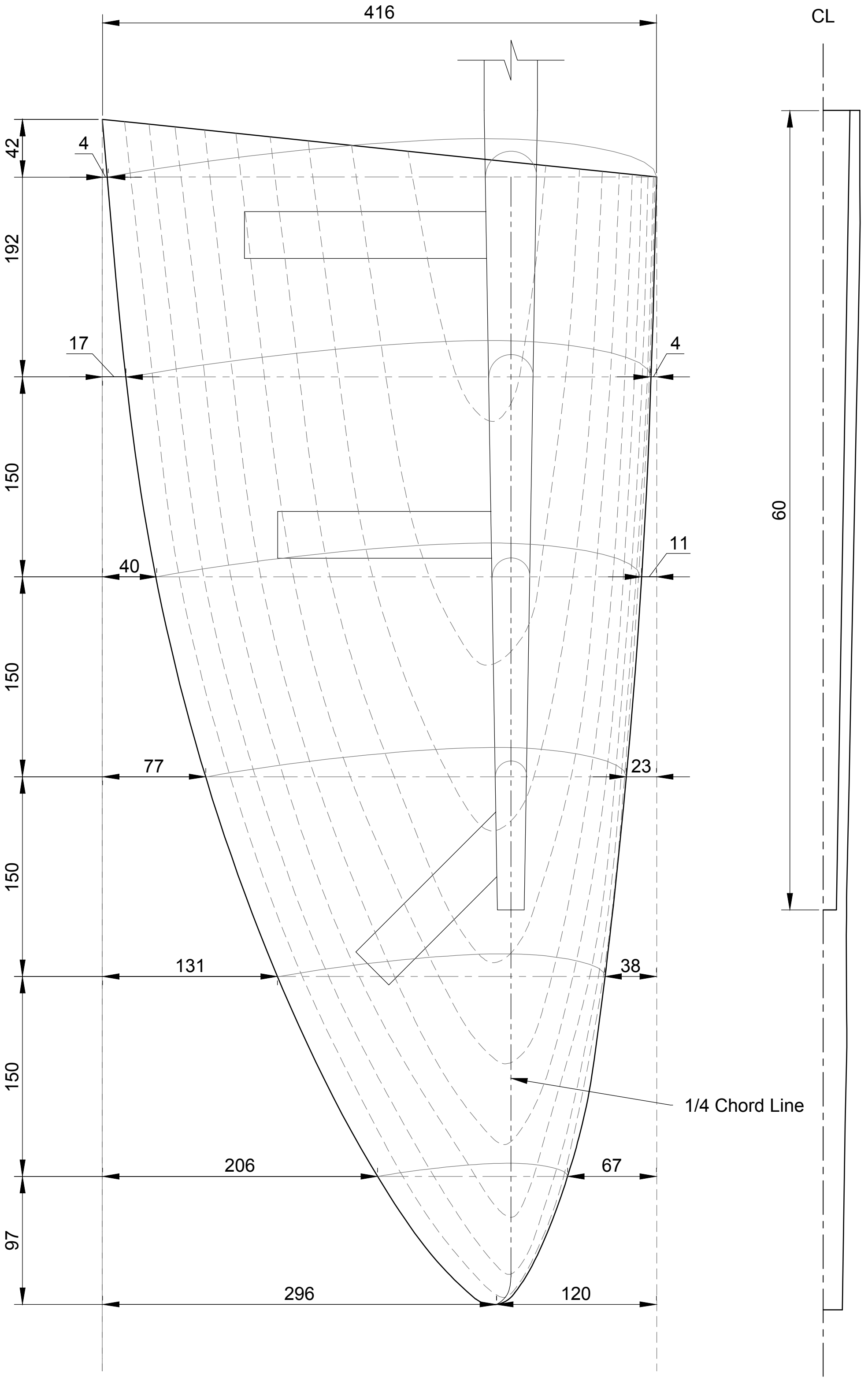

Notes:

1 - Construction details to be found in Drawing 06.
2 - Bronze rudder stock and tangs.
3 - Arrangement to be modified should the rudder stock be subcontracted.

JEAN-BAPTISTE ROGER GUILLAUME SOUPPEZ			
Rudder Blade Geometry			
PROJECT: Thames A Rater		FORMAT: A4	UNITS: mm
DATE: 27/06/2015	DRAWN BY: JBS	DRAWING n°: 05	SCALE: 1:5

CENTREPLATE CROSS SECTION

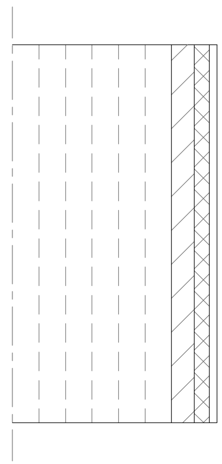

CL

RUDDER CROSS SECTION

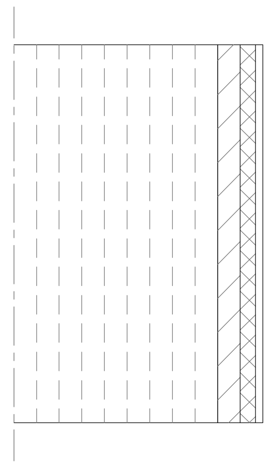

CL

Centreplate Laminate Schedule (from CL)

Location	Ply	gsm	n° of plies	Wf	Ply t (mm)	Comment
Inner	Mahogany Veneer	n/a	6	n/a	3	Oriented along the span
	E-Glass UD	450	2	0,50	0,55	Oriented along the span.
	E-Glass WR	300	1	0,40	0,58	Resin rich.
Outer	Gel coat	n/a	n/a	n/a	1	Polished finished.

Rudder Laminate Schedule (from CL)

Location	Ply	gsm	n° of plies	Wf	Ply t (mm)	Comment
Inner	Mahogany Veneer	n/a	9	n/a	3	Oriented along the span.
	E-Glass UD	450	2	0,50	0,55	Oriented along the span.
	E-Glass WR	300	1	0,40	0,58	Resin rich.
Outer	Gel coat	n/a	n/a	n/a	1	Polished finished.

Notes:

1 - Appendages to be constructed from the buttocks templates shown in Drawings 04 and 05, glued using epoxy.
2 - Veneers and unidirectionals (UD) should run along the span of the foil.
3 - FRP layers should respect the advised weight fraction; a 10% margin will be allowed on the FRP thickness.
4 - Woven rovings (WR) cannot be replaced by Chopped Strand Mat (CSM) as epoxy will not disolve binder.
5 - Final thickness to be checked against design requirement.

JEAN-BAPTISTE ROGER GUILLAUME SOUPPEZ			
Centreplate and Rudder Laminate Schedule			
PROJECT: Thames A Rater		FORMAT: A4	UNITS: mm
DATE: 27/06/2015	DRAWN BY: JBS	DRAWING n°: 06	SCALE: 1:1

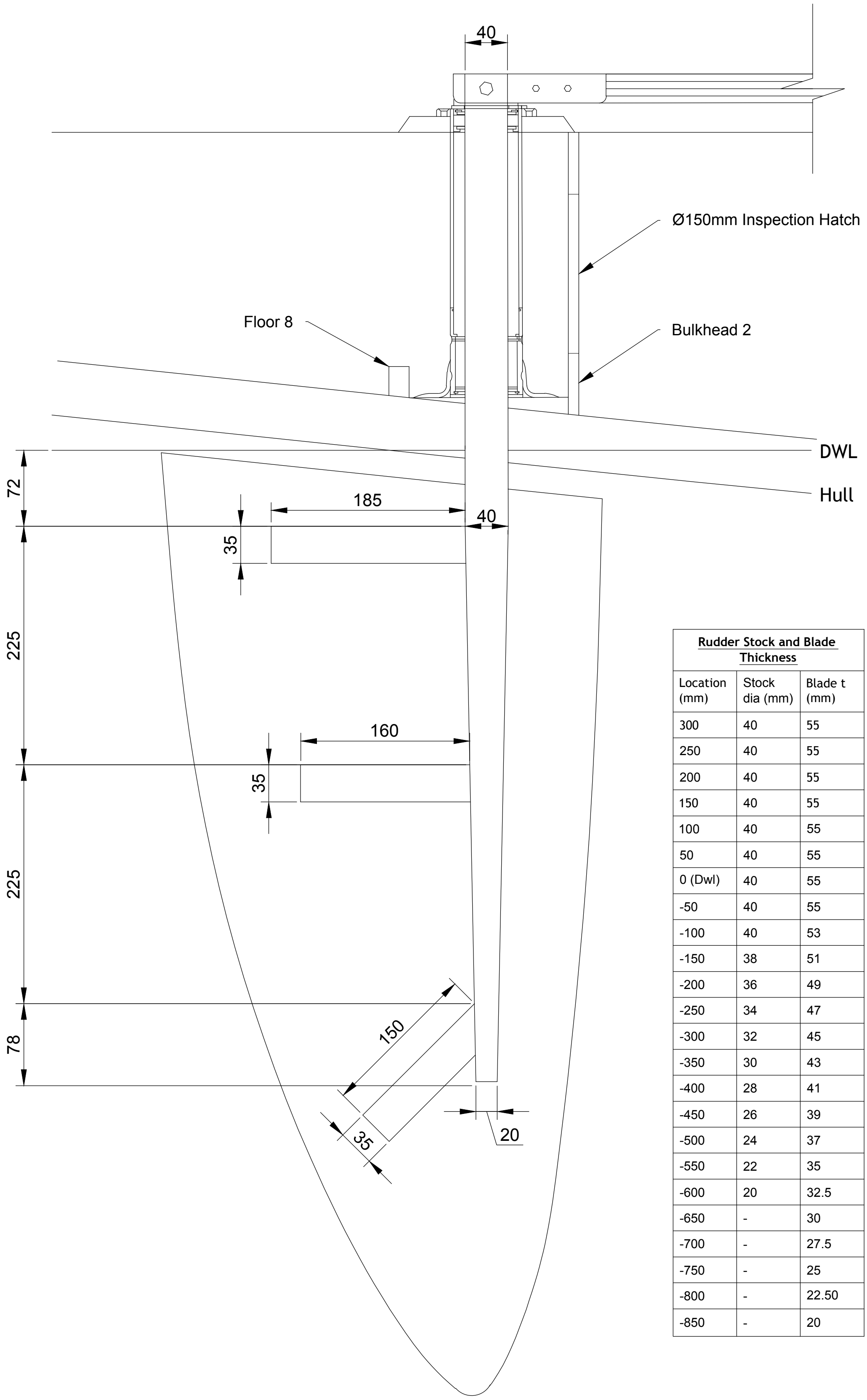

Rudder Stock and Blade Thickness

Location (mm)	Stock dia (mm)	Blade t (mm)
300	40	55
250	40	55
200	40	55
150	40	55
100	40	55
50	40	55
0 (Dwl)	40	55
-50	40	55
-100	40	53
-150	38	51
-200	36	49
-250	34	47
-300	32	45
-350	30	43
-400	28	41
-450	26	39
-500	24	37
-550	22	35
-600	20	32.5
-650	-	30
-700	-	27.5
-750	-	25
-800	-	22.50
-850	-	20

Notes:

1 - Bronze rudder stock and tangs (8mm thick).
2 - Arrangement to be modified should the rudder stock be subcontracted.
3 - Top and bottom bearings, and tube arrangement from *Jefa Rudder & Steering*.
4 - Structural details to be found in Drawing 06.
5 - Tiller section 40mm wide by 25mm deep, laminated mahogany.

JEAN-BAPTISTE ROGER GUILLAUME SOUPPEZ

Rudder Arrangement

PROJECT: Thames A Rater		FORMAT: A4	UNITS: mm
DATE: 27/06/2015	DRAWN BY: JBS	DRAWING n°: 07	SCALE: 1:6

A-RATER

Main:
P = 11.75 m
E = 2.25 m
Area = 23.21 m²
AR = 6.04
Reef 1 = 17.40 m²
Reef 2 = 10.44 m²

Jib:
I = 7.95 m
J = 2.30 m
LP = 2.20 m
Area = 9.30 m²
AR = 6.78

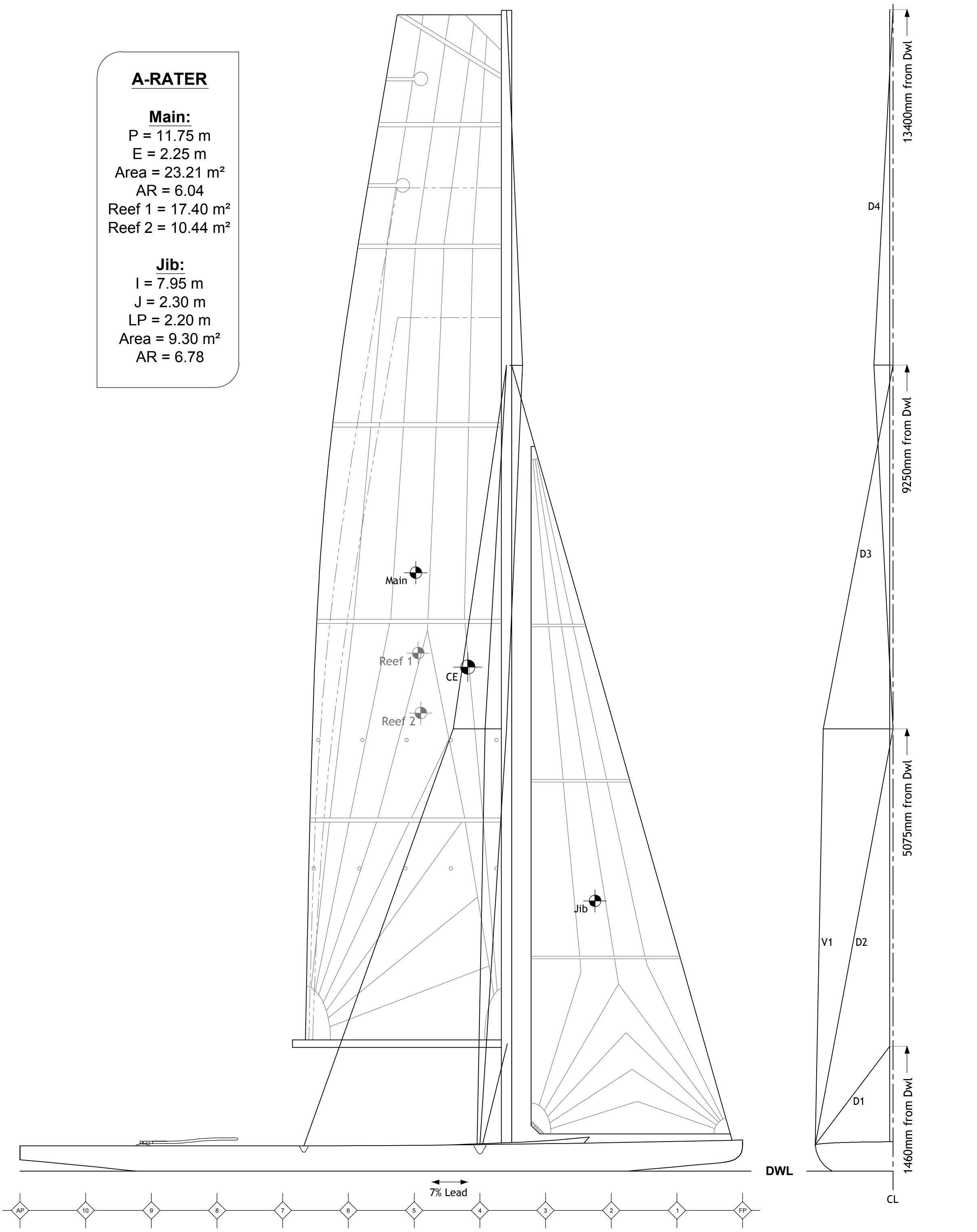

Shrouds and Stays size and dimensions (1x19 stainless steel)			
Shroud/Stay	Angle (°)	Dia (mm)	Length (mm)
D4	3.1	3.0	4085
D3	10.9	4.0	4245
D2	10.6	4.0	4855
D1	37.0	4.0	1415
V1	1.1	4.0	4775
Forestay	15.9	5.0	9240
Running Backstay	8.3	6.0	9295

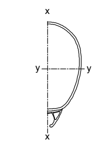
Mast Section:
Selden CC077

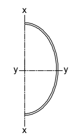
Boom Section:
Selden BC086

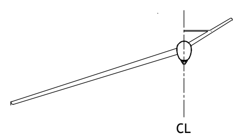

Spreader and Jumper
(Scale 1:35)

Notes:

1 - Rig design developed in accordance with the Nordic Boat Standard [90].

2 - Indicative design only, final specifications and scantlings to be defined by the manufacturer.

JEAN-BAPTISTE ROGER GUILLAUME SOUPPEZ			
Rig and Sail Plan			
PROJECT: Thames A Rater		FORMAT: A4	UNITS: mm
DATE: 27/06/2015	DRAWN BY: JBS	DRAWING n°: 08	SCALE: 1:70

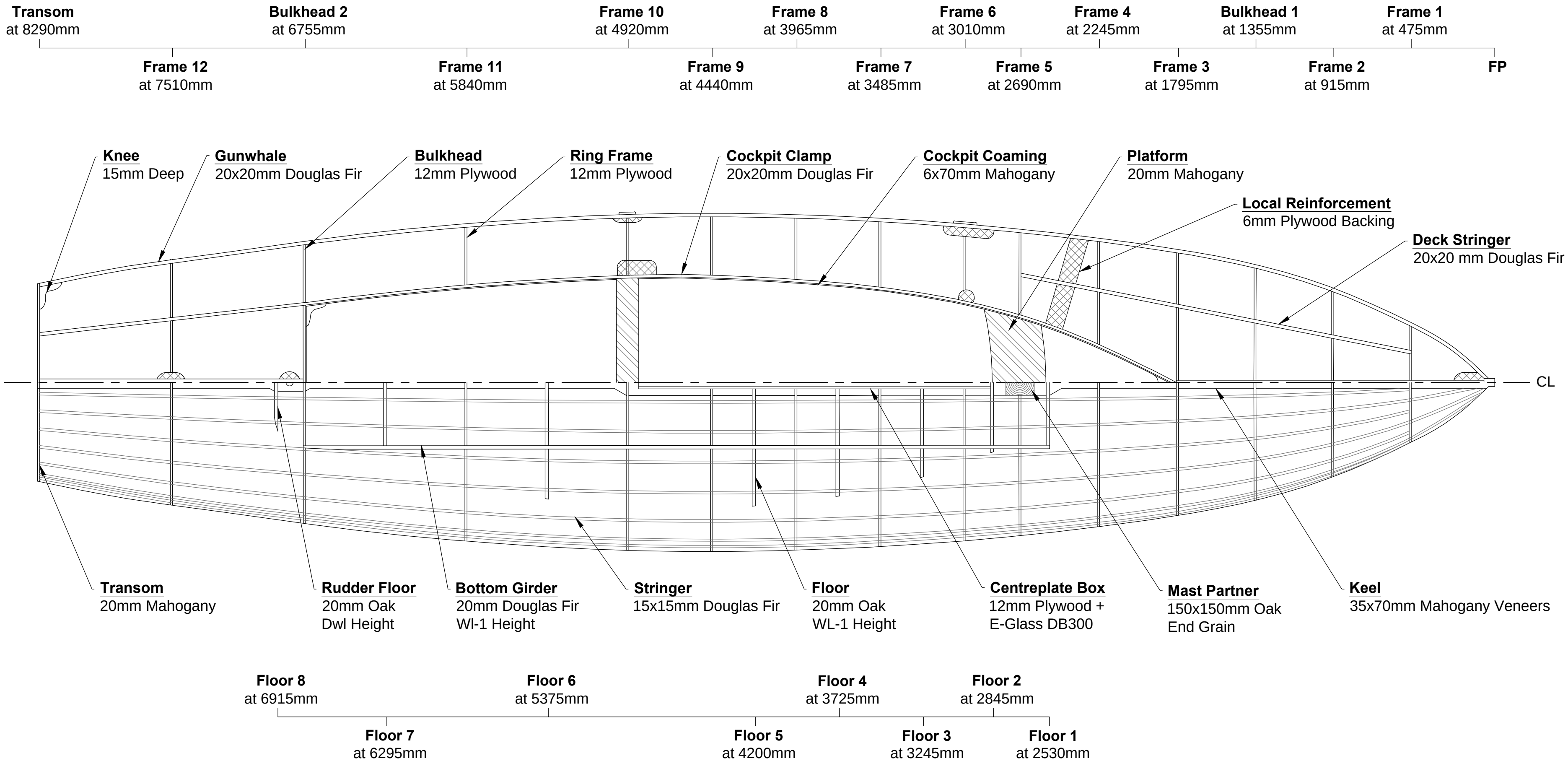

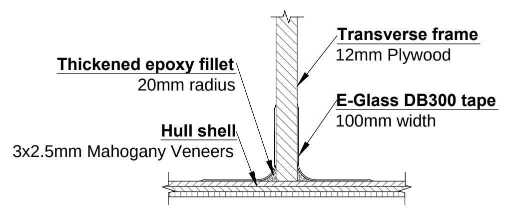

Hull/Frame connection

Scale 1:4

Notes:

1. Hull is 3x2.5mm mahogany veneers, sheathed with E-glass DB 300.
2. Deck is 6mm veneered plywood, sheathed with E-glass DB 600.
3. Frames and bulkheads are 12mm plywood, 50mm deep, as detailed in Drawing 10.
4. Frames and floors position are given related to the forward perpendicular.
5. All plywood to be marine grade (BS 1088 compliant).
6. All plywood edges to be encapsulated with epoxy.
7. Proposed scantlings and building method only.

JEAN-BAPTISTE ROGER GUILLAUME SOUPPEZ		
Hull and Deck Structure		
PROJECT: Thames A Rater	FORMAT: A4	UNITS: mm
DATE: 27/06/2015	DRAWN BY: JBS	DRAWING n°: 09	SCALE: 1:36

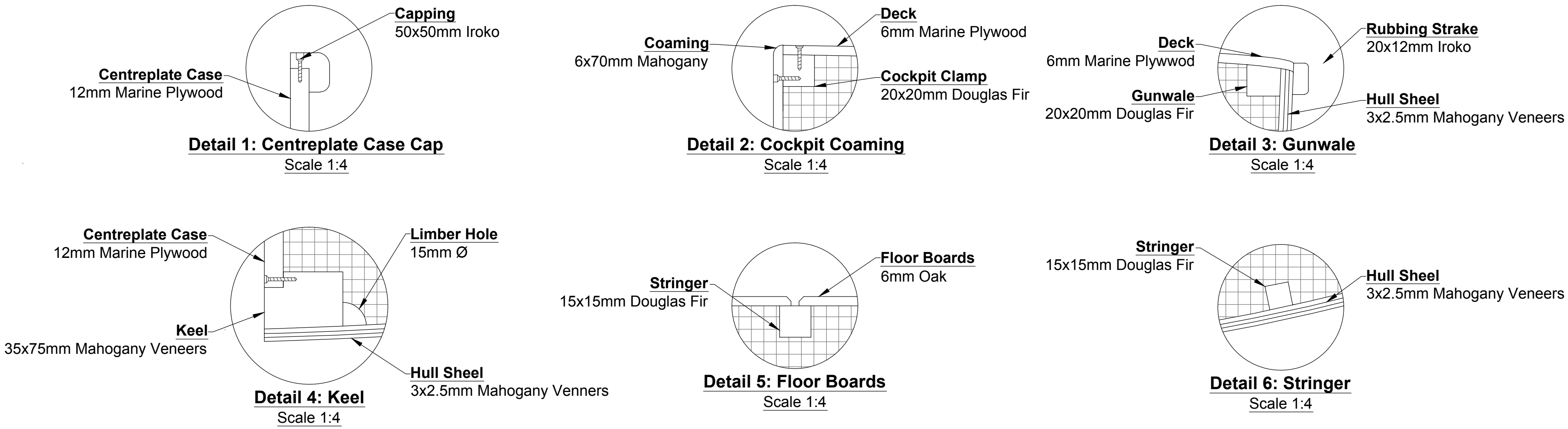

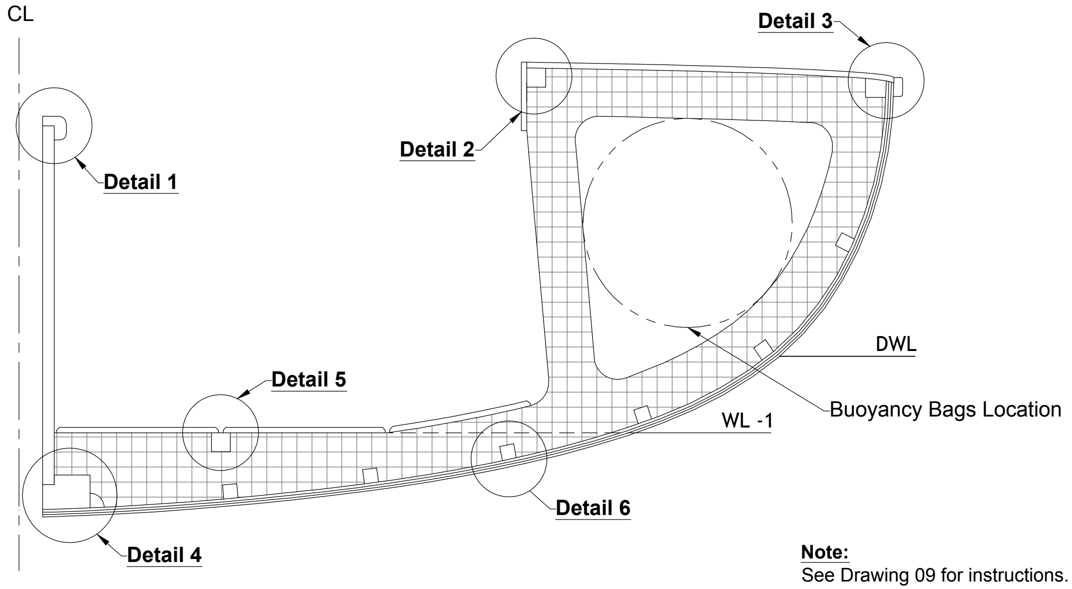

Wood description		
Common name	**Latin name**	**Density (kg/m³)**
European Oak	Quercus spp.	689
African Mahogany	Khaya anthotheca	530
Douglas Fir	Pseudotsuga Menziesii	446

Note:
See Drawing 09 for instructions.

JEAN-BAPTISTE ROGER GUILLAUME SOUPPEZ			
Midship Section (Frame 8)			
PROJECT: Thames A Rater		FORMAT: A4	UNITS: mm
DATE: 27/06/2015	DRAWN BY: JBS	DRAWING n°: 10	SCALE: 1:8

Chapter 14: Future Work

The work undertaken revealed opportunities for further work and investigations, from both an academic and production perspective. Those aspects have not been incorporated to the project at this stage as they are beyond the intended scope. Nevertheless, this chapter will present the suggestions, recommendations, and intended future work inherent to the new A Rater.

14.1 Introduction

The scope of the project has been defined as the conception and production of a wooden Thames A Rater class sailing yacht, and revealed areas that could be further investigated as well as alternative construction methods. The main opportunities identified are the design evaluation as part of the post-production, possible modifications, and a composite production line.

14.2 Design Evaluation

14.2.1 Introduction

Many aspects of the design rely on estimations, with various degrees of uncertainty that lead to safety margins. While there is a vast amount of data about estimation methods in the literature, there is no published data on how the application of those estimates compare to the actual boat built. It would therefore appear relevant to carefully record aspects of the construction, in the areas detailed hereafter.

14.2.2 Weight Estimate

Possibly the most critical of all, the weight estimate has been realised considering each item individually in this instance. This can be particularly hard to establish for laminated wood, glues and varnish. As a result, the margins added to the different weight categories vary to reflect the level of uncertainty. Weighing the boat regularly as the construction progresses will highlight the various degrees of accuracy, validate the assumptions made, and refine the margins applied.

14.2.3 Inclining Experiment

Closely linked to the weight is the centre of gravity estimate that will be ascertained as part of the inclining experiment. Once again, the comparison of the original calculations and the actual stability will provide valuable insights into the use of stability estimation in yacht design. Appropriate safety margins, particularly regarding the VGC, can then be derived.

14.2.4 Speed Trials

A significant part of the design revolved around the VPP. While accurate measurements of all degrees of freedom would be very expensive in terms of instrumentations, a simple speed trial would constitute relevant data.

The boat speed can be recorded with a simple GPS unit in a range of true wind speeds and true wind angle. The comparison of the velocity prediction and the actual speed recorded would provide an interesting comparison, and help evaluate and refine the VPP, particularly in terms of planning behaviour. In this case too, there seems to be very little published data regarding the comparison on velocity prediction and actual yacht performance.

14.2.5 Building Accuracy

Introduced in Section 2.4.2, the building accuracy is regulated by the class rule and is also of primary concern to the designer, since it is expected that the yacht will be constructed as intended. Identifying where and to which extent the final yacht diverges from the plans will allow to improve the building accuracy in future builds.

14.2.6 Timing and Costing

While unlikely to be very precise for a one-off vessel, the time and cost estimates are decisive factors. Recording the progress of the production and inherent costs to then be compared to the original approximations would refine future similar work. The emphasis will be put on the margins; in this instance, a 20% margin has been applied to both the time and cost evaluation, for all phases of the building. However, some aspects might be more reliable, thus requiring a lower margin. Conversely, more complex tasks may have a much higher degree of uncertainty, which will be translated into higher margins. The comparison of the intended and actual time and cost estimate will therefore provide improved data for future reference.

14.2.7 Documentation

Finally, some of the future work to be undertaken will include documentation, mostly for the purpose of the classification and the redaction of the owner's manual. This will rely on previous aspects of the design evaluation, such as the actual displacement and stability.

14.2.8 Conclusions

In order to improve future approximations and provide actual data on the comparison of design estimates and actual production results, a careful evaluation should be realised. The major aspects include weight, stability, speed trial and building accuracy, aiming at validating the methods employed. Moreover, specific timing and costing margins will be determined for the various stages of the construction. Finally, the classification and documentation of the yacht are to be performed.

It is hoped that the design evaluation will provide relevant data in an area where very little is available in the published literature.

14.3 Design Modifications

14.3.1 Introduction

The proposed design could be modified to better suit the customer's expectations, as well as broaden the sailing possibilities offered by the boat. As a result, aspects such as the customisation and inshore sailing capabilities including a spinnaker and trapeze will be discussed.

14.3.2 Customisation

Introduced along the report, the possibilities for customisation are endless. The wood spices can lead to very different visual effects. The deck manufacturing and appearance can be made in multiple ways. Furthermore, the hull and deck can either be varnished, or painted, in which case a large array of colours can be proposed.

In addition, the deck hardware, ropes, rig and sails are left at the customer's discretion, with a range of options, from simple and inexpensive, to top of the range products and associated cost.

Finally, further design changes can be implemented. In term of the cockpit for instance, a compartment for a disabled sailor could be arranged.

From the design proposed, there is leeway to adapt the yacht to the specific demands of any customer. This can be extended to the sailing program.

14.3.3 Inshore Sailing

The Thames A Rater class rule [111] specifies that the yachts are to race inland, and spinnaker and trapeze are therefore prohibited. However, the boat was developed as a category C, i.e. able to sail up to 2 miles offshore, and not just as an inland craft (Category D). This is to widen the sailing capabilities of the new A Rater, which could also be a nice day boat for inshore sailing.

Moreover, by sailing inshore, the prohibition of spinnaker and trapeze on waterways is not applicable anymore, which would allow for a downwind sail and improved stability, not to mention the more extreme sensations.

A yacht with an enlarged sailing program and a tremendous increase in performance can therefore be expected, likely to attract more customers.

14.3.4 Conclusions

In order to broaden the commercial potential of the new A Rater, a high level of personalisation will be offered, on both the wooden construction and equipment. Furthermore, the yacht will be able to sail inshore, and a spinnaker could easily be fitted to achieve a fast and polyvalent craft.

14.4 Composite Production Line

14.4.1 Introduction

The building of a wooden boat has certain drawbacks compared to a composite yacht, such as a longer and more expensive construction, and a potentially higher weight. The setup of a composite production line would remedy those issues, and provides the tools required to build a large fleet in a shorter amount of time. To do so, a female mould tool is to be created.

14.4.2 Female Mould Tool

14.4.2.1 Terminology

There seems to be a certain amount of confusion regarding the terminology involved with mould making. Three terms are to be defined: plug, mould, and mould tool:

- The plug is the basis on which the mould or mould tool will be made. A plug can be manufactured from a foam block with a 5-axis machine, or using station moulds and closely spaced stringers. The plug can either be male or female, meaning that the mould will respectively be constructed over the top of, or inside the plug.
- A mould is built for a one-off vessel only, and is therefore structurally minimalist.
- A mould tool refers to a mould that is to be as part of a production line, i.e. used more than once, and should consequently be structurally reinforced.

14.4.2.2 Female Mould Tool.

In the case of the A Rater, once laminated, the hull shell is essentially a male plug. There is therefore an opportunity at this stage of the building (and before the hull turn-over) to construct a female mould tool on top of the hull shell. This is easily done by laminating layer of fiberglass on top of the hull, ensuring the wood is separated from the composite laminate by a plastic layer so the mould tool can be released.

Appropriate stiffening reinforcement will be provided to ensure the mould tool retains the hull shape accurately over time. Once constructed, the mould tool makes the manufacturing of multiple composite hulls possible.

The same principle applies to the appendages: the original ones will be laminated wood; a female mould tool can then be made.

14.4.3 Composite Design

For the new composite boat, new scantlings are to be designed. This can take various forms depending on the required degree of performance to be achieved, but more importantly the budget allocated by the customer. An extremely low-cost hull can be built with chopped strand mat (CSM) and polyester resin. Conversely, a much lighter but much more expensive hull can be manufactured from unidirectional carbon fibre and epoxy resin. In any case, the new structural arrangement is to comply with the ISO 12215 Part 5 [54] and the mould tool can accommodate any kind of composite (fibre and resin) combination.

A composite design will provide a much faster building, effectively eliminating the time consuming backbone setup, and making for a much faster lamination. Furthermore, the composite hull can be lighter than a wooden one. Remembering the minimum lightship weight imposed by the class rule, this means that the yacht still cannot be made lighter. However, it allows for an increased amount of ballast in the centreboard; the higher ballast ratio improving stability and performance.

14.4.4 Composite Production

A composite production line can be set up thanks to the female mould tool. The manufacturing of the deck can either be wooden or composite. Indeed, a female mould tool for the deck can be made from the wooden one. By doing so, a yacht can be delivered in a much shorter amount of time, and at a lower cost, making it more attractive to potential customers and help with the development of a fleet on the Norfolk Broads, where the new A Rater is intended to be sailed.

14.4.5 Advertising

A production line involves attracting a certain amount of customers, thus requiring means of promoting the yacht. One of the most efficient ways is certainly the realisation of 3D renders. This has not been considered yet as the time expense was not deemed relevant for an academic research project. An advertising campaign would however justify the time and computational resources involved with the realisation of 3D renders, which will therefore be part of the future work.

14.4.6 Conclusions

In order to develop a larger fleet, increase the manufacturing rate and lessen the cost, a production line has been suggested. This is entirely compatible with the building of the wooden A Rater, and can result in an efficient composite production line.

14.5 Conclusions

Three main areas of interest beyond the intended scope of the project appear to be relevant future work.

First, a careful comparison of design estimates and actual data for the purpose of determining the reliability of the evaluations and safety margins adopted will be undertaken.

Then, a broader sailing program including inshore sailing, a spinnaker and trapeze is intended. Design modifications will therefore be performed.

Finally, the setup of a composite production line aiming at a large scale manufacturing of a lighter and more performant yacht is easily realisable.

Those three aspects are therefore to be further investigated to provide valuable insight for future yacht designs and widen the commercial opportunities for the new A Rater.

Chapter 15: Conclusions

Reflecting on the requirements and objectives originally stated in the design brief, the conclusion will aim at assessing the relevance of the design. In addition, the conclusions drawn from the various aspects of the yacht's conception tackled in this project will be summarised. Ultimately, the new A Rater appears to meet and exceed all the original expectations, and some particularly interesting findings have been highlighted.

15.1 Introduction

The aim of the project was clearly stated as providing a new generation of A Raters that will conserve the traditional spirit of the class, while incorporating modern design and production technology. Furthermore, the new yacht is to be introduced to the Norfolk Broads, inland waterways for which it has been specifically conceived. The strict requirements of the client, shipyard, environment, sailors, class rule and regulatory bodies have all been considered and incorporated into the design and production.

15.2 Design Evaluation

15.2.1 Hull

A major obstacle to the hull design was the Thames A Rater class rule requiring an exact replica of an existing A Rater, with a tolerance of one and a half inch. A substantial amount of research was necessary to eventually obtain an original linesplan. Estimating modelling and building accuracies, 20mm of the allowed tolerance has been dedicated to optimising the hull shape.

Thanks to the Delft Systematic Yacht Hull Series and parametric optimisation, the hydrodynamics of the yacht has been improved, reducing the high speed resistance by 3%, thus demonstrating the feasibility of design optimisation based on semi-empirical resistance prediction methods.

12.2.2 Appendages

The appendages not being regulated by the Thames A Rater class rule, a large amount of time and resources was dedicated to their design. Computational fluid dynamics was used to contrast a range of planforms, and select the most efficient. Compared to the original centreplate and rudder, a 1.8% and 10.5% increase in lift/drag ratio have been achieved respectively.

Considering the structural requirements of each appendage led to the thickness/chord ratio (t/c). For the centreplate, a 7.2% t/c provides a minimum drag, whereas the 13% t/c of the rudder, dictated by the rudder stock diameter, results in a delayed stall angle. Furthermore, the choice of a NACA 00 series hydrofoil section is a significant improvement compared to the flat plates of the original A Raters.

Tremendous progress has therefore been made on the hydrodynamics of the appendages, highlighting the importance of computational fluid dynamics in modern yacht design.

15.2.3 Rig and Sails

Vortex Lattice Method has been applied to the sails to contrast, refine and optimise the design, providing a greater aerodynamic drive force. The mainsail aspect ratio was slightly diminished while the jib one was increased, both aiming at a higher performance. In addition, the flat foredeck will promote the mirror boundary effect on the jib when sailing close hauled, thus increasing the effective aspect ratio.

The proposed rig was created in accordance with the Nordic Boat Standard, and was designed to be as light as possible to reduce weight and lower the centre of gravity. Its position was decided to achieve a balanced yacht with a 7% lead.

15.2.4 Cockpit Design

A new cockpit layout was developed, taking into account the downflooding angle as well as ergonomics and anthropometrics for a practical and comfortable sailing environment. But the major improvement lies in the definition of new compartments, better suited to modern yacht racing and allowing the crew more flexibility.

15.2.5 Structural Design

The primary structural elements have been designed in accordance with the ISO 12215, meeting the requirements of a Category C yacht for added safety and reliability, justified by the extreme racing nature of the A Raters. Research also revealed the very little interest of regulatory bodies in wooden boats, with minimum guidance on structural arrangements, and no information inherent to smaller secondary components.

As a result, both empirical and experience based scantling rules have been applied for the design of various components, revealing the heavy influence of traditional methods in modern boatbuilding.

15.2.6 Stability

Relying on a careful weight and centres estimate at this stage, the stability has been evaluated against the ISO 12217. This is however mostly dependant on the location of the vertical centre of gravity, that can only be ascertained through an inclining experiment; the procedure has therefore been detailed. In addition, the requirements to obtain the intended Category C classification have been outlined, and compliance has been demonstrated.

15.2.7 Velocity Prediction Program

Key stone of the design development and evaluation, the velocity prediction program is nowadays a critical part of naval architecture. A complete six degrees of freedom program has been developed. The hydrodynamics rely on the Delft series for its higher flexibility, while the aerodynamic model combines Hazen's theory with the more recent Offshore Racing Congress coefficients.

Being dedicated to a light planning craft, the velocity prediction program was implemented with three main innovations.

First of all, a crew module allowing to specify the weight and height of each crew member enables to refine the hydrostatics and performance prediction for any combination of crew. This appears particularly relevant to a yacht where the crew mass is over a third of the sailing displacement.

Secondly, to cope with the varying displacement and hydrostatics, the traditional righting lever $\overline{Gz}$ has been replace by $\overline{KN}$, normally preferred by the shipping industry, to better characterise the stability. This is an atypical choice that proved to be better suited to simple programs, i.e. not featuring a lines processing stability module, and would be strongly recommended for future velocity prediction software.

Finally, the Savitzky planning theory, intended for motor crafts, has been adapted to the A Rater approximated as a flat plate, thus incorporating planning behaviour as part of the performance prediction to better model the actual capabilities of the yacht.

Decisive improvements in the velocity prediction program have therefore been achieved, especially relevant to light planning crafts which tends not be accurately modelled by commercially available software.

15.2.8 Production

The construction represented a challenge as it strongly differs from common production principles. Indeed, the yacht is to be manufactured at the International Boatbuilding Training College, where the labour is undertaken by students, and is not charged for: only materials will be billed. Furthermore, being built by students induces a potentially higher standard of craftsmanship than a commercial shipyard since there is no time and labour cost pressure; however, the consistency of the work is likely to greatly vary from a worker to another.

Cold moulding has been advised for its greater strength, lightweight, low maintenance, fast construction and low waste, making it more suitable than traditional carvel.

While a critical path analysis proved not to be applicable to one-off wooden boats, production planning, timing and costing have been estimated. Due to the high level of uncertainties, large safety margins have been considered. A total of 2400 man hours and an overall cost ready to sail of £28.2k ($56.2) have been determined, large variations are however to be expected.

Finally, a high degree of personalisation will be offered to the customer, which will impact on the appearance of the yacht as well as its cost.

15.2.9 Recommendations for Future Work

The work undertaken revealed further opportunities, in terms of design evaluation, modifications and large scale composite manufacturing.

First of all, a careful design evaluation has been suggested. Naval architecture relies on multiple assumptions and approximations, for which many guidelines have been published. However, there appears to be a complete lack of information regarding the comparison of the estimates made at a design stage and the final yacht. It therefore appears relevant to conduct a thorough evaluation during the construction to assess the accuracy and reliability of the assumptions made.

Then, further design opportunities can be explored, the main one being the adaptation into an inshore craft. This would lift the spinnaker and trapeze restrictions applying inland, thus considerably increasing the performance of the A Rater and widening its sailing program.

Finally, the foremost suggestion for future work is the setup of a composite production line. The wooden hull manufactured can be the basis of a female mould tool, from which a number of hulls can be manufactured. This would allow for a much faster building time, a more economical and lighter yacht, and a large commercial potential.

The new A Rater provides the basis of future work, whether academic with the accuracy of the estimates to be monitored during the construction, or commercial with further design possibilities and the setup of a composite production line.

15.3 Client Review

The final component of the conclusion is the feedback received from the client. This constitutes the most crucial part of the design evaluation, and defines whether the project is a success or not.

The author would like to thank Mr Simon McClean for its time and for providing the following review, dated June 20, 2015:

"I have been sailing all my life in boats that have ranged from 3M dinghies to 30M super maxi racing yachts. Speaking as a yachtsman, businessman (and potential client for your design!) I have read through your dissertation several times and I think it is an exceptional piece of work.

For me, yachts should be safe, fun, fast, affordable, aesthetically pleasing and manoeuvrable. It is my considered opinion that your design project has easily hit the mark in respect of all these areas.

The most important aspect of these criteria is safety and by incorporating a reefing sailplan into the design as *well as ensuring that your vessel conforms to relevant knockdown and stability criteria (as seen in section 9.5) you will be offering a design that will appeal to all levels of sailing ability, from the relative novice (who can utilise a reefed sail profile, or just smaller sails) through to the seasoned racer who will undoubtedly relish the challenge of campaigning these yachts at the very highest echelons of the sport.*

This, therefore, creates a winning design that will keep pace with the owners competence and sailing ability.

I cannot comment on the technical nature of the formulae you have used in the dissertation as these are all beyond my experience. I would add, though that the depth of consideration you have made in Ch10 for the VPP seems exceedingly thorough.

I also feel that your dissertation considers an often overlooked concept in any business, namely that of social responsibility. It is clear from what I read in Ch 11 that the production of this type of vessel will potentially create much needed employment in Lowestoft with all the concomitant benefits this will bring. It is my intent to use this design to advance the concept of classic sailing yachts on The Norfolk Broads in a way that offers owners the experience of sailing beautiful contemporary yachts that owe their existence to a traditional design. The Souppez A Rater will fit that bill rather well."

The design has therefore been positively received by the client, who mostly appreciated the safety, fun, affordability, aesthetics and performance, with special mentions of the reefed mainsail and the local production considerations. In the high level of satisfaction of the client resides the success of the design.

15.4 Conclusions

The design and production of a new Thames A Rater class sailing yacht to be introduced on the Norfolk Broads has been undertaken. The final design appears to satisfy all requirements from the multiple stakeholders involved as well as both the Thames A Rater class rule and the RCD/ISO standard. Many design aspects have been implemented and significant findings have been highlighted. In addition, areas of future work with a significant academic and commercial potential have been suggested. Finally, the client's feedback proved that the design and project have been successfully conducted.

References

[1] Amdahl G. M. (1967). Validity of the single processor approach to achieving large scale computing capabilities. *AFIPS sprint joint computer conference*. California: IBM Sunnyvale.

[2] American Bureau of Shipping (1997). *Guide for Building and Classing Offshore Racing Yachts*. American Bureau of Shipping.

[3] American Wood Council (2007.) *Beam design formulas with shear and moment diagrams*. Washington: American Wood Council.

[4] ANSYS Inc. (2013). *ANSYS CFX 15.0* (Version 15.0.0.685484). [Software].

[5] Baigent G (Undated). *Light brigade: the New Zealand school of yacht design*. New Zealand.

[6] Barnaby K. C. (1982). *Schoenherr friction coefficients - Smooth turbulent flow*. The University of Michigan naval tank.

[7] Barrass C. B. and Derrett D. R (2002). *Ship stability for masters and mates*. 7th edition. Oxford: Butterworth-Heinemann.

[8] Bentley Systems (2012). *Hydromax - Maxsurf stability* (Version 19.0 V8i) [Software].

[9] Bentley Systems (2012). *Maxsurf modeller* (Version 19.0 V8i) [Software].

[10] Birmingham R. (2005). *Boatbuilding techniques*, 3rd edition. London: Adlard Coles Nautical.

[11] Blount D. L. and Fox D. L. (1976). Small Craft power prediction. *Marine technology*, Vol 13, No 1, pp 14-45.

[12] British Pathé Archives (1923). *Cowes on Thames* [Video]. Available online: http://www.britishpathe.com/video/cowes-on-thames/query/bourne+end [Accessed 9th December 2014]

[13] British Pathé Archives (1929). *Cowes on Thames* [Video]. Available online: http://www.britishpathe.com/video/cowes-on-thames-1/query/bourne+end [Accessed 9th December 2014].

[14] British Pathé Archives (1933). *The little boats' day* [Video]. Available online: http://www.britishpathe.com/video/the-little-boats-day/query/bourne+end [Accessed 9th December 2014].

[15] British Standard (1992). *BS EN 294: 1992 Safety of machinery - Safety distance to prevent danger zones being reached by the upper limbs*. London: British Standard.

[16] British Standard (1997). *BS EN 847-1: 1997 Tools for woodworking - Safety requirements - Part 1: Milling tools and circular table saw*. London: British Standard.

[17] British Standard (1997) *BS EN 847-2: 1997 Tools for woodworking. Safety requirements. Part 2: Milling tools and circular saw blades*. London: British Standard.

[18] British Standard (1998). *BS EN 859: 1998 Safety of woodworking machines. Handfed surface planning machines*. London: British Standard.

[19] British Standard (1999) 120 *BS EN 1870-1:1999 Safety of wood working machines - Circular sawing machines - Part 1: Circular saw benches (with and without sliding table) and dimension saw*. London: British Standard.

[20] Broads Authority (1988). *Norfolk and Suffolk Broads Act*. Available online: http://www.broads-authority.gov.uk/ [Accessed 21st January 2015].

[21] Celik I. B. (Undated). *Procedure for estimation and reporting of discretization error in CFD applications*. West Virginia University.

[22] Cook, N. J. (1985). *The designers guide to wind loading of buildings and structures*. Butterworth.

[23] Delft Systematic Yacht Hull Series (2014). *DSYHS database*. Retrieved from: http://dsyhs.tudelft.nl/ [March 20th, 2014]

[24] Fossati R. (2009). *Aero-hydrodynamics and the performance of sailing yachts*. London : Adlard Coles nautical.

[25] Froude W. (1872). Experiments of the surface-friction experienced by a plane moving through water. *Report to the British Association for the Advancement of Science*, London.

[26] Froude W. (1874). Report to the Lords Commissioners of the Admiralty on experiments for the determination of the frictional resistance of the water on a surface under various conditions. *Report to the British Association for the Advancement of Science*, London

[27] FutureShip (2009). *FS-Equilibrium* (Rel14.0228) [Software].

[28] Germanischer Lloyd (2009). *Guidelines for the design and construction of large modern yacht rigs*. Germanischer Lloyd Aktiengesellschaft

[29] Gerr D (2000). *The element of boat strength*. International marine, McGraw-Hill.

[30] Gerristma J. (1971). *Course keeping qualities and motions in waves of a sailing yacht*. Technical report, Delft University of Technology.

[31] Gerritsma J. and Keuning J.A. (1986). Further experiments with keel-hull combinations. *SNAME first Tampa bay sailing yacht symposium*, S. Petersburg.

[32] Gerristma J., Moeyes G. and Onnink R. (1997). Test results of a systematic yacht hull series. *5th HISWA symposium yacht architecture*.

[33] Gerritsma J., Onnink R. and Versluis A. (1981). Resistance and stability of the Delft systematic yacht hull series. *International shipbuilding progress* (Vol. 28).

[34] Gerritsma J., Onnink R. and Versluis A. (1996). The bare hull resistance of the Delft systematic yacht hull series. *The International HISWA symposium on yacht design and yacht construction*.

[35] Gougeon Made, 2005. *The Gougeon Brothers on boat construction*. 5th Edition, Gougeon Brothers Inc.

[36] Grubisic I. (2003). *Reliability of weight prediction in the small craft concept design*. Croatia: The university of Zagreb.

[37] Hadler J. B. (1958). *Coefficient for international towing tank conference 1957 model-ship correlation line*. DTMB Report 1185.

[38] Hansen H. (2006). *Enhanced wind tunnel techniques and aerodynamic force models for yacht sails*. PhD Thesis, University of Auckland.

[39] Hansen H., Richards P. J. and Jackson P. S. (2010). Reef and flat or twist and ease: an improved trim parameter model for yacht sails. *Intl J Small Craft Tech, Trans RINA*, Vol 152, Part B1.

[40] Health and Safety Executive (1974). *Health and safety at work act*. Health and Safety Executive.

[41] Health and Safety Executive (1992). *Management of health and safety at wok regulation*. Health and Safety Executive.

[42] Health and Safety Executive (1992). *Personal protective equipment regulation*. Health and Safety Executive.

[43] Health and Safety Executive (1995) *Reporting injuries, diseases and dangerous occurrences regulation*. Health and Safety Executive.

[44] Health and Safety Executive (1998). *Lift operation lift equipment regulation*. Health and Safety Executive.

[45] Health and Safety Executive (1998). *Safe use of woodworking machinery*. Health and Safety Executive.

[46] Health and Safety Executive (1999). *Control of Substances Hazardous to Health*. Health and Safety Executive.

[47] Hazen G. S. (1980). A model of sail aerodynamics for diverse rig types. *New England sailing yacht symposium*.

[48] Hoerner S. F. (1965). *Fluid-dynamic drag: theoretical, experimental and statistical information*. Great Britain: Published by the Author.

[49] Hope L. (1903). *Small yacht construction and rigging*. New York City: Forest and Stream publishing company.

[50] International Towing Tank Conference (1978). Report of the Resistance Committee. *15th International Towing Tank Conference*, The Hague.

[51] International Towing Tank Conference (1999). ITTC recommended procedures: performance, propulsion, 1978 ITTC performance prediction method. *22th International Towing Tank Conference*, Seoul.

[52] International Towing Tank Conference (2002). ITTC recommended procedures and guidelines: model manufacture, ship models. *23th International Towing Tank Conference*, Venice.

[53] International Organisation for Standardization (2002). *ISO 12215 Small craft - Hull construction and scantlings. Part 3: Materials: steel, aluminium alloys, wood, other materials*. International Organisation for Standardization.

[54] International Organisation for Standardization (2008). *ISO 12215 Small craft - Hull construction and scantlings. Part 5: Design pressures for monohulls, design stresses, scantlings determination*. International Organisation for Standardization.

[55] International Organisation for Standardization (2008). *ISO 12215 Small craft - Hull construction and scantlings. Part 6: Structural arrangements and details*. International Organisation for Standardization.

[56] International Organisation for Standardization (2009). *ISO 12215 Small craft - Hull construction and scantlings. Part 8: Rudders*. International Organisation for Standardization.

[57] International Organisation for Standardization (2012). *ISO 12215 Small craft - Hull construction and scantlings. Part 9: Sailing craft appendages*. International Organisation for Standardization.

[58] ISO – International Organisation for Standardisation (2002). *ISO 12217 - Small Craft - Stability and buoyancy assessment and categorization. Part 2: Sailing boats of hull length greater or equal to 6m*. International Organisation for Standardization.

[59] Kemp, D. (1904). *Dixon Kemp's manual of yacht and boat sailing*. New and tenth edition. Edited by B. Heckstall-Smith. London: Horace Cox.

[60] Kemp, D. (1913). *Dixon Kemp's manual of yacht and boat sailing and yacht architecture*. New and eleventh edition. Edited by B. Heckstall-Smith and Linton Hope. London: Horace Cox.

[61] Keuning J. A. and Binkhorst B-J. (1997). Appendage resistance of a sailing yacht hull. *13th Chesapeake sailing yacht symposium*, Amsterdam.

[62] Keuning J. A., Katgert M. and Vermeulen K. J. (2007). *Further analysis on the forces on keel and rudder of a sailing yacht*. Delft University of Technology.

[63] Keuning J. A. and Katgert M. (2008). *A bare hull resistance prediction method derived from the results of the delft systematic yacht hull series extended to higher speeds*. Delft University of Technology.

[64] Keuning J. A. and Katgert M. (2010). *The influence of heel on the bare hull resistance of a sailing yacht*. Delft University of Technology,.

[65] Keuning J. A., Onnink R., Versluis A. and Van Gulik A. A. M. (1996). The Bare hull resistance of the Delft systematic yacht hull series. *The international HISWA symposium on yacht design and yacht construction*, Amsterdam.

[66] Keuning J. A. and Sonnenberg U. B. (1998). Approximation of the hydrodynamic forces on a sailing yacht based on the Delft systematic yacht hull series. *15th International symposium on yacht design and construction*, Amsterdam.

[67] Keuning J. A. and Sonnenberg U. B. (1998). Development in the velocity prediction based on the Delft systematic yacht hull series. *International conference on the modern yacht*. Portsmouth.

[68] Keuning J. A. and Sonnenberg U. B. (1999). *Approximation of the calm water resistance on a sailing yacht based on the Delft systematic yacht hull series*. Delft University of Technology.

[69] Keuning J. A. and Verwerft B. (2009). A new method for prediction of the side force on keel and rudder of a sailing yacht based on the results of the Delft systematic yacht hull series. *The 19th Chesapeake sailing yacht symposium*, Annapolis.

[70] Keuning J. A. and Verwerft B. (2009). A new method for prediction of the side force on keel and rudder of a sailing yacht based on the results of the Delft systematic yacht hull series. *The 19th Chesapeake sailing yacht symposium*, Annapolis.

[71] Kristensen H. O. and Lützen M. (2013). *Prediction of resistance and propulsion power of ships*. Technical University of Denmark and University of Southern Denmark.

[72] Laity M. (undated). Caprice. *Classic Boats*. pp.51-56.

[73] Laity M. (2001). Thames Clubs. *Classic Boats*. pp.58-63.

[74] Laity M. (2007). Bell Boy. *Classic Boats*. October 2007, pp.34-37.

[75] Larsson L. and Eliasson R. (2007). *Principles of yacht design*. Third Edition, London: Adlard Coles Nautical.

[76] Launder B and Spalding D (1972). *Mathematical models of turbulence*. Academic press, London.

[77] Le Deroff J. Y. and Lachikine P (2001). *Righting moment measurement on Laser class*. Ecole nationale de voile.

[78] Loscombe R. (1998). Structural design considerations for laminated wood yachts. *International conference on the modern yacht*. Portsmouth.

[79] Loscombe R. (2012). *Marine craft structure theory*. Southampton Solent University.

[80] MacNaughton Yacht Design (2010). *Scantlings rules: could molded construction*. MacNaughton Yacht Design

[81] Marchaj C. A. (1988). *Aero-hydrodynamics of sailing*. London: Adlard Coles Nautical.

[82] MathWorks (2010). *Matlab* (Version 7.11.0.584). [Software].

[83] Mérillon M. D. (1900). *Concours internationaux d'exercices physiques et de sports*. Paris: Imprimerie Nationale.

[84] Microsoft Office (2010). *Microsoft Excel* (Version 14.0.7145.5000). [Software].

[85] Milgram J.H. (1970). Sail force coefficients for systematic rig variations. *SNAME technical and research report*: R-10

[86] MIT (2008). *Lifting Surfaces*. MIT - Department of Mechanical Engineering.

[87] Nicolson I. (1983). *Surveying small craft*. London: Stanford maritime.

[88] Nicolson I. (1994). *Surveying small craft*, 3rd edition. London: Adlard Coles Nautical

[89] Nomoto K. and Tatano H. (1979). Balance of helm of sailing yachts: a ship hydrodynamics approach on the problem. *6th HISWA Symposium*, Amsterdam.

[90] Nordic Boat Standard (1990). *Nordic Boat Standard*. Det Norske Veritas classification A/S. Oslo

[91] Offshore Racing Congress (2013). *ORC VPP Documentation*. Updated 4th July 2013.

[92] Pardey L. (2010). *Details of classic boat construction*. Pardey Books.

[93] Phillips M. (2005). *Ulva*. Available online: http://www.tradboatrally.com [Accessed: 12/01/15].

[94] Presque D. and Paulet D. (2005). *Naval architecture: knowledge and practice*. 2nd edition. Paris: La Villette.

[95] Recreation Craft Directive (2006). *Recreation Craft Directive RYA compliance guide*. Royal Yachting Association.

[96] Remmlinger U. (2014). *Bare hull resistance prediction based on the Delft Systematic Yacht Hull Series*. Ulirch Remmlinger, Germany.

[97] Rhinoceros (2012). *Rhinoceros - Modelling tools for designers* (Version 5.1.20927.2230) [Software].

[98] Robbins Timber (2015). *Marine products: Guide and price list*. Robbins Timber.

[99] Rössel C. G. (1993). Lofting Demystified. *Wooden Boat*.

[100] Sail7 (2012). *Sail7* (Version v.0.05 alpha) [Software].

[101] SailCut (2011). *SailCut* (Version 4-2011). [Software].

[102] Savitsky, D. (1964). *Hydrodynamic design of planning hulls*. SMANE transactions.

[103] Savitsky D. and Brown W. P. (1976). Procedures for hydrodynamic evaluation of planning hulls in smooth and rough water. *Marine technology*, Vol 13, No 4, pp381-400.

[104] Seldén (2015). *Seldén carbon spars*. Seldén.

[105] Souppez J. B. (2013). *Design and production of a one-off 32 feet wooden racing yacht dedicated to Southampton Solent University*. Southampton Solent University final year dissertation.

[106] Souppez J. B. (2014). *On the use of Unstructured Meshes for Free Surface Flow Around a Yacht Hull*. The University of Auckland.

[107] Souppez J. B. (2014). *On the use of unstructured meshes for free surface flow around a yacht hull*. The University of Auckland.

[108] Souppez J. B. (2014). *Development and validation of a computational fluid dynamics hydrodynamic model of the Stewart 34 for velocity prediction program applications*. The University of Auckland yacht engineering research project

[109] Souppez J.B. (2014). *Upwind wind tunnel testing of the Stewart 34*. The University of Auckland.

[110] Stewart J. (2002). *The design of a Thames A Class Rater*. Southampton Solent University final year dissertation.

[111] Thames Sailing Club (2007). *The Thames A Rater Association Rules*. Thames Sailing Club, Revised and Updated: March 2007.

[112] Upper Thames Sailing Club (2015). *Upper Thames Sailing Club gallery*. Available online: http://bew.utsc.org.uk/ [Accessed: 12/01/15].

[113] Vacanti D. (2005). Keel and Rudder Design. *Professional boatbuilder*, June/July 2005.

[114] Van Oossanen P. (1993). Predicting the speed of sailing yachts. *SNAME transactions*. Vol. 101, pp 337-397. Wageningen.

[115] Viola I.M., Bot P. and Riotte M. (2012). Upwind sail aerodynamics: A RANS numerical investigation validated with wind tunnel pressure measurements. *Int. J. Heat Fluid Flow*.

[116] Wallis S. (2012). *Aero-Hydrodynamics: sail forces*. Southampton Solent University.

[117] Wallis S. (2012). *3D foil theory*. Southampton Solent University.

[118] Wallis S. (2011). *Buckling theory, masting and rigging*. Southampton Solent University.

[119] Wallis. S (2011). *Marine craft design and development: keel and ballast*. Southampton Solent University.

[120] Wallis S. (2011). *Marine craft design and development: Weight estimate*. Southampton Solent University.

[121] Wallis S. (2012). *Savitsky planning craft theory*. Southampton Solent University

[122] Wolfson Unit (2008*). HullScant: hull scantlings ISO-12215* (Version FV21:4). [Software].

[123] Wolfon Unit (2009). *WinDesign 4.0* (Version 4.2.29N). [Software].

[124] Young W. C. and Budynas R. G. (2002). *Roark's formulas for stress and strain*. 7th edition. London: McGraw-Hill.

Appendix A: Project Organisation

Jean-Baptiste R. G. SOUPPEZ: Design and Production of a Wooden Thames A Rater Class Sailing Yacht

Client:	Simon McClean	Shipyard:	IBTC - Lowestoft	Class:	Thames A Rater	Regulation:	RDC/ISO Standards

1. Contact with client		**2. Letter of intent**		**3. Project approved by Auckland Uni**		**4. Contract signed**		**5. Kick off meeting**		**6. Detailed project schedule**	
Completed:	29/10/2014	Completed:	06/11/2014	Completed:	07/11/2014	Completed:	13/11/2014	Completed:	03/12/2014	Completed:	04/12/2014
7. Design brief		**8. Design**		**9. Class compliance**		**10. Production**		**11. Deliverables**		**12. Project submitted to client**	
Client	03/12/2014	Hull	20/02/2015	Structure	27/04/2015	Planning	30/04/2015	Report	31/05/2015	Completed:	08/06/2015
Shipyard	03/12/2014	Appendages	08/03/2015	Scantlings	27/04/2015	Schedule	03/05/2015	Drawings	04/06/2015		
Environment	07/12/2014	Sails	15/03/2015	Hydrostatics	06/04/2015	Cost	07/05/2015	Appendix	06/05/2015		
Sailors	14/01/2015	Rig	02/04/2015	Stability	07/04/2015	Detailed design	15/05/2015	Proof Reading	07/06/2015		
Class	26/01/2015	Cockpit/Deck	03/04/2051	Other Regulations	28/04/2015			Completed:	07/06/2015		
Regulation	30/01/2015	Weights	06/04/2015			Drawings	27/05/2015				
Design Brief Approved	31/01/2015	VPP	23/04/2015	Class Association	27/04/2015	Production Approved	28/05/2015				
Completed:	31/01/2015	Design Approved	22/04/2015	Completed:	28/04/2015	Completed:	28/05/2015				
		Completed:	23/04/2015								
13. Project submitted to shipyard		**14. Project approved by client**		**15. Project approved by shipyard**		**16. Project submitted to Auckland Uni**		**17. Building approved**		**18 All materials delivery schedule complete**	
Completed:	08/06/2015	Completed:	20/06/2015	Completed:		Completed:	27/06/2015	Completed:		Completed:	
								Estimated:	July 2015	Estimated:	July 2015
19. Production		**20. Quality control**		**21. Launch**		**23. Classification**		**24. Sea trial**		**25. Handover**	
Lofting		Completed:		Completed:		Completed:		Completed:		Completed:	
Section Moulds		Estimated:	March 2016	Estimated:	April 2016	Estimated:	April 2016	Estimated:	April 2016	Estimated:	May 2016
Backbone											
Hull											
Deck											
Appendages											
Fit out											
Painting											
Rigging											
Completed:											
Estimated:	March 2016										

Appendix B: VPP Results

B.1 Apparent Wind

B.1.1 Apparent Wind Speed

Apparent Wind Speed (kts)				
TWA	4kts TWS	8kts TWS	12kts TWS	16kts TWS
30	6.6	10.8	14.5	17.8
35	6.9	11.0	14.9	18.2
40	7.1	11.2	15.1	18.6
45	7.3	11.3	15.2	18.8
50	7.4	11.3	15.1	18.7
60	7.4	11.2	14.8	18.3
70	7.3	10.7	14.1	17.5
80	6.9	10.0	13.3	16.6
90	6.3	9.3	12.4	15.6
100	5.6	9.1	11.4	14.5
110	4.7	8.3	10.8	13.3
120	3.9	7.2	10.2	12.4
130	3.1	6.1	9.1	11.7
140	2.6	5.2	8.0	10.6
150	2.3	4.6	7.2	9.8
160	2.1	4.3	6.7	9.2
170	2.0	4.1	6.4	8.9
180	2.0	4.0	6.2	8.8

B.1.2 Apparent Wind Angle

Apparent Wind Angle (°)				
TWA	4kts TWS	8kts TWS	12kts TWS	16kts TWS
30	18.4	19.8	22.2	24.2
35	19.5	21.4	24.0	26.2
40	20.7	23.2	26.0	28.3
45	22.1	25.4	28.6	31.1
50	24.1	28.5	32.4	35.2
60	26.6	32.2	37.0	40.5
70	30.0	37.1	43.2	47.4
80	33.9	42.2	49.7	54.5
90	38.6	47.7	56.3	61.8
100	44.4	53.8	63.2	69.1
110	52.3	61.3	69.3	76.5
120	63.5	71.4	76.3	82.4
130	79.7	83.9	90.6	89.3
140	99.5	100.8	107.3	106.8
150	120.0	120.3	124.3	125.6
160	140.2	140.3	142.2	143.8
170	160.2	160.1	160.9	161.9
180	180.0	180.0	180.0	180.0

B.2 Boat Speed

B.2.1 Knots

Boat Speed (kts)				
TWA	4kts TWS	8kts TWS	12kts TWS	16kts TWS
30	2.88	3.40	3.31	3.22
35	3.24	3.86	3.95	3.55
40	3.56	4.23	4.43	4.27
45	3.91	4.61	4.92	4.90
50	4.30	5.07	5.46	5.56
60	4.64	5.48	5.87	6.01
70	4.91	5.82	6.22	6.44
80	5.02	6.06	6.54	6.87
90	4.94	6.29	6.86	7.36
100	4.68	6.77	7.19	7.91
110	4.27	6.73	7.88	8.50
120	3.72	6.31	8.40	10.48
130	3.13	5.79	7.61	10.39
140	2.63	5.15	6.81	9.19
150	2.31	4.59	6.31	8.17
160	2.11	4.22	5.99	7.57
170	2.01	4.03	5.80	7.28
180	1.99	3.99	5.75	7.21

B.2.2 Meters/Second

Boat Speed (m/s)				
TWA	4kts TWS	8kts TWS	12kts TWS	16kts TWS
30	1.48	1.75	1.70	1.66
35	1.67	1.99	2.03	1.83
40	1.83	2.18	2.28	2.20
45	2.01	2.37	2.53	2.52
50	2.21	2.61	2.81	2.86
60	2.39	2.82	3.02	3.09
70	2.53	2.99	3.20	3.31
80	2.58	3.12	3.36	3.53
90	2.54	3.24	3.53	3.79
100	2.41	3.48	3.70	4.07
110	2.20	3.46	4.05	4.37
120	1.91	3.25	4.32	5.39
130	1.61	2.98	3.91	5.35
140	1.35	2.65	3.50	4.73
150	1.19	2.36	3.25	4.20
160	1.09	2.17	3.08	3.89
170	1.03	2.07	2.98	3.75
180	1.02	2.05	2.96	3.71

B.3 Heel Angle

Heel Angles (°)				
TWA	4kts TWS	8kts TWS	12kts TWS	16kts TWS
30	10.8	30.0	30.0	30.0
35	12.1	30.0	30.0	30.0
40	13.2	30.0	30.0	30.0
45	14.4	30.0	30.0	30.0
50	15.4	30.0	30.0	30.0
60	15.6	30.0	30.0	30.0
70	14.4	30.0	30.0	30.0
80	12.3	30.0	30.0	30.0
90	9.6	29.3	30.0	30.0
100	6.9	20.2	30.0	30.0
110	4.5	13.1	25.9	30.0
120	2.6	7.9	16.4	30.0
130	1.3	4.5	8.9	17.4
140	0.6	2.5	5.3	9.6
150	0.4	1.5	3.5	6.3
160	0.2	1.0	2.3	4.2
170	0.1	0.5	1.2	2.2
180	0.0	0.0	0.1	0.1

B.4 Leeway Angle

Leeway (°)				
TWA	4kts TWS	8kts TWS	12kts TWS	16kts TWS
30	3.07	4.44	5.45	6.32
35	2.66	3.50	4.06	5.72
40	2.36	3.01	3.32	4.12
45	2.08	2.59	2.75	3.16
50	1.79	2.18	2.22	2.41
60	1.53	1.83	1.84	1.97
70	1.27	1.54	1.53	1.60
80	1.06	1.33	1.29	1.29
90	0.89	1.13	1.07	1.01
100	0.74	0.77	0.87	0.76
110	0.60	0.57	0.60	0.56
120	0.46	0.43	0.37	0.41
130	0.33	0.30	0.29	0.20
140	0.23	0.22	0.24	0.18
150	0.18	0.17	0.19	0.17
160	0.14	0.13	0.14	0.14
170	0.08	0.08	0.08	0.08
180	0.00	0.00	0.00	0.00

B.5 Rudder Angle

Rudder Angle (°)				
TWA	4kts TWS	8kts TWS	12kts TWS	16kts TWS
30	0.290	0.868	0.596	0.368
35	0.394	1.112	0.788	0.474
40	0.500	1.252	0.946	0.668
45	0.634	1.426	1.132	0.868
50	0.810	1.668	1.412	1.170
60	0.972	2.046	1.878	1.628
70	1.092	2.696	2.594	2.330
80	1.108	3.512	3.498	3.218
90	1.034	4.422	4.672	4.362
100	0.898	3.506	6.252	5.878
110	0.728	2.716	6.652	7.954
120	0.544	2.040	4.780	7.482
130	0.380	1.488	3.354	6.492
140	0.268	1.076	2.560	4.608
150	0.210	0.850	2.090	3.848
160	0.184	0.736	1.808	3.466
170	0.172	0.686	1.666	3.286
180	0.180	0.750	1.846	3.682

B.6 Trim Angle

Trim Angle (°)				
TWA	4kts TWS	8kts TWS	12kts TWS	16kts TWS
30	-0.161	-0.234	-0.499	-1.023
35	-0.185	-0.307	-0.675	-1.335
40	-0.204	-0.375	-0.853	-1.574
45	-0.224	-0.450	-1.013	-1.823
50	-0.238	-0.511	-1.134	-2.061
60	-0.268	-0.646	-1.323	-2.310
70	-0.286	-0.734	-1.436	-2.502
80	-0.293	-0.772	-1.515	-2.532
90	-0.287	-0.740	-1.519	-2.550
100	-0.270	-0.658	-1.490	-2.494
110	-0.243	-0.533	-1.354	-2.230
120	-0.211	-0.399	-1.082	-1.718
130	-0.170	-0.259	-0.709	-1.097
140	-0.135	-0.165	-0.405	-0.729
150	-0.095	-0.082	-0.219	-0.413
160	-0.067	-0.040	-0.121	-0.240
170	-0.057	-0.029	-0.089	-0.182
180	-0.055	-0.027	-0.084	-0.173

B.7 Displacement

Displacement (m^3)				
TWA	4kts TWS	8kts TWS	12kts TWS	16kts TWS
30	0.652	0.652	0.652	0.652
35	0.652	0.652	0.652	0.652
40	0.652	0.652	0.652	0.652
45	0.652	0.652	0.652	0.652
50	0.652	0.652	0.652	0.652
60	0.652	0.652	0.651	0.651
70	0.652	0.652	0.650	0.649
80	0.652	0.651	0.647	0.643
90	0.652	0.650	0.646	0.636
100	0.652	0.650	0.645	0.625
110	0.652	0.649	0.641	0.612
120	0.652	0.648	0.634	0.607
130	0.652	0.650	0.629	0.603
140	0.652	0.651	0.635	0.606
150	0.652	0.652	0.645	0.621
160	0.652	0.652	0.652	0.650
170	0.652	0.652	0.652	0.652
180	0.652	0.652	0.652	0.652

B.8 Depowering

B.8.1 Reef

Reef				
TWA	4kts TWS	8kts TWS	12kts TWS	16kts TWS
30	1	1	0.849	0.724
35	1	0.976	0.771	0.668
40	1	0.924	0.727	0.615
45	1	0.88	0.69	0.579
50	1	0.839	0.665	0.562
60	1	0.836	0.684	0.58
70	1	0.873	0.722	0.614
80	1	0.929	0.775	0.661
90	1	1	0.845	0.722
100	1	1	0.934	0.798
110	1	1	1	0.897
120	1	1	1	1
130	1	1	1	1
140	1	1	1	1
150	1	1	1	1
160	1	1	1	1
170	1	1	1	1
180	1	1	1	1

B.8.2 Flat

Flat				
TWA	4kts TWS	8kts TWS	12kts TWS	16kts TWS
30	1	0.666	0.564	0.471
35	1	0.667	0.689	0.659
40	1	0.745	0.784	0.788
45	1	0.833	0.889	0.907
50	1	0.949	1	1
60	1	1	1	1
70	1	1	1	1
80	1	1	1	1
90	1	1	1	1
100	1	1	1	1
110	1	1	1	1
120	1	1	1	1
130	1	1	1	1
140	1	1	1	1
150	1	1	1	1
160	1	1	1	1
170	1	1	1	1
180	1	1	1	1

Appendix C: Production Planning Overview

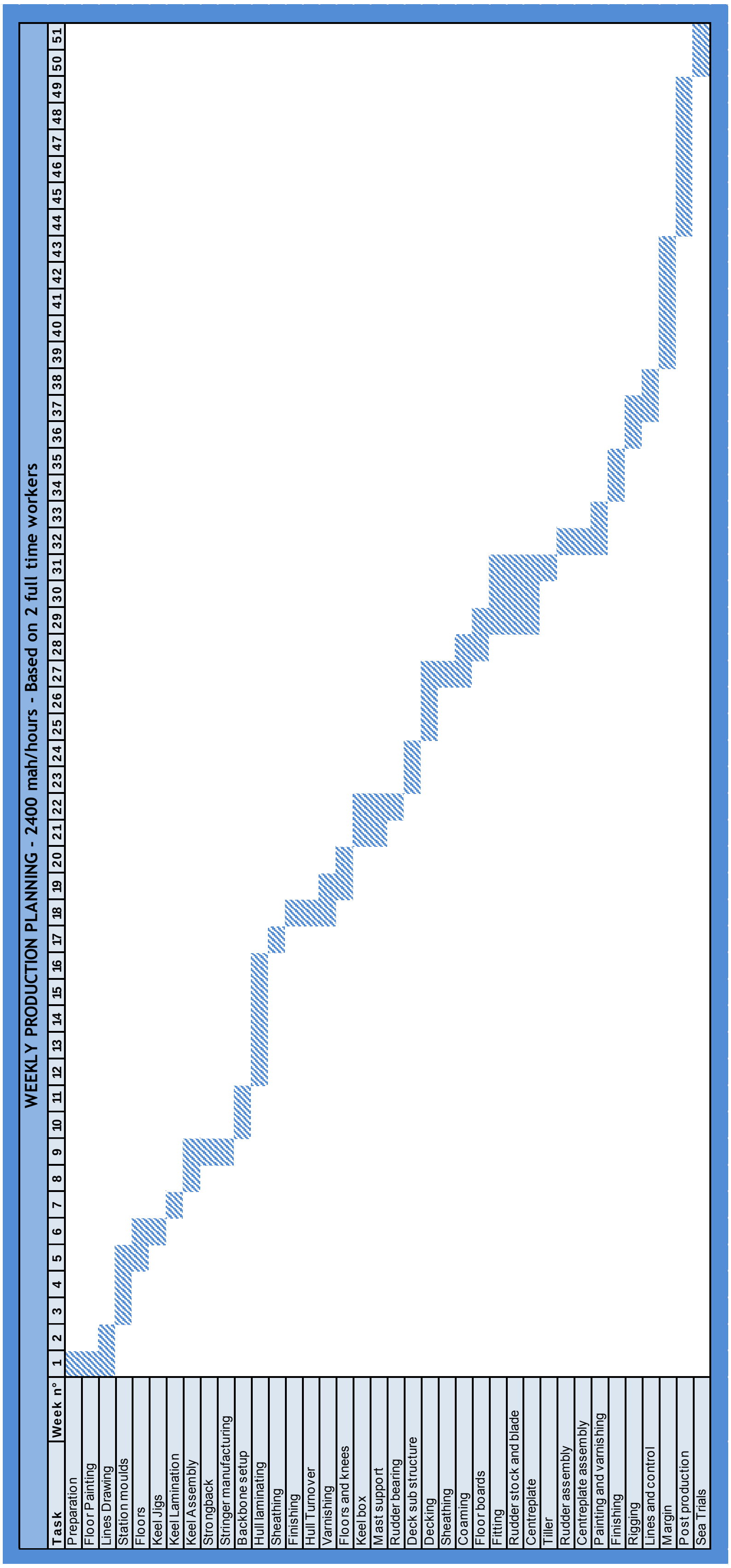

Jean-Baptiste R. G. SOUPPEZ

Master of Engineering Studies in Yacht Engineering
Department of Mechanical Engineering
The University of Auckland
June 2015